

**A RISK-BASED OPTIMIZATION MODELING FRAMEWORK FOR
MITIGATING FIRE EVENTS FOR WATER AND FIRE RESPONSE
INFRASTRUCTURES**

A Dissertation

by

LUFTHANSA RAHMAN KANTA

Submitted to the Office of Graduate Studies of
Texas A&M University
in partial fulfillment of the requirements for the degree of

DOCTOR OF PHILOSOPHY

December 2009

Major Subject: Civil Engineering

**A RISK-BASED OPTIMIZATION MODELING FRAMEWORK FOR
MITIGATING FIRE EVENTS FOR WATER AND FIRE RESPONSE
INFRASTRUCTURES**

A Dissertation

by

LUFTHANSA RAHMAN KANTA

Submitted to the Office of Graduate Studies of
Texas A&M University
in partial fulfillment of the requirements for the degree of

DOCTOR OF PHILOSOPHY

Approved by:

Co-Chairs of Committee,	Kelly Brumbelow Emily M. Zechman
Committee Members,	Ralph A. Wurbs Sergiy Butenko
Head of Department,	John M. Niedzwecki

December 2009

Major Subject: Civil Engineering

ABSTRACT

A Risk-based Optimization Modeling Framework for Mitigating Fire Events for Water and Fire Response Infrastructures. (December 2009)

Lufthansa Rahman Kanta, B.S., Bangladesh University of Engineering and Technology;

M.S., Texas A&M University

Co-Chairs of Advisory Committee: Dr. Kelly Brumbelow
Dr. Emily M. Zechman

The purpose of this dissertation is to address risk and consequences of and effective mitigation strategies for urban fire events involving two critical infrastructures – water distribution and emergency services. Water systems have been identified as one of the United States’ critical infrastructures and are vulnerable to various threats caused by natural disasters or malevolent actions. The primary goals of urban water distribution systems are reliable delivery of water during normal and emergency conditions (such as fires), ensuring this water is of acceptable quality, and accomplishing these tasks in a cost-effective manner. Due to interdependency of water systems with other critical infrastructures – e.g., energy, public health, and emergency services (including fire response) – water systems planning and management offers numerous challenges to water utilities and affiliated decision makers.

The dissertation is divided into three major sections, each of which presents and demonstrates a methodological innovation applied to the above problem. First, a risk based dynamic programming modeling approach is developed to identify the critical

components of a water distribution system during fire events under three failure scenarios: (1) accidental failure due to soil-pipe interaction, (2) accidental failure due to a seismic activity, and (3) intentional failure or malevolent attack. Second, a novel evolutionary computation based multi-objective optimization technique, Non-dominated Sorting Evolution Strategy (NSES), is developed for systematic generation of optimal mitigation strategies for urban fire events for water distribution systems with three competing objectives: (1) minimizing fire damages, (2) minimizing water quality deficiencies, and (3) minimizing the cost of mitigation. Third, a stochastic modeling approach is developed to assess urban fire risk for the coupled water distribution and fire response systems that includes probabilistic expressions for building ignition, WDS failure, and wind direction. Urban fire consequences are evaluated in terms of number of people displaced and cost of property damage. To reduce the assessed urban fire risk, the NSES multi-objective approach is utilized to generate Pareto-optimal solutions that express the tradeoff relationship between risk reduction, mitigation cost, and water quality objectives. The new methodologies are demonstrated through successful application to a realistic case study in water systems planning and management.

DEDICATION

This dissertation is dedicated to my parents, Lutfor and Mahmuda Rahman; to my husband, Saquib Ejaz; and to our beloved daughters, Lamiya Zahin (March 13, 2000 – August 2, 2004) and Nashita Zahin.

ACKNOWLEDGMENTS

I would like to express my sincerest gratitude to my primary advisor, Dr. Kelly Brumbelow, for giving me the opportunity to work on this research project. The work presented here in this dissertation would not have been possible without the help and support of my primary advisor. I sincerely appreciate his guidance, support and patience during difficult periods of this work. I would like to express my sincere gratitude to my co-chair, Dr. Emily Zechman, for her support and encouragement throughout the process. Both of my advisors support and encouragement kept me focused and energized. I would also like to thank Dr. Ralph Wurbs and Dr. Sergiy Butenko for their valuable advice and support as my research advisory committee throughout the period of my studies.

Parts of this dissertation were produced with the support of the National Science Foundation (NSF) Infrastructure Management and Hazards Response Program under Grant No. CMS-0600448. All opinions expressed in this dissertation are the author's and do not necessarily reflect the views of NSF.

I would like to acknowledge my best friend and officemate, Jacob Torres, for being a valuable research collaborator. I would also like to acknowledge my officemates and fellow graduate students for their feedback and support including Arun Aryasomayajula, Chandana Damodaram, Marcio Giacomoni, and Mohammadmehdi Shafiee. I would like to thank all my friends who offered support and encouragement whenever needed.

I would like to thank my parents and my husband Saquib Ejaz who encouraged me to come back to school after losing our beloved daughter Lamiya Zahin and who gave me support throughout the toughest period of my life. Finally, I am very grateful to the Almighty for the survival of our second daughter Nashita Zahin; she is my biggest inspiration in pursuit to the doctoral program at Texas A&M University.

NOMENCLATURE

AWWA	American Water Works Association
AWWARF	American Water Works Association Research Foundation
AC	Asbestos Cement
BCS	Cities of Bryan and College Station, Texas
CCN	Construction Classification Number
CI	Cast Iron
DI	Ductile Iron
DP	Dynamic Programming
EC	Evolutionary Computation
EF	Exposure Factor
ES	Evolution Strategy
FF	Fire Flow
GA	Genetic Algorithm
GIS	Geographic Information System
GLM	Generalized Linear Model
GPM	Gallons per Minute
HC-AF	High Cost Accidental Failure
HC-IF	High Cost Intentional Failure
HHM	Hierarchical Holographic Modeling
HM2EA	Hypervolume Maximizing Multi-objective Evolutionary Algorithm

IRAM	Infrastructure Risk Analysis Model
ISO	International Organization of Standards
LC-AF	Low Cost Accidental Failure
LC-IF	Low Cost Intentional Failure
MBVA	Model Based Vulnerability Analysis
MC	Monte Carlo
MMAF	Multi Mode Attack and Failure
MOP	Multi-objective Problem
MUFS	Model of Urban Fire Spread
NPGA	Niched Pareto Genetic Algorithm
NSES	Non-dominated Sorting Evolution Strategy
NSF	National Science Foundation
NSGA	Non-dominated Sorting Genetic Algorithm
NSGA-II	Fast Elitist Non-dominated Sorting Genetic Algorithm
OHC	Occupancy Hazard Classification
PAES	Pareto Archived Evolutionary Strategy
PGD	Permanent Ground Displacement
PGV	Peak Ground Velocity
P_LP	Probability of Intentional Attack on Likely Pipes
RAM-W	Risk Assessment Methodology for Water Utilities
SPEA	Strength Pareto Evolutionary Algorithm
US	United States

USEPA United States Environmental Protection Agency

WDS Water Distribution System

TABLE OF CONTENTS

	Page
ABSTRACT.....	iii
DEDICATION.....	v
ACKNOWLEDGMENTS.....	vi
NOMENCLATURE.....	viii
TABLE OF CONTENTS.....	xi
LIST OF FIGURES.....	xiv
LIST OF TABLES.....	xviii
1. INTRODUCTION.....	1
2. VULNERABILITY, RISK, AND MITIGATION ASSESSMENT OF WATER DISTRIBUTION SYSTEMS FOR INSUFFICIENT FIRE FLOWS.....	5
2.1. Introduction.....	5
2.2. Water Systems' Vulnerability, Risk, and Fire Flows.....	8
2.3. Water Systems' Failure Scenarios and Estimation of Failure Probabilities.....	10
2.4. Methodology for Vulnerability and Risk Assessment.....	12
2.5. A Dynamic Programming Solution for Vulnerability and Risk Assessment.....	13
2.5.1. Dynamic Programming Algorithmic Attributes.....	15
2.5.2. Formulation of Damage Function.....	16
2.5.3. Total Probability of Failure.....	18
2.5.4. Dynamic Programming Algorithmic Steps.....	20
2.6. Application of Risk-based DP Model to a Case Study.....	20
2.6.1. Description of Data and Estimation of Probabilities.....	21
2.6.2. Application of Risk-based DP Algorithm.....	23
2.6.3. Sensitivity Analysis on the Ratio of Probability of Attack on "likely" Pipe to "unlikely" Pipe.....	25
2.7. Results of Vulnerability and Risk Assessment.....	25
2.7.1. Results at Hydrant HY29.....	26
2.7.2. Results at Hydrant HY66.....	27
2.8. Analysis and Recommendation of Mitigation Strategies.....	31

	Page
2.9. Benefit-cost Analysis for Proposed Mitigation Strategies.....	35
2.10. Final Remarks.....	38
3. A MULTI-OBJECTIVE EVOLUTIONARY COMPUTATION APPROACH TO HAZARDS MITIGATION DESIGN FOR WATER DISTRIBUTION SYSTEMS.....	40
3.1. Introduction.....	40
3.2. Problem Statement.....	42
3.3. Multi-objective Evolutionary Algorithms.....	44
3.4. Non-dominated Sorting Evolution Strategy (NSES).....	45
3.4.1. Representation.....	46
3.4.2. Mutation.....	49
3.4.3. Selection.....	50
3.4.4. Non-dominated Sorting.....	50
3.4.5. Crowding Distance Estimation.....	51
3.5. Performance Measure of NSES Algorithm.....	51
3.5.1. Measure of Diversity.....	53
3.5.2. Measure of Pareto Optimality.....	57
3.6. Application of NSES to Water Distribution System Problem.....	59
3.7. Results.....	62
3.7.1. Algorithmic Parameters.....	62
3.7.2. Algorithmic Convergence.....	63
3.7.3. Comparison of Non-dominated Solutions.....	65
3.8. Sensitivity to Variation in Water Distribution System's Fireflow Locations.....	69
3.9. Final Remarks.....	73
4. A STOCHASTIC MODELING APPROACH FOR URBAN FIRE RISK ANALYSIS INCLUDING PERFORMANCE OF WATER AND FIRE RESPONSE INFRASTRUCTURES.....	77
4.1. Introduction.....	77
4.2. Computerized Fire Models.....	81
4.3. Components of Urban Fire Risk Assessment.....	83
4.3.1. Building Ignition Frequency.....	84
4.3.2. Wind Properties.....	85
4.3.3. Water System Failure Probabilities.....	86
4.3.4. Determination of Fire Consequences.....	88
4.3.5. Estimation of Urban Fire Risk.....	89
4.4. Application of Urban Fire Risk Assessment Methodology to a Coupled Water and Fire Model.....	92

	Page
4.4.1. Description of Data and Estimation of Probabilities.....	92
4.4.2. Evaluation of Fire Consequences.....	96
4.5. Analyzing and Characterizing the Results.....	97
4.6. Managing Urban Fire Risk for the Case Study.....	106
4.6.1. Model Formulation.....	107
4.6.2. Implementation of NSES to Mitigate WDS Fire Damages....	109
4.6.3. Mitigation Results.....	112
4.7 Final Remarks.....	117
5. SUMMARY AND CONCLUSIONS.....	122
REFERENCES.....	128
VITA.....	135

LIST OF FIGURES

FIGURE		Page
2.1	Building map of Micropolis with water distribution network shown with thin lines, sources shown with black squares, “likely” pipes for intentional attack with black thick dotted lines, and hydrants included in the vulnerability and risk analysis indicated with stars....	22
2.2	Number of failures versus risk at hydrant HY29 with fire flow = 31.5 l/s (500 gpm).....	26
2.3	Number of failures versus risk at hydrant HY29 with fire flow = 31.5 l/s (500 gpm).....	27
2.4	Results at hydrant HY29 for maximum failure number $X_{max} = 5$ and ratio of probability of attack on “likely” pipes to “unlikely” pipes $\eta = 5$, vulnerable pipes (decision variables) shown in solid blue lines for $P_{LP} = 0.1$, vulnerable pipes (decision variables) shown in solid red lines for $P_{LP} = 0.2$, and “likely” pipes for intentional attack shown in black thick dotted lines.....	28
2.5	Number of failures versus risk at hydrant HY66 with fire flow = 31.5 l/s (500 gpm).....	29
2.6	Number of failures versus risk at hydrant HY66 with fire flow = 31.5 l/s (500 gpm).....	29
2.7	Results at hydrant HY66 for maximum failure number $X_{max} = 5$ and ratio of probability of attack on “likely” pipes to “unlikely” pipes $\eta = 5$, vulnerable pipes (decision variables) shown in solid blue lines for $P_{LP} = 0.2$, vulnerable pipes (decision variables) shown in solid red lines for $P_{LP} = 0.4$, and “likely” pipes for intentional attack shown in black thick dotted lines.....	30
2.8	Mitigation designs for Micropolis water distribution system.....	33
2.9	Number of failures versus risk at hydrant HY29 with low cost mitigation for accidental failure (mitigation package 1) with $P_{LP} = 0.02$ and $\eta = 5$	34

FIGURE	Page	
2.10	Number of failures versus risk at hydrant HY29 with low cost mitigation for intentional failure (mitigation package 3) with $P_{LP} = 0.6$ and $\eta = 5$	34
3.1	Flowchart for NSES	47
3.2	Chromosome representation.....	48
3.3	Crowding distance estimation in NSGA-II	52
3.4	Pareto optimal solutions obtained with NSES for MOP2.....	55
3.5	Pareto optimal solutions obtained with NSES for MOP4.....	55
3.6	Mean of the deviation metric Δ obtained for each of the test problems is shown in column graph, standard deviation of the deviation metric Δ is shown with error bar, lower value of Δ indicates better performance.....	56
3.7	The calculation of ‘Hypervolume’ in NSES for the test problem MOP2 using LebMeasure algorithm; solutions on the Pareto front are shown in black dots; each rectangle represents incremental hypervolume in the non-dominated objective space contributed by each point on the front; the worst point is (1,1).....	58
3.8	Building map of Micropolis with water distribution network shown with thin lines	61
3.9	Convergence of NSES for multi-objective water distribution system problem in terms of hypervolume metric.....	64
3.10	Convergence of NSES for multi-objective water distribution system problem in terms of number of non-dominated solutions.....	64
3.11	X-Y-Z scatter plot of the Pareto-optimal solutions for the WDS after 150 generations, the WDS performance at existing condition is shown with a black square, solutions chosen for further discussion are enclosed in circles.....	66
3.12	Results (decision variables) of application of NSES to the multi-objective WDS problem.....	68

FIGURE	Page
3.13	Sensitivity analysis of application of NSES to the multi-objective WDS problem with six hydrant arrangements..... 70
3.14	X-Y-Z scatter plot of the Pareto-optimal solutions for the WDS with six hydrant arrangements after 150 generations, the WDS performance at existing condition is shown with a black square, solutions chosen for further discussion are enclosed in circles..... 72
4.1	Methodological steps in urban fire risk analysis..... 80
4.2	Flowchart for Monte Carlo procedure to evaluate scenario risk..... 91
4.3	Building map of Micropolis with WDS shown in thin lines, water sources are shown in black squares, and fire hydrants are shown in black dots..... 93
4.4	Histogram of fire consequences conditioned on ignition for Micropolis..... 98
4.5	Gamma fitted distribution of consequences not conditioned on ignition for Micropolis..... 99
4.6	Building map of Micropolis with fire spread profile for highest risk scenario (scenario-1)..... 104
4.7	Building map of Micropolis with WDS shown in thin lines and water quality monitoring locations are shown in black dots..... 110
4.8	X-Y-Z scatter plot of the Pareto-optimal solutions for the hydrant set-1 after 350 generations, the WDS performance at existing condition is shown with a square..... 113
4.9	X-Y-Z scatter plot of 15 Pareto-optimal solutions in fireflow-cost-water quality space (hydrant set-1), the WDS performance at existing condition is shown with a square..... 115
4.10	X-Y-Z scatter plot of the Pareto front in scenario risk-cost-water quality space (hydrant set-1), the WDS performance at existing condition is shown with a square..... 115
4.11	X-Y-Z scatter plot of 10 Pareto-optimal solutions in fireflow-cost-water quality space (hydrant set-2), the WDS performance at

FIGURE		Page
	existing condition is shown with a square.....	118
4.12	X-Y-Z scatter plot of the Pareto front in scenario risk-cost-water quality space (hydrant set-2), the WDS performance at existing condition is shown with a square	118

LIST OF TABLES

TABLE		Page
2.1	Benefit-cost Comparison for Proposed Mitigation Strategies for 2 Failed Pipes.....	36
2.2	Benefit-cost Comparison for Proposed Mitigation Strategies for 4 Failed Pipes.....	37
3.1	Multi-objective Test Problems Where n Denotes the Number of Decision Variables.....	53
3.2	Comparison of Solutions in Fireflow Water Quality Cost Objective Space.....	67
3.3	Comparison of Pareto-optimal Solutions from Sensitivity Analysis...	72
4.1	Parameters of the Generalized Barrois Model Fitted to Observations in Finland (Tillander and Keski-Rahkonen 2002).....	85
4.2	Annual Frequency Distribution of Wind Direction	95
4.3	Highest Risk Scenarios for Micropolis Generated from Monte Carlo Analysis	101
4.4	Scenarios Involved Pipe Failures for Micropolis Generated from Monte Carlo Analysis.....	103
4.5	Comparison of Pareto-optimal Solutions in the Objective Space for Hydrant Set-1.....	114
4.6	Comparison of Pareto-optimal Solutions in the Objective Space for Hydrant Set-2.....	117

1. INTRODUCTION

Water systems have been identified as one of the United States' critical infrastructures (White House 2003) and are vulnerable to various threats caused by natural disasters or malevolent actions (such as terrorist attack, vandalism, or insider sabotage). Water supply infrastructure is also strongly connected to the critical infrastructures of energy, public health, chemical industry, agriculture and food, and emergency services such as fire response. Thus, any potential damage in water supply infrastructure would be a threat to those infrastructures as well, and vice versa.

The primary goals of urban water distribution systems are to provide water to consumers with adequate quantity and with acceptable quality. Water systems also play a critical public safety role: delivering water in emergency conditions such as pipe failure, power outage, and fire. Thus water systems planning and management offer numerous challenges to water utilities, affiliated decision makers, and regulators throughout the country. Effective planning and management of the system helps in achieving both the primary goals of the system and better security against natural and manmade hazards. For many years significant studies have been performed to recognize and manage the threats toward water systems; however, much recent attention has focused on chemical and biological threats.

This dissertation follows the style of *Journal of Water Resources Planning and Management*.

This dissertation addresses a subject area within two critical infrastructures – water and emergency services – which is currently underdeveloped: the risk and consequences of and effective mitigation strategies for urban fire events. Most urban fire services depend upon the fire suppression capacity of urban water distribution systems (WDS). However, the hydraulic behavior of WDS's is complex, and the occurrence of fire events is variable yet uncertain.

The objective of this research is to development of a risk-based optimization methodology to analyze the vulnerability and risk of water utilities; and to design mitigation for urban fire events for both water and fire response infrastructure. This new approach generates a risk-based WDS vulnerability assessment tool, a set of Pareto-optimal WDS fire mitigation designs, and a set of Pareto-optimal risk management plans for urban fire events. The desired outcome of this project is to serve as a guide for utilities, emergency response personnel, and affiliated decision makers to address and assess urban fire risk and appropriate risk management strategies. The specific goals of this research are to:

- Develop a risk-based optimization model to assess vulnerability and risk to a water distribution system against possible fire events;
- Develop a new evolutionary algorithm-based multi-objective modeling framework to mitigate WDS's fire damage;
- Develop a stochastic modeling framework of risk analysis for simulating fire damage consequences from urban fire spread model; and

- Develop a multi-objective simulation-optimization framework to mitigate and manage urban fire risk.

A risk based dynamic programming (DP) modeling approach is developed to identify the critical components of a water distribution system during fire events under three failure scenarios: (1) accidental failure due to soil-pipe interaction, (2) accidental failure due to a seismic activity, and (3) intentional failure or malevolent attack. The risk analysis framework is used to understand the changing nature of system vulnerability versus failure causes. The risk associated with the failure of each component under the above mentioned failure scenarios along with the corresponding damage consequences can help utility managers understand the value of risk mitigation.

A new evolutionary algorithm (EA) based multi-objective technique, Non-dominated Sorting Evolution Strategy (NSES), is developed for systematic generation of optimal mitigation strategies for urban fire events. A WDS hydraulic simulation model is coupled with this evolutionary multi-objective modeling framework to mitigate vulnerability and risk with three competing objectives: (1) minimizing fire damages, (2) minimizing water quality deficiencies, and (3) minimizing the cost of mitigation. This multi-objective approach produces a set of Pareto-optimal solutions in the objective-space of fire damage, water quality, and cost that helps utility managers understand the trade-offs between those objectives.

Finally, an urban fire risk assessment methodology is developed by introducing a stochastic modeling approach. Three major fire variables: ignition, wind direction, and water system's failure, are considered during this analysis by introducing both fire

hazard and wind direction probabilities and an actual WDS failure scenarios along with their failure probabilities. A coupled model of water and fire response infrastructure is utilized to evaluate the fire consequences in terms of building specific data such as number of people displaced and cost of property damage. A Monte Carlo simulation is utilized to generate all possible fire scenarios as well as the distribution of consequences. Finally, fire mitigation strategies are developed based on scenario-based results using an evolutionary multi-objective optimization framework to manage the system wide urban fire risk.

The above described research is presented here as three sections written as journal articles that illustrate the methodological developments, applications, and results. The vulnerability and risk assessment procedure of WDS for insufficient fire flows is presented in Section 2. Section 3 illustrates the development of a novel multi-objective approach (NSES) to mitigate urban fire events for WDS. Section 4 describes the development of a stochastic modeling framework for fire hazard and fire risk assessment methodology by utilizing a coupled model of water and fire response infrastructure. Finally, Section 5 presents conclusions based on the whole body of the dissertation and potential future areas of research.

2. VULNERABILITY, RISK, AND MITIGATION ASSESSMENT OF WATER DISTRIBUTION SYSTEMS FOR INSUFFICIENT FIRE FLOWS

2.1. Introduction

Water systems have been identified as one of the United States' critical infrastructures (White House 2003) and are naturally vulnerable to physical, chemical/biological, and cyber threats. These threats towards water systems had been recognized long before September 11, 2001 and the water utility industry had taken some security measures against such threats, but not as many as since September 11, 2001. Water infrastructure is also strongly connected to the critical infrastructures of energy, public health, chemical industry, agriculture and food, and emergency services such as fire response. Thus, any potential damage in water infrastructure would be a threat to those infrastructures as well, and vice versa. The present study of vulnerability, risk, and mitigation assessment for water distribution systems is motivated by the need to determine the most critical components of a water distribution system during fire events and the risks associated with those system components.

Typically, vulnerability means susceptibility to damage; therefore vulnerability analysis can be defined as the process that identifies the risk areas and the mechanisms by which potential damages can occur without considering the likelihoods of damages. Risk, on the other hand, is the “combination of the probability of an event and its consequence” (ISO 2001). Traditionally, the process of risk analysis has three core

elements – risk assessment, risk management, and risk communication (National Research Council 1994). Thus risk assessment is the systematic analysis to identify probabilities and magnitudes of losses to the recipients from failures involving natural and/or manmade events; risk management is the process of minimizing the assessed risk; and risk communication is the process of exchanging and sharing the risk information between stakeholders and decision makers (Modarres 2006).

Vulnerability analysis for water systems has been a topic of intense study in recent years. Haines et al. (1998) recognized the potential threats against water supply systems as physical threats, chemical/biological threats, and cyber threats and proposed a methodology to reduce the vulnerability by hardening of water systems based on the philosophy of Hierarchical Holographic Modeling (HHM) (Haines 1981). Haines (2002) proposed a strategic plan combined with the hardening of the water supply system by applying a well planned maintenance program and by standardizing the components of water supply and distribution systems. The HHM philosophy was also adopted by Ezell et al. (2000) in development of the probabilistic Infrastructure Risk Analysis Model to identify, assess, and manage risks to infrastructure. Tidwell et al. (2005) proposed an alternative approach of threat assessment of water supply systems using Markov Latent Effect modeling in which an assessment score was obtained to provide a measure of the credibility of a threat. Lewis (2006) developed a comprehensive method to analyze infrastructure vulnerability in different sectors called Model Based Vulnerability Analysis (MBVA) and thereby suggested a method of allocating limited resources to improve infrastructure security and to reduce the risks.

The United States Environmental Protection Agency (USEPA), in association with American Water Works Association Research Foundation (AWWARF) and the U.S. Department of Energy's Sandia National Laboratories, developed Risk Assessment Methodology for Water Utilities (RAM-W) to identify water system vulnerabilities and thereby to determine the level of security needed to reduce risk (AWWARF and Sandia National Laboratories 2002).

The studies cited above have taken a somewhat generic approach to vulnerabilities, but others have used an approach focused on more specific threats and consequences. Ostfeld and Salomons (2004) presented a methodology applying a genetic algorithm to find the optimum locations for a set of monitoring stations, called an early warning detection system, in a distribution network to detect accidental or deliberate intrusions of harmful chemicals and microorganisms to the water distribution system. Al-Zahrani and Moied (2001), among others, performed a similar study. Skolicki et al. (2006) used an evolutionary computation-based approach to identify vulnerable distribution system components with loss of nodal service pressures used as an assessment criterion.

This article departs from previous studies in its emphasis on firefighting flows provided by the water distribution system. The main goal of this research is to extend the basic knowledge of vulnerabilities in the water systems during occurrence of fire and to incorporate the risk associated with the water system failure for fire events in decision making processes to address potential problems. The specific goals of this research are to:

- Develop a methodology to examine the vulnerability and risk to water distribution systems during urban fire events;
- Develop strategies to mitigate the assessed risk to water distribution systems; and
- Examine the effectiveness of proposed mitigation strategies using benefit-cost analysis.

2.2. Water Systems' Vulnerability, Risk, and Fire Flows

Water systems are generally constructed to provide sufficient water to the users with specific pressure, volume, and quality. These systems consist of various physical components for example, pipes, valves, junctions, pumps, elevated storage tanks, water treatment plants, etc. To ensure safe delivery to water users, water systems are generally designed to fulfill base demands with additional capacity for emergency demand conditions such as broken pipes and valves, firefighting demands, pump and power outages, etc. (Mays 2004). These types of emergency demand conditions might arise because of mechanical failure of the system during a natural disaster or due to intentional attacks. In such conditions the system might not deliver water to end users with sufficient flow and/or pressure. Local design requirements vary, but a typical set of standards is that of the cities of Bryan and College Station, Texas, where under normal conditions, a static pressure of 241.3 kilonewtons per square meter (kN/m^2) (35 pounds per square inch [psi]) is maintained throughout the system under normal conditions, and a minimum of 137.9 kN/m^2 (20 psi) pressure is to be maintained throughout the system during fire flow events (Cities of Bryan and College Station [BCS] 2005); with this

minimum pressure requirement a flowrate of 63 liters per second (l/s) (1,000 gallons per minute [gpm]) is required at fire hydrants serving single family residential buildings, and a flowrate of 158 l/s (2,500 gpm) is required at hydrants for multi-family residential/commercial/industrial buildings during fire flow events (BCS 2005). The minimum pressure requirement is needed to overcome head losses between hydrants and fire-engine pumps (Mays 2004). Additional fire flow information is included in AWWA (1998) and Mays (2000), among others.

Water systems can be viewed as a collection of links connected to the nodes (Rossman 2000). The performance of the system depends upon the performance of the individual system components. To ensure reliable delivery of water for fire fighting and other uses, water mains are generally constructed in a grid pattern so that if a single section fails, the damaged section can be isolated and the remainder of the system will still provide adequate flows and pressures at hydrants and other demand locations. However, if multiple segments fail the water distribution system may not include sufficient redundancy to ensure adequate service conditions. Thus, the process of vulnerability assessment is one of identifying critical combinations of system failures that impair the water system from meeting its designed capacity.

While vulnerability assessment identifies the potential risk areas, risk assessment measures probabilities and magnitude of losses to recipients. Traditionally, risk assessment addresses four basic questions: (1) what can go wrong? (2) how likely is it? (3) what are the consequences if it does go wrong? (4) how certain is this knowledge? (Stern and Fineberg 2003). Thus the first step in WDS's risk assessment would be

identification of failure scenarios during fire events; the second step would be estimation of probabilities for identified failure scenarios; the third step would involve estimation of potential losses during fire due to failure of the water system's ability in delivering fire fighting flows; and the last step would be analysis of uncertainty. The following sections describe in detail the specific steps to accomplish the vulnerability and risk assessment for WDS during urban fire events, implementation of the proposed methodology to a case study, and results.

2.3. Water Systems' Failure Scenarios and Estimation of Failure Probabilities

In WDS vulnerability and risk assessment the first two steps are identification of all possible failure scenarios and estimation of the corresponding failure probabilities. During this analysis, three failure scenarios are considered for examining vulnerability and risk to water distribution system during fire events: (1) accidental failure due to soil-pipe interaction, (2) accidental failure due to a seismic event, and (3) malevolent actions or terrorist attack.

Deterioration of pipes due to aging often cause pipe breaks and leaks and has been a major concern of water utility industries. Yamijala et al. (2009) proposed a logistic generalized linear model (logistic GLM) for estimating the probability of pipe breakage due to soil-pipe interaction. Using historical (2000-2005) pipe break data from a major U.S. city, they developed a statistical model to estimate the probability of pipe failure for a water distribution system. The results from their analysis showed that the variables that are statistically significant at a level of 5% for the studied system were: (1)

pipe diameter, (2) pipe material, (3) pipe length, (4) land use type, and (5) soil type. For any given water system with known soil profile and zoning data, the likelihood of pipe failure at least once in a five year period caused by soil-pipe interaction for each individual pipe in the system can be estimated using the logistic GLM (Yamijala et al. 2009). Hence, in this article the logistic GLM (Yamijala et al. 2009) is used to estimate pipe failure probabilities due to pipe aging.

Seismic wave propagation often causes transient soil deformation and can produce well-dispersed damage to buried pipelines (Eidinger 2005). Studies showed that pipes that are made of cast iron or asbestos cement perform poorly during seismic events; ductile iron pipes, being more durable than cast iron, generally perform better than the other two. The level of ground shaking at any pipeline location is generally measured in terms of peak horizontal ground velocity (PGV). When the soil mass experiences long duration strong ground shaking, then landslides or liquefaction occurs and causes severe damage to the pipes. The amount of landslide or liquefaction movement is generally measured in terms of permanent ground displacement (PGD). Eidinger (2005) developed a set of fragility curves using available pipe damage data from historical earthquakes. These curves are expressed as repair rates per unit length of pipe, and as a function of peak ground velocity (PGV) or permanent ground deformation (PGD). The pipe damage algorithm or fragility curves (Eidinger 2005) are expressed as:

$$RR = K_1 * (0.00187) * PGV \text{ (for wave propagation)} \quad (2.1)$$

$$RR = K_2 * (1.06) * PGD^{0.319} \text{ (for permanent ground deformation)} \quad (2.2)$$

where, RR = repairs per 1000 ft (305 m) of main pipe; PGV = peak ground velocity in inch/second (1 inch = 0.0254m); PGD = permanent ground deformation in inch (0.0254m); K_1 = ground shaking constants for fragility curve; and K_2 = permanent ground deformations constants for fragility curve. The constants K_1 and K_2 vary with different pipe material, joint type, soil, and pipe diameter. Detailed list of values for K_1 and K_2 can be found in Eiding (2005). In this article only ground shaking hazard is considered, hence, equation (2.1) is applied.

Intentional attacks have been a major concern in the U.S. since the events of September 11, 2001. Although the threat of terrorist attacks to water supply systems have been well-studied and documented both before and after September 11, 2001, the probability of occurrence of a potential terrorist attack on water infrastructure is impossible to predict and difficult to estimate. Thus a parametric approach is conceived to estimate the risks. Detailed description of this approach is discussed in section 2.6.1.

2.4. Methodology for Vulnerability and Risk Assessment

The next step in traditional risk assessment procedure is consequences evaluation. Any inadequacy or diminished capacity of the WDS due to system failure would lead to severe consequences during fire events such as loss of homes, loss of businesses, loss of lives, or all of the above. Thus the consequences can be expressed in terms of WDS performance during critical combination of system failure. Therefore, assessed risk to WDS would be the product of probability of component failure and the diminished system performance. This problem of vulnerability and risk assessment for

water distribution system can be viewed as an optimization problem which maximizes the system risk during urban fire event caused by failure or disruption of specific system components. Mathematically the problem can be formulated as follows:

$$\text{Maximize } R = J(U | D, \text{hydraulics}) * P(U) \quad (2.3)$$

where, R = system risk; J = a damage function calculated on the basis of pressure and/or flow at an active fire hydrant node; U = set of damaged system components (decision variables); D = set of non-firefighting demands imposed on the water system and the fire flow needed at an active hydrant; *hydraulics* = the governing physical principles on the water supply system; and $P(U)$ = total probability of failure for the set of decision variables under all three failure scenarios.

Along with the objective function in Eq. (2.3), a constraint on the problem is the maximum number of component failures that may be included in U , which is representative of a number of pipe failures due to physical attacks and/or accidents.

2.5. A Dynamic Programming Solution for Vulnerability and Risk Assessment

The proposed model is formulated in an optimization-simulation framework where an optimal solution to the problem is achieved by interfacing the dynamic programming (DP) optimization model (Mays 1996) with a hydraulic simulation model, EPANET 2.0 (Rossman 2000). The hydraulic simulation model is used to solve the pipe hydraulics to evaluate the objective function at each iteration.

“Dynamic Programming transforms a sequential or multistage decision problem that may contain many interrelated decision variables into a series of single stage problems, each containing only one or a few variables” (Mays 1996). Thus the DP procedure is recursive which includes the following attributes (Mays 1996):

- Each problem can be disintegrated into a sequence of single-decision problems at various stages (points where decisions are made).
- Each stage has a number of feasible state variables that connect the subsequent stages.
- The decision at each stage transforms the current state into some state at the next stage through the state transition function.
- The optimal policy at any stage is independent of the strategies adopted at antecedent stages.
- A recursive relationship is developed to choose the best solution from state to state across the stages.

Classical optimization techniques such as Linear Programming, Dynamic Programming, Lagrange Multiplier, and Gradient Method, among others, are commonly used in many hydrosystems application. However, the proposed methodology is developed by utilizing a DP-based optimization technique for two primary reasons: (1) identifying the most critical components of a water supply system (i.e., those whose failure maximizes the risk) can be considered as a multistage decision problem, which is DP's forte; and (2) the hydraulics of pipe networks include significant non-linearities

that would prohibit application of other techniques, but to which DP is immune. The structure and implementation of DP to the WDS problem are described below.

2.5.1. Dynamic Programming Algorithmic Attributes

The DP decision variables correspond to the elements of the system which are to be damaged or fail (U in Eq. 2.3). It is obvious that failure of a pump station or elevated storage tank would likely cause maximum damage to the system, and consequence determination would be a matter of straightforward hydraulic simulation. On the other hand, failure of multiple pipes in the system to cause maximized risk is a more complex matter of multistage decisions. Therefore, only water mains are considered in this study as potential failure elements, and the decision variables are defined as binary decisions of damage/no damage for each pipe in the system. The stages of the DP solution are defined as the pipes for which a decision variable must be determined. Thus, if there are 500 pipes in a water system model, 500 stages would exist, and 500 decision variables would need to be determined. Thus,

$$u_k = \begin{cases} 0, & \text{if pipe } k \text{ is undamaged / does not fail} \\ 1, & \text{if pipe } k \text{ is damaged / fails} \end{cases} \quad (2.4)$$

where, k = index on system stage; u_k = decision variable at stage (pipe) k .

With system stages defined as progression through damage/failure decisions for each system pipe, system state at a given stage is defined as the cumulative number of

positive damage/failure elements (i.e., the cumulative sum of this and all previous decision variables). A terminal constraint on state value is needed to reflect the maximum number of damaged/failed pipes that should be considered, and an initialization constraint is required to begin accumulation at zero. The state transition function, initialization constraint, and terminal constraint, respectively, are thus:

$$X_k = X_{k-1} + u_k \quad (2.5)$$

$$X_0 = 0 \quad (2.6)$$

$$X_N \leq X_{max} \quad (2.7)$$

where, X_k = state variable at stage k ; X_0 = state variable at “zero-th” stage; N = number of stages; X_N = state variable at final stage; and X_{max} = maximum number of damaged/failed pipes to be considered.

As discussed above, fire flow requirements include both pressure and flow criteria. The damage function J is thus formulated and described below.

2.5.2. Formulation of Damage Function

To determine the available flow at an active fire hydrant node during a fire event, the pressure at that node is fixed at its minimum allowable value (as discussed above, 137.9 kN/m² [20 psi]) and available flow is determined using the hydraulic model. In the hydraulic model, the flow through a fire hydrant can be modeled at fixed pressure by specifying the node to be an “emitter” (Rossman 2000), i.e., a discharge of water to the

atmosphere through an open orifice. Flow through an emitter is proportional to the square root of pressure available at that node:

$$Q_{em} = C_{em} \sqrt{P_{em}} \quad (2.8)$$

where, Q_{em} = flow through the emitter (l/s or gpm); P_{em} = available pressure at the emitter node (kN/ m² or psi); and C_{em} = emitter discharge coefficient [l/s/(kN/ m²)^{0.5} or gpm/psi^{0.5}] (Rossman 2000). To determine the maximum flow available at a fire hydrant, the available pressure is assumed to be 137.9 kN/ m² (20 psi), and a discharge coefficient for that emitter is determined according to the hydrant's physical characteristics. For a 25.4 cm (10 in) diameter connection fire hydrant $C_{em} = 44.5$ l/s/(kN/ m²)^{0.5} (1850 gpm/psi^{0.5}), and for a 7.62 cm (3 in) diameter connection $C_{em} = 4.01$ l/s/(kN/ m²)^{0.5} (166.5 gpm/psi^{0.5}). Then a single period hydraulic simulation is performed, and the free orifice flow at the hydrant is determined. The maximum available flow at the fire node is the emitter flow minus any base demand (Rossman 2000); that is, if normal consumer demands were also associated with a node, they would be subtracted to find the flow available exclusively for fire fighting. The damage function J is thus calculated as:

$$J = \begin{cases} \alpha \frac{Q_{req} - Q_{available}}{Q_{req}} + \beta \frac{L_{operable}}{R_{max}}; & \text{if } Q_{available} < Q_{req} \\ 0; & \text{if } Q_{available} = Q_{req} \\ \frac{Q_{req} - Q_{available}}{Q_{req}}; & \text{if } Q_{available} > Q_{req} \end{cases} \quad (2.9)$$

where, Q_{req} = required flow for firefighting according to regional fire code; $Q_{available}$ = maximum net available flow at fire node from hydraulic simulation.

The rationale behind the formulation in Eq. (2.9) is to indicate “damage” as positive when available flows are less than required at the active fire hydrant, and that damage value is amended by a normalized distance to the nearest operable backup hydrant. If more than the required flow is available, the “damage” value is negative. Negative damage values indicate residual flow capacity at the hydrant. To transform this damage function to a more tangible quantity, potential property losses can be calculated as the product of the damage function and total building replacement cost within some radius of the hydrant under analysis. In this study, a radius of 244 m (800 ft) was used.

2.5.3. Total Probability of Failure

The estimation of $P(U)$ involves both event tree and fault tree analysis (Pate-Cornell 1984). The three failure scenarios discussed in section 2.3 are broadly grouped into two independent events: (1) accidental failure, which involves both soil-pipe interaction and seismic activity, and (2) intentional failure. Considering the case of accidental failure, a pipe k can fail either due to aging (i.e., soil-pipe interaction) or due to seismic activity. If there is an earthquake, the pipe k is more susceptible to failure due to earthquake than due to soil-pipe interaction; if there is no earthquake, the only accidental failure mode is soil-pipe interaction. The sequence of failure of a set of pipes (decision variables) linked by conditional probabilities of an earthquake event was modeled using an event tree. Assuming the accidental failures (due to soil-pipe

interaction and seismic event) are independent of intentional failures, the failure probability due to all three failure modes for a set of pipes was modeled using a fault tree (Pate-Cornell 1984).

The DP solution algorithm defined in the equations above is implemented in a computer code that utilizes iterative solution of the water distribution system hydraulics as each stage's decision variable is evaluated under the constraint values defined in Eq. (2.5) through Eq. (2.7). The EPANet Programmer's Toolkit (Rossman 1999) was used in a Microsoft Visual Basic 6.0 code for this purpose. At each stage, flows and pressures in the distribution system are solved for both possible values of the decision variable, and the decision variable value maximizing the objective function is retained. Computation of the DP solution for a given set of constraints produces several outputs: the optimal decision set U^* ($= [u_1^*, u_2^*, \dots]$) that represents the set of pipes whose collective failure maximizes the risk; a total probability of failure value, $P(U^*)$, for the optimal decision set; a maximized risk value, R^* ; and operational status of all non-active fire hydrants (i.e., could those hydrants supply needed fire flow at minimum pressure). Thus the optimal decision set U^* represents the vulnerable system components; total probability $P(U^*)$ represents the likelihood of system damage; and the maximized risk value R^* represents the system risk during a specific fire event. Further details on development of the DP algorithm are discussed by Kanta (2006).

2.5.4. Dynamic Programming Algorithmic Steps

The algorithmic steps of the DP procedure are:

Step 1. Initialize the system risk R and the decision set U .

Step 2. Incorporate current decision values, U , into the water model and update the network accordingly. The current decision values include both the previous stages' decisions and the current stage's decision.

Step 3. Run EPANET to obtain damage function J using current values of decision variables U .

Step 4. Calculate total probability of failure value, $P(U)$, for the current decision set U .

Step 5. Calculate system risk using Eq. (2.3).

Step 6. Compute maximum system risk, R^* , by comparing risk values between the current stage and the previous stage. Update the decision set U as the optimal decision set U^* accordingly.

Step 7. If terminal constraint, Eq. (2.7), is satisfied then stop; otherwise, go to Step 2.

2.6. Application of Risk-based DP Model to a Case Study

To demonstrate the vulnerability and risk assessment methodology for WDS fire events, a hypothetical case study was performed for the virtual small town "Micropolis" (Brumbelow et al. 2005, 2007). Detailed description of available data and implementation of the methodology to Micropolis WDS are presented in the following sections.

2.6.1. Description of Data and Estimation of Probabilities

“Micropolis” (Brumbelow et al. 2005, 2007) has an approximate area of 5.2 km² (2 mi²) and a population of 5,000. The city has two major sources of water, a surface-water reservoir and a well field. Water from these sources is treated in a treatment plant. The current version of its water system model consists of a pumping station consisting of 3 pumps, one elevated storage tank, 1088 pipes, 1210 non-hydrant nodes, 52 fire hydrants, and 196 valves (Fig.2.1). Among the 1088 pipes there are 577 water mains and the remaining pipes are service and hydrant connections. In addition to the water distribution system model, there is a detailed building map, a soil map, and a geographic information system (GIS) database for Micropolis that were used throughout the vulnerability, risk, mitigation, and benefit-cost analysis.

From the GIS database of Micropolis and the soil map of the area, the detailed information about pipe diameter, length, pipe material, pipe corrosivity to soil, soil type, and overlying land use data were extracted for each of the 577 water mains. Then using the logistic generalized linear model of Yamijala et al. (2009) the annual probability of failure of each of those 577 pipes was calculated.

To estimate pipe damage due to seismic risks the PGV-dependent model of Eidinger (2005) – Eq. (2.1) – was used. Data from the 1994 Northridge, California, earthquake on PGV values was used to estimate an exponential distribution for PGV. Repair rates for cast iron (CI), asbestos cement (AC), and ductile iron (DI) pipes were estimated using Eidinger’s fragility curves. Ten thousand Monte Carlo (Hasofer et al. 2007) simulations of PGV magnitude were carried on with repair locations randomly

assigned to pipes within each material class. The results of the Monte Carlo simulations were then aggregated to produce a seismic failure probability for each individual pipe.

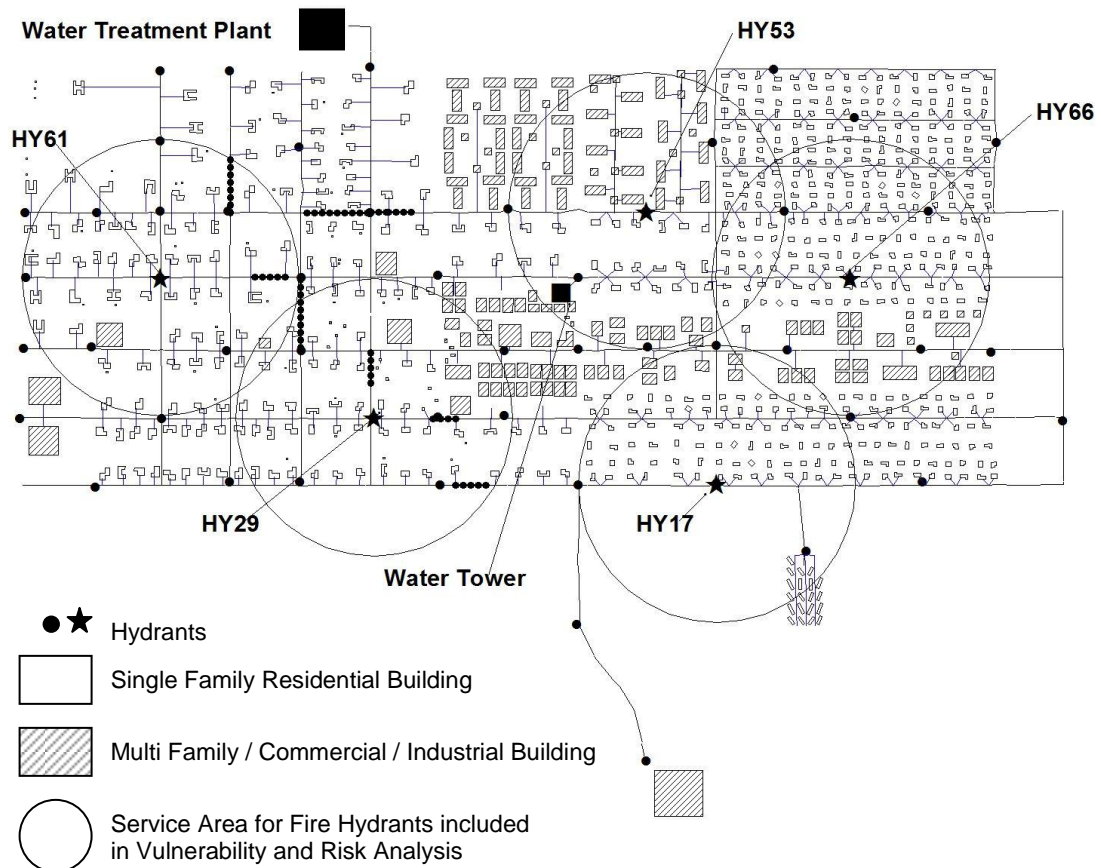


Fig. 2.1. Building map of Micropolis with water distribution network shown with thin lines, sources shown with black squares, “likely” pipes for intentional attack with black thick dotted lines, and hydrants included in the vulnerability and risk analysis indicated with stars

To estimate the probability of pipe failure due to intentional attack a parametric approach was used. The 577 water mains were grouped into: (1) “likely” pipes for terrorist attack, and (2) “unlikely” pipes for terrorist attack. The likely pipes were pipes that are more accessible, unprotected, and/or above ground, such as pipes that run under bridges. Ten pipes were chosen as “likely” pipes, and the rest were assumed to be “unlikely pipes” (Fig.2.1). “Likely” pipes were assumed to have probability of attack as much as η ($\in \{1,2,3,\dots,10\}$) times that of “unlikely” pipes. Probability of failure for the “likely” pipes was set at values of 0.01, 0.02, 0.03, 0.04, 0.05, 0.075, 0.1, 0.2, 0.4, 0.6, 0.8, and 1 in different risk analysis trials to determine the effect of changing likelihood of malevolent attack versus constant probability of accidental failure. A risk threshold was hypothesized as the value of the probability of attack on the “likely” pipes which dominates the intentional failure over accidental failure. A sensitivity analysis was performed with varying η to assess the risk threshold between accidental failure and intentional failure.

2.6.2. Application of Risk-based DP Algorithm

The risk-based DP algorithm defined above is here demonstrated for the case of “Micropolis” (Brumbelow et al. 2005, 2007). To reduce computation time, a subset of 470 mains was selected out of the total of 577 on the basis of the pipe significance index (SI) (Arulraj and Rao 1995). For simplicity of analysis, only a single active fire hydrant is considered at a time in this application, although the specific hydrant is varied. Five fire hydrants throughout the city were selected for intensive analysis. Among these five

hydrants, HY17, HY29, and HY61 are located in single family residential areas; HY53 is located in a multifamily residential area; and HY66 serves both a single family residential area and a commercial/ industrial area of the city of Micropolis. The service areas are circles around each of the five hydrants (Fig.2.1) of radius 244 m (800 ft); it is assumed that a fire inside a service area might lead to the hydrant being tapped for fire suppression. In the analyses, required fire flows at each hydrant were determined on the basis of the surrounding area type and the requirements. Because Micropolis is a small municipal system serving a population of about 5,000, a lesser fire flowrate of 31.5 l/s (500 gpm) was used for analysis (Mays 2000). Minimum residual pressure was 137.9 kN/m² (20 psi) for all hydrants. The maximum search radius R_{max} for a nearby operable hydrant was set at 244 m (800 ft) for all analyses.

Kanta (2006) presents the vulnerability analysis at all five hydrants mentioned above, and those results indicate that the Micropolis water system's fire protection capabilities possess no robustness to attack on or failure of pipe elements, and limited resilience. This observation is not surprising as the system is intended to replicate the imperfect circumstances of a typical small municipal system. The algorithm was applied in an iterative fashion. For each of the five chosen fire hydrant locations, the maximum allowable number of failures (X_{max}) was increased from 1 to a value where the damage function reached a plateau. Values of the weighting coefficients α and β were set at 0.99 and 0.01, respectively through a sensitivity analysis after Kanta (2006). The hydraulic model simulation was performed at 9:00 am in the morning as the demand at that particular time of the day reached maximum.

2.6.3. Sensitivity Analysis on the Ratio of Probability of Attack on “likely” Pipe to “unlikely” Pipe

To understand the changing nature of vulnerability and risk with respect to the ratio of probability of attack on “likely” pipes to “unlikely” pipes, η , a sensitivity analysis was performed with fire at hydrants HY29 and HY66 with varying $\eta \in \{1,2,3,\dots,10\}$. A risk threshold between accidental failure and intentional failure was also noted. From the sensitivity analysis it has been observed that when the hydrant is far away from the “likely” pipes, for instance the case of hydrant HY66, the decisions on vulnerable pipes from the risk-based DP model are insensitive to the ratio η ; and the risk threshold is 0.2 for any value of η . In contrast, the DP solutions based on the active fire hydrants close to the “likely” pipes are quite sensitive to the ratio, η . This is the case of hydrant HY29. In such a case it was observed from the analysis that higher the ratio, η , lower is the risk threshold and vice versa. Moreover, the risk threshold between accidental failure and intentional failure remains 0.2 for $\eta \leq 5$ and decreases with an increase in η . Based on the observation, a value of $\eta = 5$ was used for the subsequent analysis.

2.7. Results of Vulnerability and Risk Assessment

The vulnerability and risk assessment results for hydrants HY29 and HY66 are discussed in detail in the following sections. Kanta (2006) discusses the full set of results of vulnerability analysis (excluding risk) for all five hydrants with fire flow requirements specified by BCS (2005).

2.7.1. Results at Hydrant HY29

System risk versus number of failures at hydrant HY29 are shown in Fig.2.2 and Fig.2.3. A required flowrate of 31.5 l/s (500 gpm) was considered for analysis. The optimal decision set (points of vulnerability) is shown in Fig.2.4.

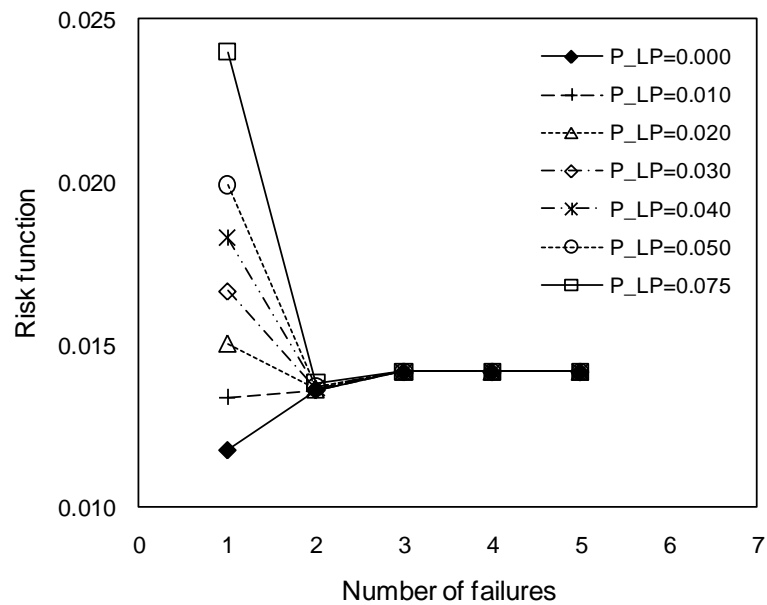


Fig. 2.2. Number of failures versus risk at hydrant HY29 with fire flow = 31.5 l/s (500 gpm)

For a single failure ($X_{max}=1$) the risk function reaches a value 0.011 when the probability of attack on “likely” pipes (P_{LP}) is 0.0. This risk function value for a single failure increases as the probability of attack on “likely” pipes (P_{LP}) increases and reaches its maximum at 0.269 when probability of attack on “likely” pipes (P_{LP}) equals 1.0. As the number of failures increases the system risk value increases with

increase in intentional failure probability and reaches its maximum value at $P_{LP} = 1.0$. From the optimal decision sets (Fig.2.4.) it can be noted that the accidental failure modes dominate solutions when probability of attack on “likely” pipes (P_{LP}) is less than 0.2; the intentional failure modes dominate solutions when P_{LP} equals or exceeds 0.2.

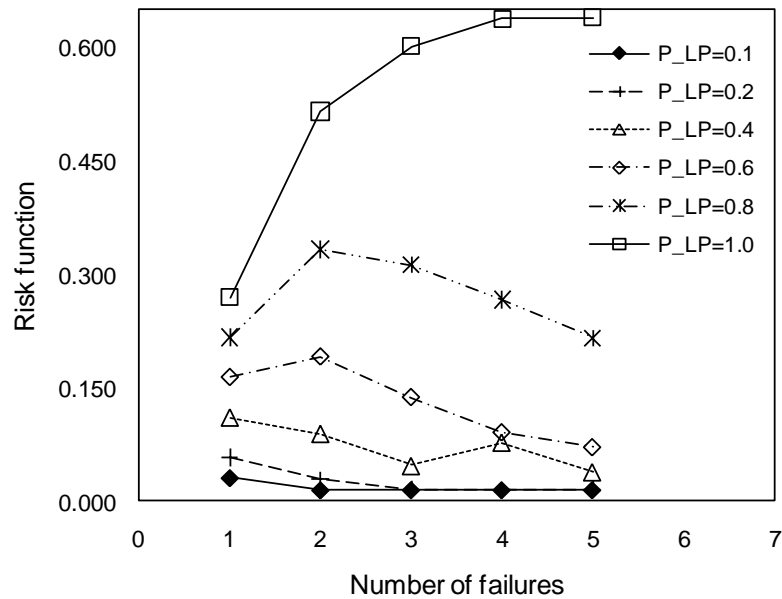


Fig. 2.3. Number of failures versus risk at hydrant HY29 with fire flow = 31.5 l/s (500 gpm)

2.7.2. Results at Hydrant HY66

System risk versus number of failures at HY66 are shown in Fig.2.5 and Fig.2.6 for a required flowrate of 31.5 l/s (500 gpm). The optimal decision set is shown in Fig.2.7.

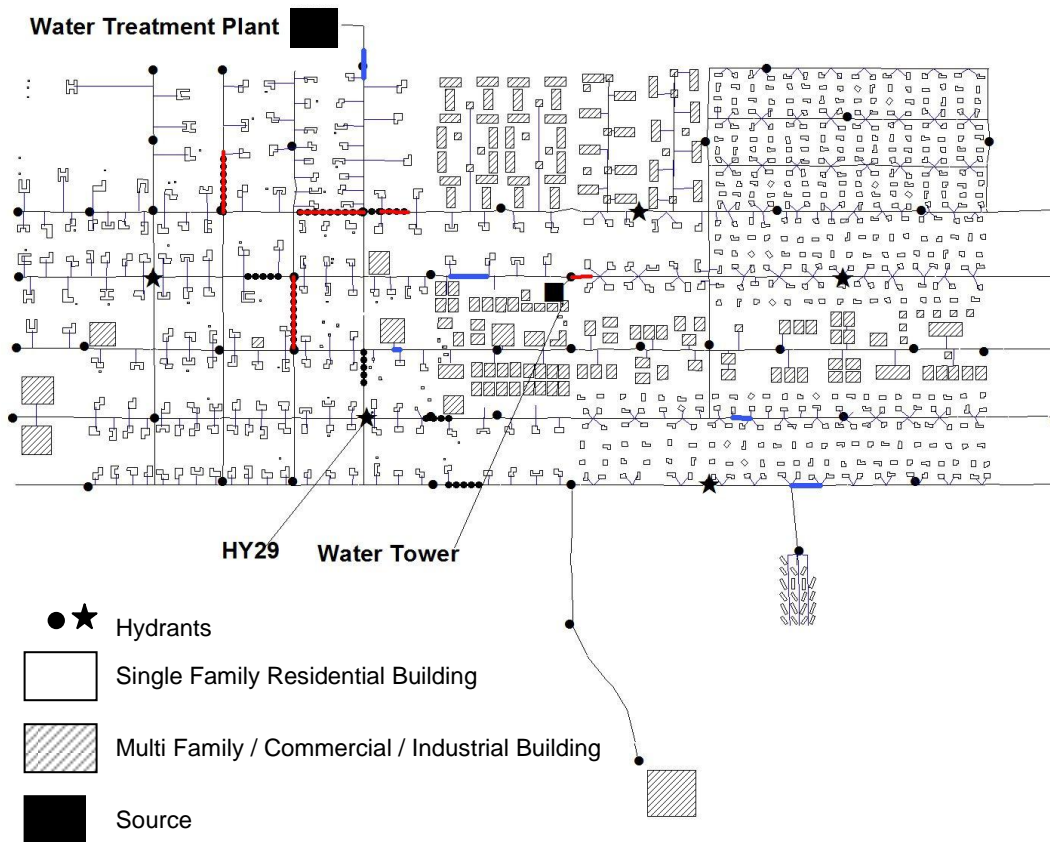


Fig. 2.4. Results at hydrant HY29 for maximum failure number $X_{max} = 5$ and ratio of probability of attack on “likely” pipes to “unlikely” pipes $\eta = 5$, vulnerable pipes (decision variables) shown in solid blue lines for $P_{LP} = 0.1$, vulnerable pipes (decision variables) shown in solid red lines for $P_{LP} = 0.2$, and “likely” pipes for intentional attack shown in black thick dotted lines

Referring to Fig.2.5 and Fig.2.6, for a single failure with probability of attack on “likely” pipes (P_{LP}) equals 0.0, the system risk is 0.011, this risk function value increases as P_{LP} increases and reaches its maximum (0.175) when $P_{LP} = 1.0$. As it

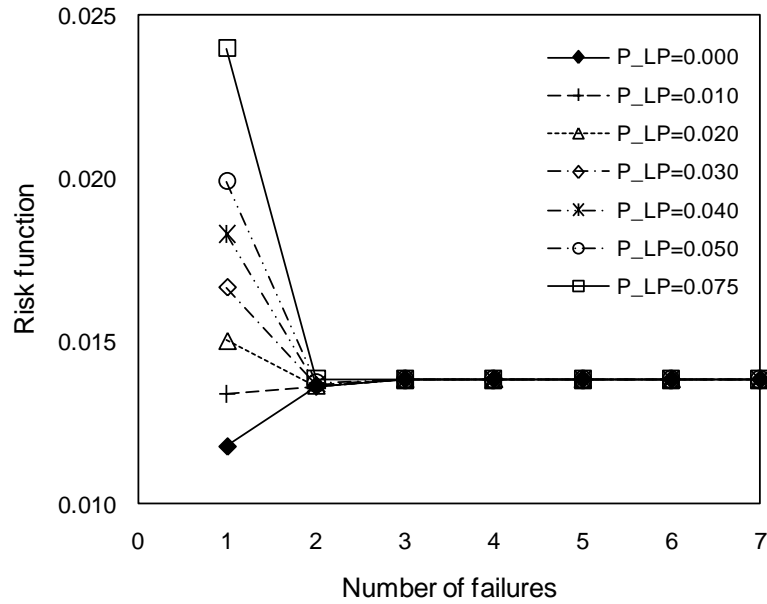


Fig. 2.5. Number of failures versus risk at hydrant HY66 with fire flow = 31.5 l/s (500 gpm)

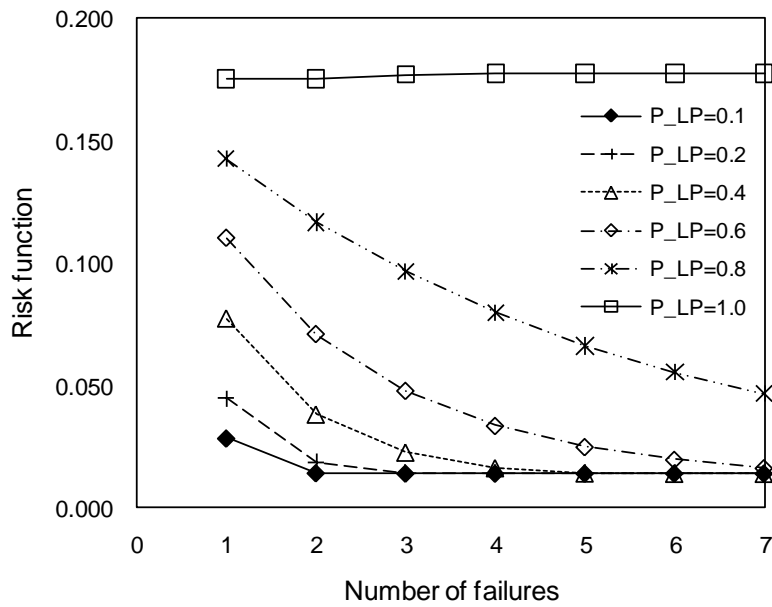


Fig. 2.6. Number of failures versus risk at hydrant HY66 with fire flow = 31.5 l/s (500 gpm)

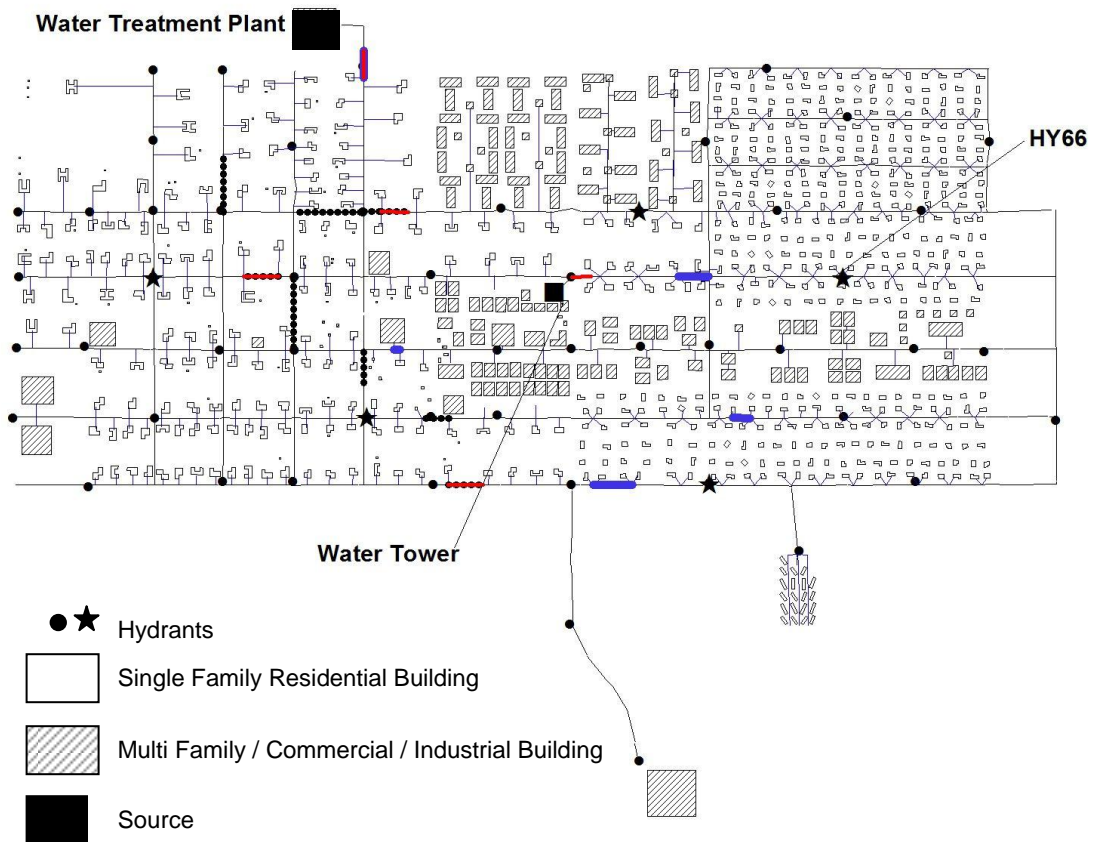


Fig. 2.7. Results at hydrant HY66 for maximum failure number $X_{max} = 5$ and ratio of probability of attack on “likely” pipes to “unlikely” pipes $\eta = 5$, vulnerable pipes (decision variables) shown in solid blue lines for $P_{LP} = 0.2$, vulnerable pipes (decision variables) shown in solid red lines for $P_{LP} = 0.4$, and “likely” pipes for intentional attack shown in black thick dotted lines

was the case of hydrant HY29, the optimal decision sets of the results from hydrant HY66 (Fig.2.7.) indicates that the accidental failure modes dominate solutions when probability of attack on “likely” pipes (P_{LP}) is less than or equals to 0.2; the intentional

failure modes dominate solutions when P_{LP} exceeds 0.2. Similar results were found in other hydrant locations. System risk obviously increases as intentional failure probability increases. These results suggest a definite quantifiable threshold where system elements generating greatest risk change due to changing failure sources.

2.8. Analysis and Recommendation of Mitigation Strategies

To reduce the assessed risk to Micropolis WDS during fire events a risk management approach was adopted through mitigation. Mitigation is the course of action which, if taken in advance, will reduce the threat toward the water system and will help in improving the system's performance. Considering all three failure scenarios discussed in WDS vulnerability and risk assessment, there are several ways to mitigate WDS fire consequences: (1) complete seismic replacement of all pipes in the network, (2) design and construction of alternate new pipelines within the service area of the system, (3) installing multiple water storage tanks designed with seismic load resistant. All of these alternatives would reduce the risks from water system's failure hazard, but they might not be cost-effective. Therefore, a hardening approach of optimal decision sets, identified from the risk-based DP methodology, was considered.

From the risk-based DP solutions presented in above sections, it was found that some elements of the Micropolis WDS were repeatedly among the most vulnerable components for fire flows at different hydrants (i.e., they were frequently included in the optimal decision set U^* determined by the risk-based DP algorithm). On the basis of these results, four mitigation strategies were considered: (1) low-cost mitigation focused

on accidental failure (LC-AF) (hardening 18 vulnerable pipes), (2) high-cost mitigation focused on accidental failure (HC-AF) (hardening 32 vulnerable pipes), (3) low-cost mitigation focused on intentional failure (LC-IF) (hardening 10 “likely” pipes for intentional failure; among 10 “likely” pipes, pipe enlargement applied at MA536, MA549, MA672, MA691, MA692, and MA693 with hardening), and (4) high-cost mitigation focused on intentional failure (HC-IF) (hardening 24 vulnerable pipes including 10 “likely” pipes for intentional failure; among 10 “likely” pipes, pipe enlargement applied at MA536, MA549, MA672, MA691, MA692, and MA693 with hardening). The mitigation designs are shown in Fig.2.8. All of these mitigation strategies involve hardening a specific set of pipes, i.e., replacing the existing pipes with more durable cement lined class 50 ductile iron pipes of same diameter or larger diameter (as included in mitigation design (3) and (4)) and further simulations were performed on the hardened water supply system to assess its changed vulnerability and risk under each mitigation strategy. In the mitigation scenario simulations, “hardened” pipes were assumed to have 0 probability of failure.

During mitigation scenario simulation, accidental failure methods were evaluated using probability of attack on “likely” pipes, $P_{LP} = 0.02$ and intentional failure methods were simulated with $P_{LP} = 0.6$. From mitigation scenario simulation it was found that the proposed mitigation measures reduced the system risks to varying degrees. As an example, system risk versus number of failures at hydrant HY29 with mitigation design (1) and (3) are shown in Fig.2.9 and Fig.2.10 respectively.

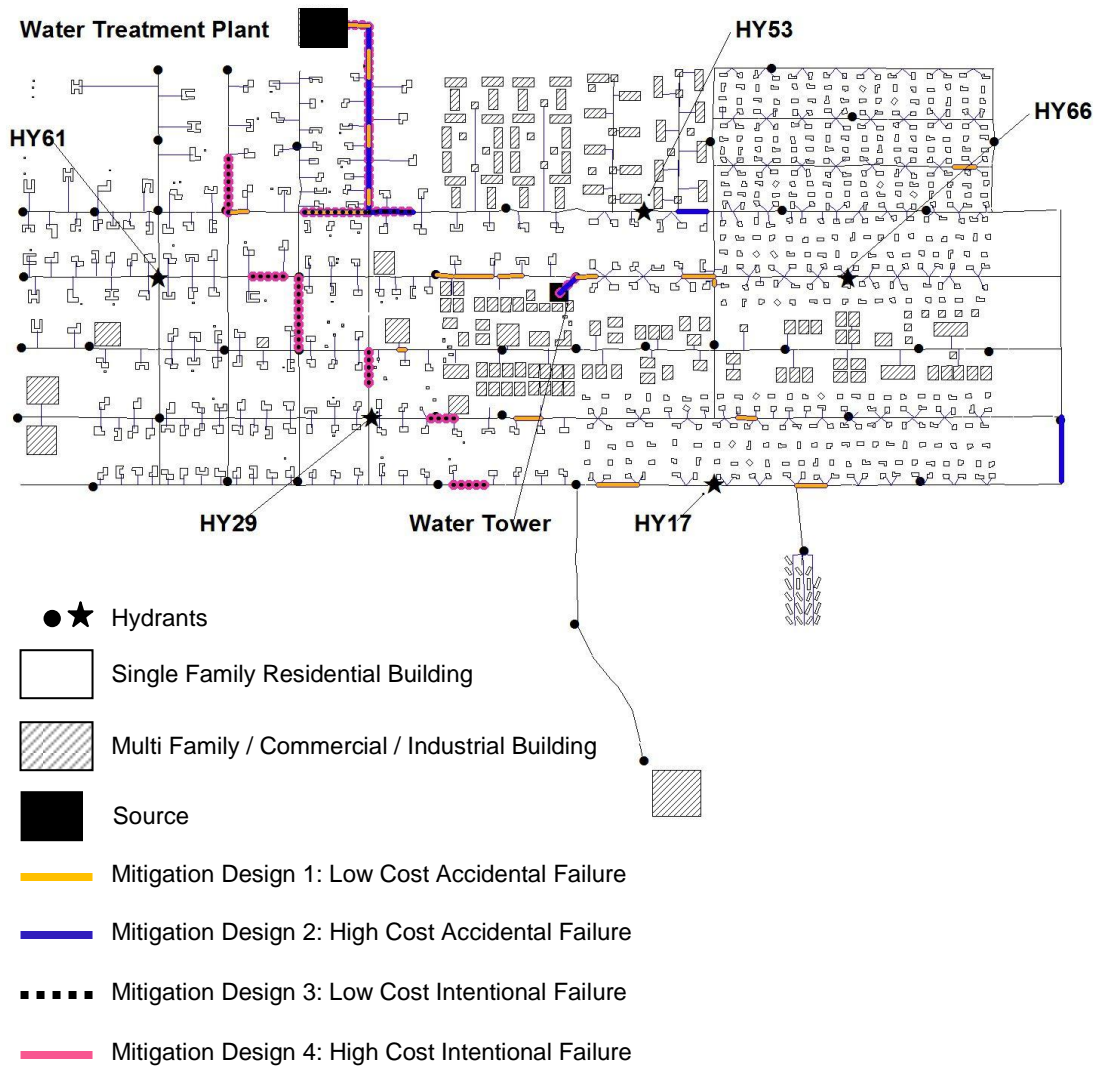


Fig. 2.8. Mitigation designs for Micropolis water distribution system

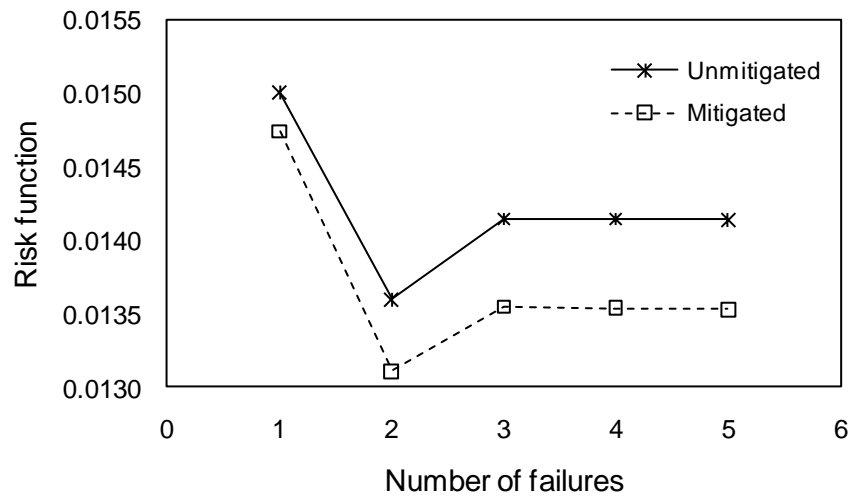


Fig. 2.9. Number of failures versus risk at hydrant HY29 with low cost mitigation for accidental failure (mitigation package 1) with $P_{LP} = 0.02$ and $\eta = 5$

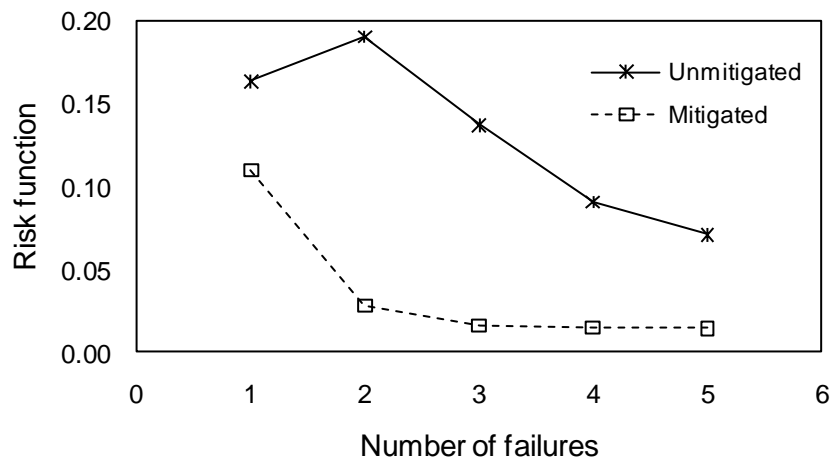


Fig. 2.10. Number of failures versus risk at hydrant HY29 with low cost mitigation for intentional failure (mitigation package 3) with $P_{LP} = 0.6$ and $\eta = 5$

2.9. Benefit-cost Analysis for Proposed Mitigation Strategies

Benefit-cost analysis was used to determine the economic feasibility of the mitigation options. The annual failure probabilities presented above were transformed to probabilities over 50 year service lives/planning horizons using the binomial distribution (Clemen and Reilly 2001). Benefits were calculated as the product of risk reduction over the 50 year planning horizon – reduction in the product of damage function value (J) and probability of simultaneous failure of pipes in the optimal decision set ($P(U)$) – and the total building replacement cost within each hydrant service area. The benefit from adopting mitigation is thus equivalent to how much building replacement cost is saved from fire damage by implementing mitigation. Cost of each mitigation option is the cost of pipe replacement, estimated as \$58.17/m (\$17.73/ft) for 0.051 m (2-inch), \$59.55/m (\$18.15/ft) for 0.102 m (4-inch), \$69.91/m (\$21.31/ft) for 0.152 m (6-inch), \$74.0/m (\$22.31/ft) for 0.203 m (8-inch), and \$107.0/m (\$32.62/ft) for 0.305 m (12-inch) diameter pipes (Saylor 2004). Accidental failure methods are evaluated using $P_{LP} = 0.02$, intentional failure methods are evaluated using $P_{LP} = 0.6$. Table 2.1 and Table 2.2 present the benefit-cost analysis at all five hydrants for this system.

The benefit-cost analysis for the Micropolis water system reflects the system's added resiliency by implementing the mitigation measures. The mitigation strategies that focused on accidental failures ((1) and (2)) reduced the system's vulnerability and risk for any number of pipe failure ($X_{max} \geq 1$) during a fire event and produced positive net-benefits. However, mitigation strategies that are focused on intentional failure ((3) and (4)) produced a negative net benefit for all of the five hydrant locations with $X_{max} = 1$;

Table 2.1. Benefit-cost Comparison for Proposed Mitigation Strategies for 2 Failed Pipes

Service Area	Mitigation Method	Estimated Cost (\$)	Property Value (\$)	Change in Risk Index	Estimated Benefit (\$)	Net Benefit (\$)
HY17	LC-AF	58,375	8,907,202	0.0141	125,906	67,531
	HC-AF	98,903		0.0255	226,795	127,892
	LC-IF	59,954		0.1010	899,203	839,248
	HC-IF	100,846		0.1131	1,007,416	906,570
HY29	LC-AF	58,375	17,302,280	0.0125	216,381	158,006
	HC-AF	98,903		0.0484	837,616	738,713
	LC-IF	59,954		-0.2407	-4,164,719	-4,224,673
	HC-IF	100,846		-0.2172	-3,758,739	-3,859,585
HY53	LC-AF	58,375	48,972,083	0.0043	210,264	151,889
	HC-AF	98,903		0.0320	1,565,913	1,467,010
	LC-IF	59,954		0.1616	7,911,980	7,852,026
	HC-IF	100,846		0.1606	7,865,523	7,764,677
HY61	LC-AF	58,375	12,755,650	0.0061	78,266	19,891
	HC-AF	98,903		0.0379	482,923	384,020
	LC-IF	59,954		0.1434	1,829,489	1,769,535
	HC-IF	100,846		0.1728	2,203,793	2,102,947
HY66	LC-AF	58,375	21,717,610	0.0196	426,226	367,851
	HC-AF	98,903		0.0104	226,513	127,610
	LC-IF	59,954		0.0641	1,391,680	1,331,726
	HC-IF	100,846		0.0792	1,719,525	1,618,679

but produced positive net benefits for all of the fire locations when $X_{max} \geq 2$ except for hydrant HY29. This condition implies that the proposed mitigation designs for intentional failure are not effective for a small scale attack; however, for a large scale attack that mitigation strategies may be effective in producing positive net-benefits in the

long run. This behavior of the proposed mitigation calls for a more systematic design. Optimizing the mitigation designs may help produce plans that would be cost effective in case of fire flow condition at all of the above mentioned hydrant locations.

Table 2.2. Benefit-cost Comparison for Proposed Mitigation Strategies for 4 Failed Pipes

Service Area	Mitigation Method	Estimated Cost (\$)	Property Value (\$)	Change in Risk Index	Estimated Benefit (\$)	Net Benefit (\$)
HY17	LC-AF	58,375	8,907,202	0.0080	71,384	13,009
	HC-AF	98,903		0.0231	205,816	106,913
	LC-IF	59,954		0.2484	2,212,321	2,152,367
	HC-IF	100,846		0.2710	2,414,292	2,313,446
HY29	LC-AF	58,375	17,302,280	0.0152	263,258	204,883
	HC-AF	98,903		0.0146	252,108	153,205
	LC-IF	59,954		0.1228	2,124,117	2,064,163
	HC-IF	100,846		0.1630	2,821,020	2,720,174
HY53	LC-AF	58,375	48,972,083	0.0047	231,076	172,701
	HC-AF	98,903		0.0264	1,293,047	1,194,144
	LC-IF	59,954		0.3009	14,737,021	14,677,067
	HC-IF	100,846		0.2987	14,629,026	14,528,180
HY61	LC-AF	58,375	12,755,650	0.0082	104,345	45,970
	HC-AF	98,903		0.0385	491,200	392,297
	LC-IF	59,954		0.2811	3,586,153	3,526,199
	HC-IF	100,846		0.3107	3,963,181	3,862,335
HY66	LC-AF	58,375	21,717,610	0.0066	142,267	83,892
	HC-AF	98,903		0.0105	228,778	129,875
	LC-IF	59,954		0.2206	4,791,524	4,731,570
	HC-IF	100,846		0.2296	4,986,459	4,885,613

2.10. Final Remarks

This paper illustrates an optimization-simulation methodology for water distribution system which addresses the risk, consequences, and mitigation strategies during fire events. Although research on vulnerability of water supply systems has been studied intensively in recent years; this paper introduces a new risk-based DP optimization approach which enables the water utilities to analyze the vulnerability and risk of the system during fire events.

The proposed methodology has three major steps. First, the pipe failure probabilities are estimated considering three failure scenarios: (1) accidental failure due to soil pipe interaction, (2) accidental failure due to a seismic event, and (3) malevolent action. Next, the total probability of failure due to all three modes is incorporated in a DP optimization methodology to evaluate the system risk during occurrence of fire. This step produces the optimal risk value; the points of vulnerability of the system, which is the set of solutions (pipes) whose collective failure maximizes the risk; and the total probability of failure for the optimal decision set. Finally, based on the solutions of the DP methodology, four mitigation strategies are proposed and the suggested mitigation plans are evaluated with a benefit cost analysis.

The results from the case study illustrate that even though the vulnerable components/pipes of a WDS vary depending upon the location of fire, some of the same water mains appeared as the most vulnerable components for fire at all locations under consideration. The proposed mitigation designs are generated in an iterative fashion by implementing simulation approach based on the concept of hardening specific sets of

water mains. Simulations of the mitigation strategies show that the system risk can be reduced significantly by adapting some of the mitigation measures (mitigation package (1) and (2)) and the system's resiliency can be improved as well. However, some of the proposed mitigation plans are not adequate for small scale attack (mitigation design (3) and (4)); evidently those are much more effective during a large scale attack scenario. This observation calls for an investigation on the mitigation measures in a more systematic way.

Prior research on fire mitigation demonstrated that while pipe enlargement increases the water distribution system's resiliency for fire protection, it also increases water age problem under normal demand condition (Bristow et al. 2007). To design an optimal mitigation plan for water systems' fire events, a multi-objective optimization approach will be examined next. To address both the fire mitigation and the water age problem, a multi-objective framework will be developed to yield a Pareto optimal front for optimal mitigation of water distribution system's fire events based on three primary objectives: (1) minimizing fire damage, (2) minimizing water quality problem, and (3) minimizing mitigation cost. The new investigation in fire mitigation and its findings is discussed in detail as a separate article in Section 3.

3. A MULTI-OBJECTIVE EVOLUTIONARY COMPUTATION APPROACH TO HAZARDS MITIGATION DESIGN FOR WATER DISTRIBUTION SYSTEMS

3.1 Introduction

Water systems have been identified as one of the United States' critical infrastructures (White House 2003) and are vulnerable to various threats caused by natural disasters or malevolent actions (such as terrorist attack, vandalism, or insider sabotage). The goal of a water distribution system (WDS) is to deliver water to the consumers in sufficient quantity and quality, even in case of emergencies such as pipe failure, power outage, and urban fire events. Previous studies have examined WDS vulnerability and risk during urban fire events and investigated rehabilitation for mitigation of potential fire events with a major focus on attaining adequate fire flows by pipe hardening and pipe enlargement (Kanta and Brumbelow 2008). Any changes in water demand or water use pattern caused by pipe rehabilitation or new development often cause slower flow through the network which, in turn, results in greater decay of disinfectant (USEPA 2002). Thus pipe enlargements can also place public health at risk during normal operational periods. This type of water quality problems can be reduced by installing chlorine booster units in the system other than at the water treatment plant. Excess amounts of chlorine however, causes bad taste and the disinfectant by-products are harmful to human health.

Bristow et al. (2007) studied different mitigation strategies to improve water distribution systems' ability to meet fire fighting demand, and water main enlargements were found to be the most effective but involved relatively high costs. Brumbelow and Bristow (2008) investigated tradeoffs between WDS emergency supply and daily water quality needs and proposed 17 mitigation packages to improve the system's capacity to provide fire fighting flows without compromising the daily water quality needs. It was found from the investigation that some tradeoff exists between normal water quality and emergency demands of the WDS. All of the previous studies for WDS hazard mitigation cited here utilized simulation based methodologies which were iterative and hence call for a systematic approach. Thus a novel approach is required to effectively address the conflicting goals of the WDS: reliable delivery of water during normal as well as emergency conditions, meeting water quality standards, and finding cost-effective design and rehabilitation options.

The goal of this project is to develop a methodology to design effective mitigation strategies for urban fire events for water distribution systems with three objectives: (1) minimizing fire damages, (2) minimizing water quality deficiencies, and (3) minimizing the cost of mitigation. This goal can be achieved by identifying pipes for replacement and their corresponding diameters and the location of additional chlorine booster units. When more than one objective is considered in an optimization problem, no single solution may produce the best result with respect to all objectives. In such a case a set of solutions known as the Pareto optimal solutions or non-dominated solutions exist (Hans 1988), none of which is worse than any other with respect to all objectives.

The Pareto optimal solutions provide the decision makers more information and flexibility in selection of a solution. This article presents a novel multi-objective evolutionary algorithm named Non-Dominated Sorting Evolution Strategy (NSES) to effectively address the conflicting goals of the WDS. The application of the algorithm is first demonstrated to a set of test problems then to the multi-objective problem in WDS. The following sections describe the development of the methodology, implementation, and results in detail.

3.2 Problem Statement

The proposed model has three objectives: (1) minimizing the aggregated fire damage (f_1), (2) minimizing the maximum water quality deficiency (f_2), and (3) minimizing normalized mitigation cost (f_3). The multi-objective optimization problem, therefore, can be mathematically formulated as follows:

$$\text{Minimize } f_1 = \sum_{i=1}^n \alpha_i \frac{Q_{i_{req}} - Q_{i_{available}}}{Q_{i_{req}}} \quad (3.1)$$

$$\text{Minimize } f_2 = \max_j D_{C_j}; \quad j=1, 2, \dots, m \quad (3.2)$$

$$D_{C_j} = \begin{cases} 1; & C_{j_{available}} < 0.2, C_{j_{available}} \geq 4.0 \\ 1 - \frac{C_{j_{available}}}{3.8}; & 0.2 \leq C_{j_{available}} < 4.0 \end{cases} \quad (3.3)$$

$$\text{Minimize } f_3 = \frac{\sum_{k=1}^{np} C_k^P + \sum_{l=1}^{nb} C_l^B}{C_{worst}} \quad (3.4)$$

subject to:

$$D_k \in \{d\}; k = 1, 2, \dots, np \quad (3.5)$$

$$np \leq \phi \quad (3.6)$$

$$nb \leq \theta \quad (3.7)$$

where, $Q_{i_{req}}$ = required fire flow (l/s [gpm]) for hydrant i ; $Q_{i_{Available}}$ = available flow (l/s [gpm]) at minimum allowable residual pressure at hydrant i (typically set at 137.9 kN/m² [20 psi] by local code); α_i = weighting coefficient for hydrant i ; n = total number of fire hydrants considered for fire flow evaluation; D_{C_j} = chlorine deficiency (unitless) at monitoring node j ; $C_{j_{Available}}$ = available residual chlorine concentration (mg/l) at monitoring node j ; m = total number of monitoring nodes; C_k^P = cost of pipe k (\$); C_l^B = installation cost of booster station l (\$); C_{worst} = worst cost (\$); D_k = diameter (m [inch]) of pipe k ; d = commercially available discrete pipe sizes (m [inch]); N = total number of pipes in the network; np = number of pipe decision variables; ϕ = user defined maximum number of pipes to be replaced; nb = number of booster station decision variables; and θ = user defined maximum number of boosters to be installed.

3.3 Multi-objective Evolutionary Algorithms

Evolutionary algorithms are population based heuristic search algorithms based on the process of natural selection. Traditional optimization models sometimes pose difficulties in application to water distribution systems analysis due to the non-linearity of the water systems operation, hence require simplification of the WDS problems.

Evolutionary algorithms, in contrast, are becoming increasingly popular in application of water resources systems analysis because of its capability of incorporating the complex simulation models into heuristic search (Ranjithan 2005). Evolutionary computation (EC) based algorithms also support efficient search to identify Pareto optimal solutions in multi-objective problems.

Genetic Algorithm (GA) (Holland 1975) is the most common evolutionary computation (EC) based approach among engineering applications. GA based methods have been successfully applied to WDS design and management (e.g., Atiquzzaman et al. (2004), Prasad and Park (2004), Prasad et al. (2004), Farmani et al. (2005), and Jeong and Abraham (2006)). Similar to a GA, Evolution Strategy (ES) (Rechenberg 1965) is another EC-based approach which uses a population of individuals to search for the best solution. Each individual (or solution) in the population consists of a set of 'genes' that represent the decision variables, and the performance of each individual is evaluated by a fitness function. While GA uses both crossover and mutation, ES is typically based solely on a probabilistic mutation operator. To mutate a value of a real-valued decision variable, the new value is taken from a normal distribution with mean as the current value of the variable and standard deviation as an algorithmic parameter. The

performance of the ES-based search is very sensitive to the value of the standard deviation; thus determination of this parameter may require extensive adjustment.

Alternatively, *adaptive mutation* may be used in which the standard deviations are also included in the chromosome representation (Eiben and Smith 2007).

A wide variety of Pareto-based multi-objective evolutionary algorithms have been reported in the literature (e.g., NPGA (Horn et al. 1994), NSGA (Srinivas and Deb 1995), SPEA (Zitzler and Thiele 1999), PAES (Knowles and Corne 1999), NSGA-II (Deb et al. 2002), and HM2EA (Dorn 2004)). The goals of a Pareto-based multi-objective optimization problem are to find: (i) solutions that are close to the Pareto front, and (ii) solutions that are well distributed and spread out along the Pareto front. It has been found in the literature that NSGA-II can converge toward the true Pareto-front uniformly and can distribute non-dominated solutions along the front evenly (Prasad et al. 2004).

3.4 Non-dominated Sorting Evolution Strategy (NSES)

To solve the multi-objective optimization problem defined in section 3.2, the fast elitist Non-dominated Sorting Genetic Algorithm (NSGA-II) is modified by incorporating an ES to address difficulties for heuristic algorithms posed by WDS problems. Proposed by Deb et al. (2002), NSGA-II is a population based multi-objective genetic algorithm which produces Pareto-optimal solutions in the objective spaces. Traditionally as in GA, NSGA-II utilizes both crossover and mutation operators to facilitate both exploration and exploitation during the heuristic search and generates

better solutions in subsequent generations. The implementation of traditional crossover operator to a WDS problem could end up in a random search which might not reflect the feasible flow path within the system. To overcome this issue, a path search algorithm could be introduced which would explore an alternate flow path within the distribution network during crossover. This approach however, would significantly increase the computation time. Therefore, NSGA-II algorithm is here modified as Non-dominated Sorting Evolution Strategy (NSES) by implementing ES based search technique with the elitist non-dominated sorting algorithm. The structure and implementation of NSES operators to the WDS problem are described in the following sections. A flowchart of the NSES algorithm is provided in Fig. 3.1.

3.4.1. Representation

In any population based search, the decision variables are encoded as an array, which, when decoded, represents a solution. The efficiency of an ES-based search depends upon the representation of a solution. For example, if an individual is represented by a large array of decision variables, it may increase the time of convergence of the algorithm. Typically, ES uses real-valued vectors for representing an individual.

To represent the multi-objective problem, it is assumed that a maximum number of pipes to be replaced for mitigation/rehabilitation is known. In this paper it is assumed that additional chlorine boosters will not be added, but the general problem formulated

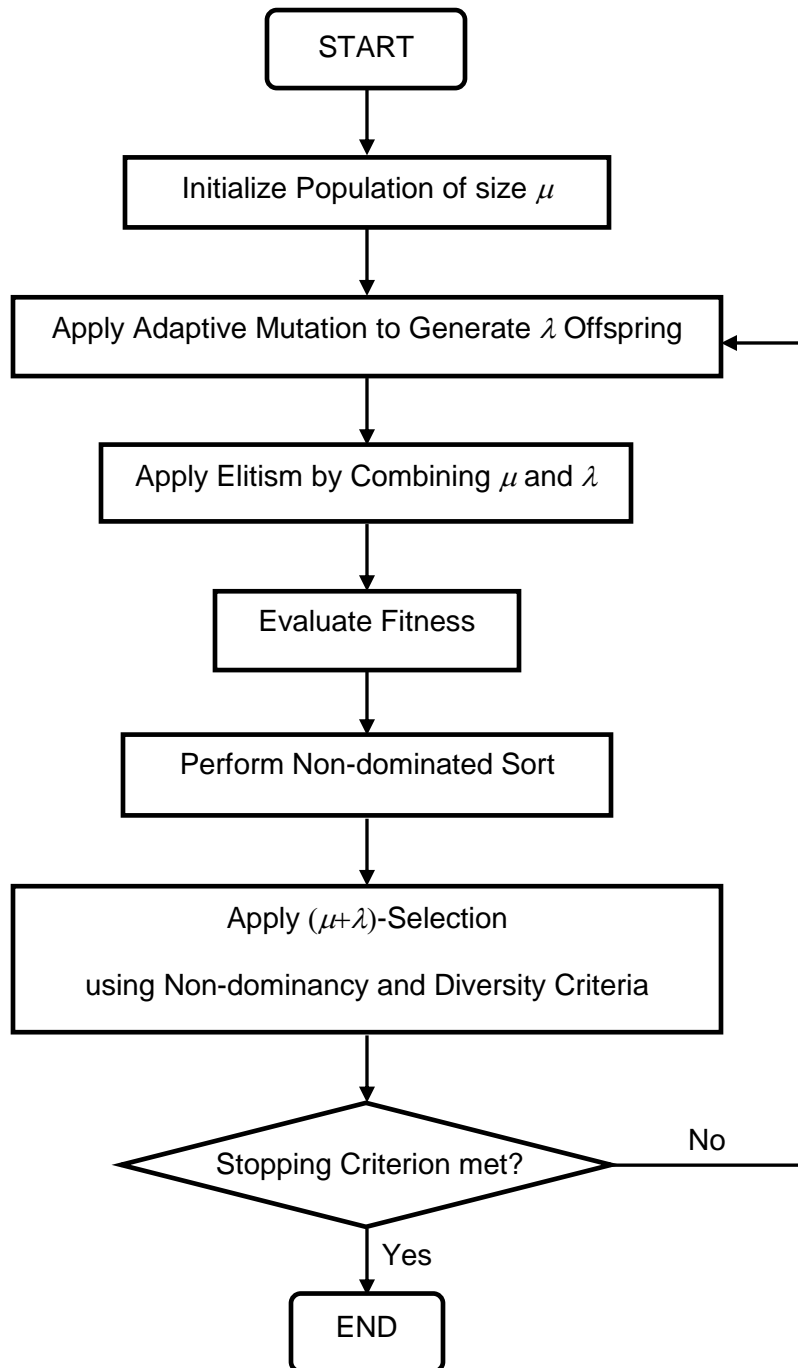


Fig. 3.1. Flowchart for NSES

above includes this possibility. Therefore, the only sets of decision variables are the pipes to be replaced and their corresponding diameters. Rehabilitation locations are represented by an array of integer values, each of which specifies the pipe ID; and the pipe diameters are represented by a separate array of integer values.

An adaptive search is applied during implementation of this methodology. For an adaptive search, each decision variable is represented by a set of two genes. One gene represents the value of the variable, x_j , and another gene represents the standard deviation, σ_{x_j} , which is used to mutate the gene representing the variable value.

Assuming the number of pipe rehabilitation decisions is n , the chromosome representation of the problem is shown in Figure 3.2.

I_1	I_2	I_n	σ_{I_1}	σ_{I_2}	σ_{I_n}
-------	-------	-------	-------	----------------	----------------	-------	----------------

Representation: Pipe ID (rehabilitation location)

d_1	d_2	d_n	σ_{d_1}	σ_{d_2}	σ_{d_n}
-------	-------	-------	-------	----------------	----------------	-------	----------------

Representation: Pipe diameter

Fig. 3.2. Chromosome representation

3.4.2. Mutation

In ES, there is a strong emphasis on the mutation operator for creating offspring. Mutation is migration from the current set of solutions to better solutions using small incremental steps. In ES, the adaptive mutation for each variable value x_j is performed in two steps: first, the standard deviation, σ_{x_j} , is mutated using a separate normal distribution to generate σ'_{x_j} ; then using the mutated standard deviation, σ'_{x_j} , the variable value x_j is mutated as x'_j . The mutation mechanism is specified as follows (Eiben and Smith 2007):

$$\sigma'_{x_j} = \sigma_{x_j} \cdot e^{\tau' \cdot N(0,1) + \tau \cdot N_j(0,1)} \quad (3.8)$$

$$x'_j = x_j + \sigma'_{x_j} \cdot N_j(0,1) \quad (3.9)$$

Here, τ and τ' are parameters such that $\tau' \propto \frac{1}{\sqrt{2n}}$ and $\tau \propto \sqrt{2\sqrt{n}}$; n is the problem size

(number of decision variables); $N(0,1)$ denotes a draw from the standard normal distribution; and $N_j(0,1)$ denotes a separate draw from the standard normal distribution for each variable j . The proportionality constants for both τ and τ' are external parameters to be set by the users.

To mutate the location of pipe rehabilitation, a special mutation operator is adopted from Zechman and Ranjithan (2009). The current pipe is mutated by random assignment of another topologically close potential pipe using an adjacency list. The

adjacency list of each pipe of a water distribution system represents a connectivity map of one pipe to other pipes in the network. In such a case, the standard deviation value, σ_{I_k} , associated with a pipe ID, I_k , indicates the maximum number of links between that pipe and the pipe to be selected.

3.4.3. Selection

In ES-based algorithm, two different types of selection operators are used: *Parent selection* and *survivor selection* (Eiben and Smith 2007). In the first generation, an initial population of size μ is generated. In each generation, *parent selection* operator is applied based on a uniform distribution to randomly select λ individuals from the pool of μ individuals, where $\lambda > \mu$. Each of these λ individuals is then mutated to create λ offspring.

After creating λ offspring, their fitness values are calculated. The *survivor selection* operator is applied to select best μ individuals deterministically, either from the set of offspring individuals only (denoted as (μ, λ) selection) or from the combined set of parent and offspring individuals (denoted as $(\mu + \lambda)$ selection). In this article, the investigation is based on a $(\mu + \lambda)$ selection.

3.4.4. Non-dominated Sorting

The non-dominated sorting approach was adopted from Deb et al. (2002). First, elitism is introduced by combining both parent individuals (μ) and offspring (λ). Then

each solution is compared with every other solution in the combined population and the individuals are sorted into several fronts such as F_1 , F_2 , F_3 , etc. The first front F_1 contains the best non-dominated solutions in the combined population. Solutions in this front have a non-dominated rank = 1. The second front F_2 contains the solutions that are dominated by the solutions in the first front F_1 but dominate all other solutions in the combined population. Solutions in this front have a non-dominated rank = 2. Similarly, the front F_3 contains the solutions that are dominated by the solutions in the fronts F_1 and F_2 but dominate all other solutions in the combined population. Solutions in this front have a non-dominated rank = 3; and so on.

3.4.5. Crowding Distance Estimation

To maintain the diversity in the population a density estimation technique is adopted from NSGA-II (Deb et al. 2002). This operator measures the density of a particular solution in terms of the average distance of two other solutions on either side of this solution along each of the m objectives. This distance is referred to as the crowding distance. Solution with larger crowding distance indicates better diversity in the population. An illustration of crowding distance estimation in NSGA-II for $m = 2$ is shown in Fig. 3.3.

3.5. Performance Measure of NSES Algorithm

The performance of an EC-based algorithm is generally evaluated to validate the Pareto optimality. The goals of a population-based multi-objective optimization are to

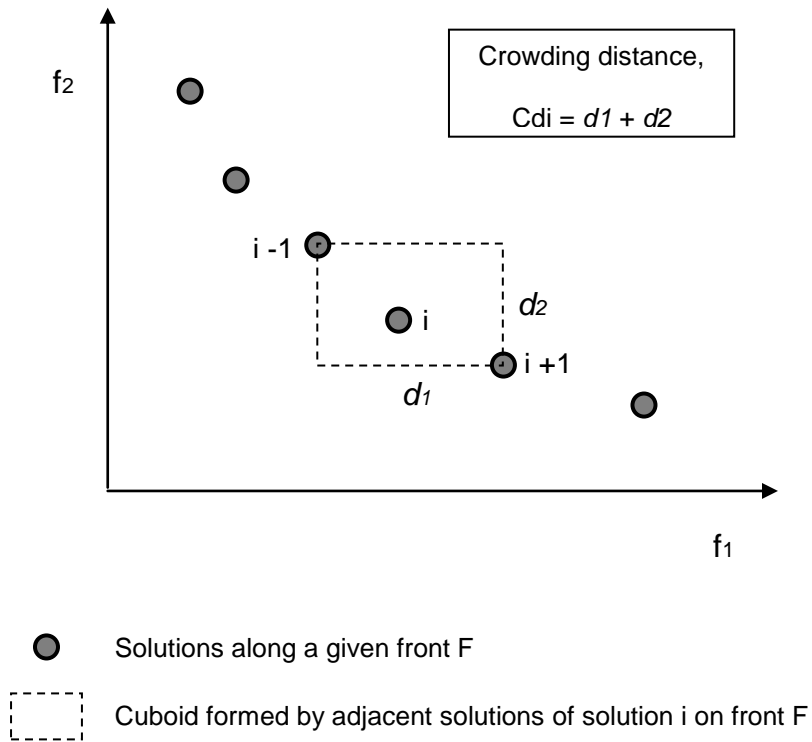


Fig. 3.3. Crowding distance estimation in NSGA-II

find a set of non-dominated solutions that are: (1) close to the true Pareto front and (2) as diverse as possible along the Pareto front. Therefore, the performance should be measured in terms of both accuracy and diversity. Different multi-objective metrics have been proposed in the literature such as *deviation metric* Δ (Deb et al. 2002), *coverage* (Zitzler and Thiele 1999), *S-factor* (Zitzler and Thiele 1998) and *hypervolume* (Fleischer 2003). In this article the NSES algorithm has been applied to a number of test problems to measure two multi-objective metrics: deviation metric Δ and hypervolume. The following sections describe the applied multi-objective metrics.

3.5.1 Measure of Diversity

To measure the diversity of the NSES solutions in the non-dominated objective space, the proposed algorithm is applied on three test problems, which have been adopted in Deb et al. (2002). A detailed description of these test problems are given in Table 3.1. All these test problems have variable degrees of difficulty. The true Pareto

Table 3.1. Multi-objective Test Problems Where n Denotes the Number of Decision Variables

Test Problem	n	Domain	Objective Functions
MOP2	3	$-4 \leq x_i \leq 4$	Minimize $f_1(x) = 1 - e^{\left(-\sum_{i=1}^n \left(x_i - \frac{1}{\sqrt{n}}\right)^n\right)}$ Minimize $f_2(x) = 1 - e^{\left(-\sum_{i=1}^n \left(x_i + \frac{1}{\sqrt{n}}\right)^n\right)}$
MOP3	2	$-\pi \leq x$ $y \leq \pi$	Minimize $f_1(x) = [1 + (A_1 - B_1)^2 + (A_2 - B_2)^2]$ Minimize $f_2(x) = [(x + 3)^2 + (y + 1)^2]$ Where: $A_1 = 0.5 \sin 1 - 2 \cos 1 + \sin 2 - 1.5 \cos 2$ $A_2 = 1.5 \sin 1 - \cos 1 + 2 \sin 2 - 0.5 \cos 2$ $B_1 = 0.5 \sin x - 2 \cos x + \sin y - 1.5 \cos y$ $B_2 = 1.5 \sin x - \cos x + 2 \sin y - 0.5 \cos y$
MOP4	3	$-5 \leq x_i \leq 5$	Minimize $f_1(x) = \sum_{i=1}^{n-1} \left(-10e^{(-0.2)\sqrt{x_i^2 + x_{i+1}^2}} \right)$ Minimize $f_2(x) = \sum_{i=1}^n (x_i ^a + 5 \sin(x_i^b))$ Where: $a = 0.8$ and $b = 3$

fronts for all of the test problems are known. The Pareto optimal solutions obtained with NSES for MOP2 and MOP4 are presented in Fig. 3.4 and Fig. 3.5 respectively.

A performance metric Δ is evaluated for each of the test problems. The metric Δ represents a measure of deviation of the solutions of the best non-dominated front in the final population (Deb et al. 2002). In multi-objective problems diversity among the Pareto-optimal solutions is very important. Thus the algorithm with a smaller deviation metric Δ shows better performance. The deviation metric Δ is computed as follows (Deb et al. 2002):

$$\Delta = \sum_{i=1}^{|F_1|} \frac{|d_i - \bar{d}|}{|F_1|} \quad (3.10)$$

where, F_1 = best non-dominated front in the final population; $|F_1|$ = number of solutions in front F_1 ; d_i = Euclidean distance in the objective space between two consecutive solutions in F_1 ; and \bar{d} = average of these distances d_i .

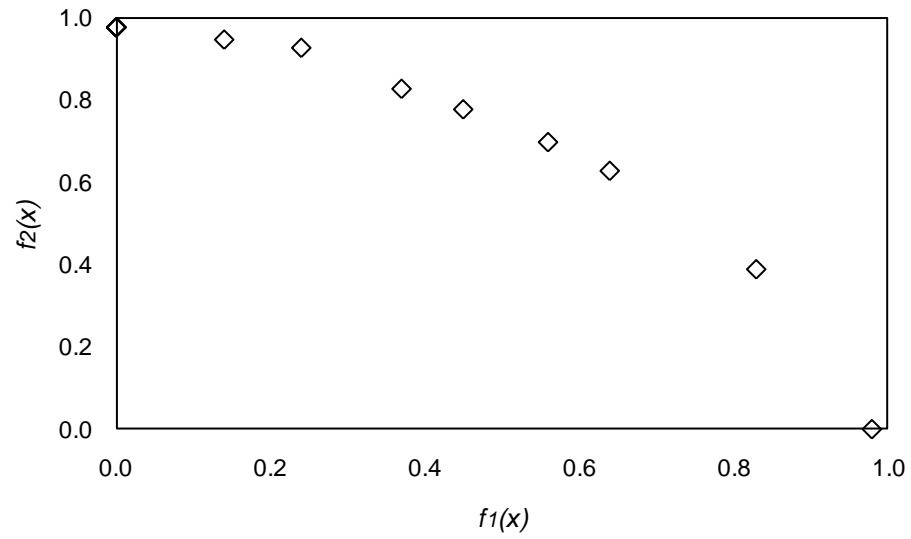


Fig. 3.4. Pareto optimal solutions obtained with NSES for MOP2

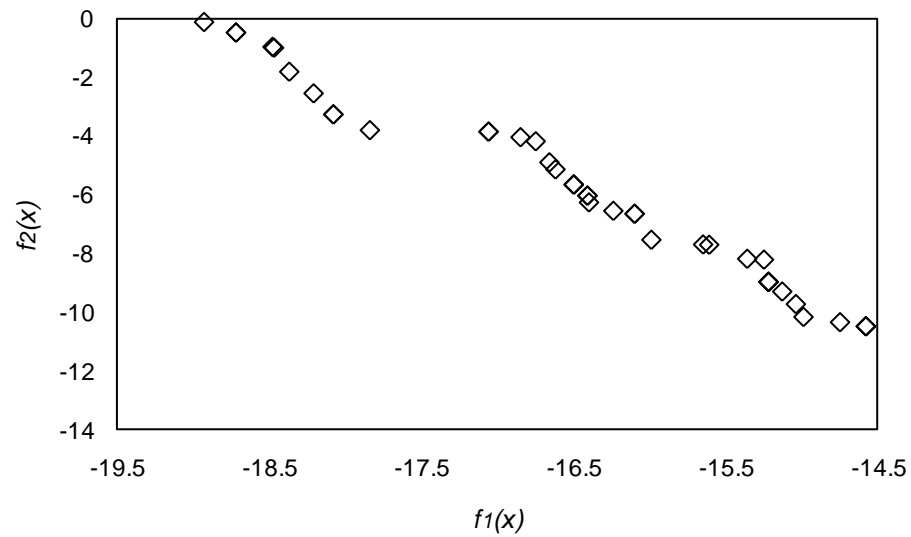


Fig. 3.5. Pareto optimal solutions obtained with NSES for MOP4

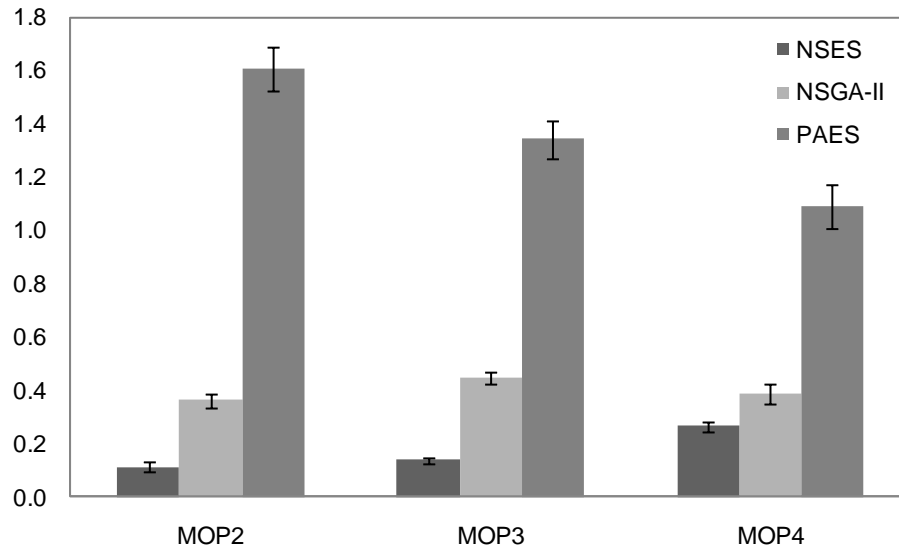


Fig. 3.6. Mean of the deviation metric Δ obtained for each of the test problems is shown in column graph, standard deviation of the deviation metric Δ is shown with error bar, lower value of Δ indicates better performance

To perform a fair comparison of the performance of NSES algorithm with that of NSGA-II and PAES, as listed in Deb et al. (2002), 10 random trials were conducted with 25,000 function evaluations ($\mu = 15$ (MOP2) and 50 (MOP3 and MOP4), $\lambda = 100$, number of generations = 250) and all three test problems were real-value encoded. The mean deviation $\bar{\Delta}$ and its variance from 10 iterations for each of the test functions using NSES is compared with that of NSGA-II and PAES and presented in Fig. 3.6. The smallest mean values of $\bar{\Delta}$ achieved for all test functions using NSES indicate that the proposed algorithm performs better than the other two. Overall, the test problem results

indicate that the NSES algorithm is able to attain diversity among the solutions in the non-dominated objective space.

3.5.2 Measure of Pareto Optimality

Zitzler and Thiele (1998) introduced a measure of accuracy, S-factor, of the Pareto front in the non-dominated objective space. The ‘S-factor’ refers to the size of the non-dominated objective space covered by the non-overlapping area of all the rectangles formed by the set of solutions in the Pareto front and a global worst point (objective function values) for any 2-objective problem. Fleischer (2003) extended this concept into higher dimensions and defined a set function that maps the Pareto optimal solutions to a scalar quantity. This single scalar is defined as ‘hypervolume’. Fleischer (2003) developed a computationally efficient algorithm, the Lebesgue Measure Algorithm, to calculate the hypervolume metric for any multi-objective (2-objective or higher) problem.

Fleischer (2003) proved through several Theorems, Lemmas, and their corollaries that a maximum value of the hypervolume metric for any multi-objective problem indicates the Pareto optimality of the associated points in the objective space in terms of both the diversity and accuracy. The deviation metric Δ (Deb et al. 2002) measures only the diversity of the points (solutions) in the best non-dominated front; thus is useful when the true Pareto front is known for the problem. However, for most real world problems the true Pareto front is unknown; hence deviation metric Δ (Deb et al. 2002) is not quite applicable. Therefore, the hypervolume metric is evaluated with

NSES for all above mentioned test problems to check both the accuracy and diversity of the proposed algorithm. Each test problem was solved for 10 random trials and the results for the different trials were similar. The results indicate the robustness of the NSES algorithm applied to the test problems. As an example, the calculation of hypervolume and the Pareto front for the test problem MOP2 for a representative trial is shown in Fig. 3.7.

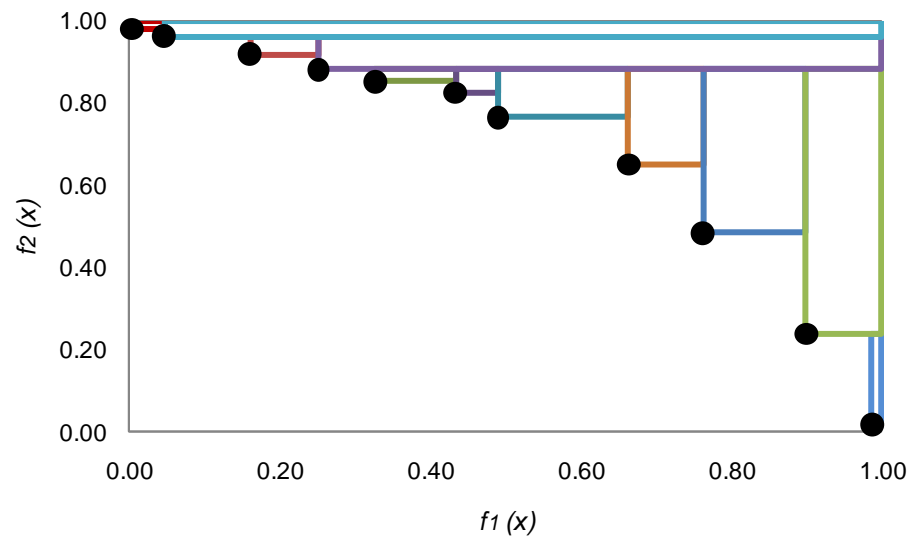


Fig. 3.7. The calculation of ‘Hypervolume’ in NSES for the test problem MOP2 using LebMeasure algorithm; solutions on the Pareto front are shown in black dots; each rectangle represents incremental hypervolume in the non-dominated objective space contributed by each point on the front; the worst point is (1,1)

3.6. Application of NSES to Water Distribution System Problem

A virtual city water distribution system data, Micropolis (Brumbelow et al. 2005, 2007), is used to demonstrate the NSES procedure to solve the multi-objective problem. “Micropolis” has an approximate area of 5.2 km^2 (2 mi^2) and a population of 5,000. The city has two major sources of water, a surface-water reservoir and a well field. Water from these sources is treated in a treatment plant. The current version of its water system model consists of a pumping station consisting of three pumps, one elevated storage tank, 1088 pipes, 1210 non-hydrant nodes, 52 fire hydrants, and 196 valves. Currently, a disinfectant dose of 4 mg/l is added at the treatment plant and there is no additional chlorine booster station in the system. Among 1088 pipes, there are 577 water mains each of which is considered as a potential pipe rehabilitation location. The diameter of rehabilitated pipes could be selected from the set of {0.15, 0.20, 0.25, 0.30, 0.36, 0.41, 0.46, 0.51, 0.61} m [{6, 8, 10, 12, 14, 16, 18, 20, 24} inch] diameter commercially available class 50 ductile iron pipes. The fire fighting capacity of the water system could be evaluated at all 52 fire hydrants, which would make the analyses computationally expensive. Therefore, to represent the system-wide fire fighting performance without contributing to computational burden, three fire hydrants are considered which cover the central business district, industrial area adjacent to the central business district, and heavily populated multi-family residential area on the north-eastern part of the city.

To evaluate the aggregate fire damage (Eq. 3.1), the weighting coefficients, α_i , are determined as replacement building cost of assets within a search radius of 304.8 m (1000 ft) of each hydrant over the total cost of assets within the search radius of all three

fire hydrants. A required fire flow of 63 l/s (1000 gpm) is considered at all three fire hydrants. Apart from the fire hydrants and the demand nodes, there are a total of 751 nodes representing valve nodes and junctions. From the set of 751 nodes, ten are selected as representative water quality monitoring nodes. The Surface Water Treatment Rule (SWTR) requires the water distribution systems to maintain a “detectable” disinfectant residual level of 0.2 mg/l (for chlorine) throughout the system. Moreover under the Stage 1 Disinfectant/Disinfection By-Products Rule, the residual should not exceed 4.0 mg/l for chlorine in any reach of the system (USEPA 2004). This is due to the fact that excessive levels of chlorine produces taste and odor problems, forms disinfectant by-products, and might accelerate pipe corrosion. Thus the water quality deficiency, expressed in Eq. (3.2), is defined to map the government regulation for drinking water quality and is evaluated at all ten monitoring nodes during each iteration. Finally, a normalized cost is evaluated as cost of pipe replacement for a current solution over the worst possible cost of rehabilitation (Eq. 3.4). The worst possible cost is evaluated by setting up a set of scenarios which maximizes the fire flow without cost or water quality constraints. The network is shown in Fig. 3.8.

The solution approach defined in the previous section is implemented in a computer code in Visual Basic 6.0 that utilizes iterative solution of the water distribution system’s hydraulics and water quality under the objectives and constraints defined by Eq. (3.1) through Eq. (3.7). The NSES model is coupled with EPANet Programmer’s Toolkit (Rossman 1999) to simulate the hydraulics and water quality in the network.

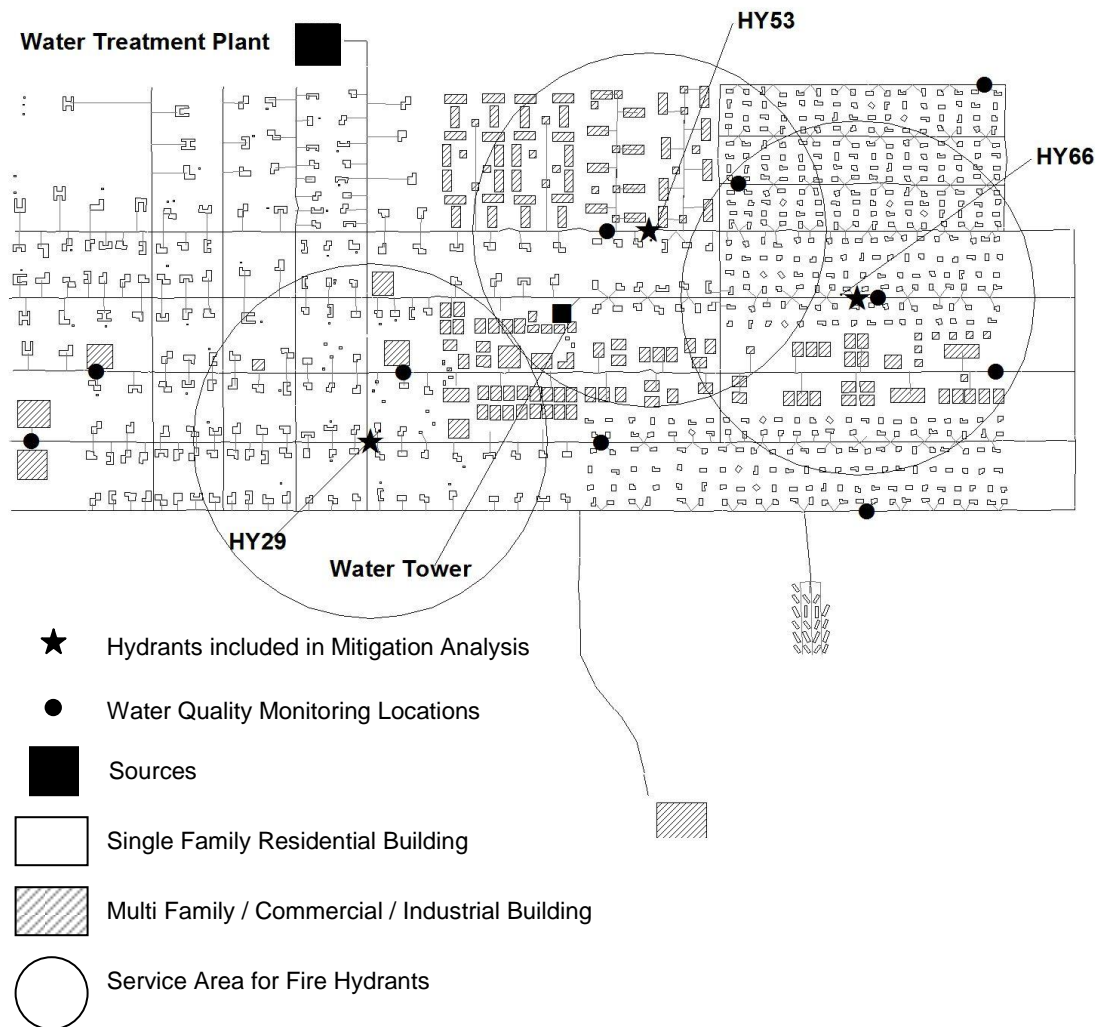


Fig. 3.8. Building map of Micropolis with water distribution network shown with thin lines

To evaluate the aggregated fire damage, the fire demands are added to the hydrants (one at a time) and a single period simulation is performed. To evaluate the water quality deficiency the hydraulics and water quality in the network are simulated separately without a fire flow demand over a 168-hour time period to allow the system to reach a

dynamic equilibrium condition with respect to disinfectant concentrations. It is assumed that a maximum number of 50 pipes or less needed to be replaced to increase the system-wide firefighting capability.

3.7 Results

Two sets of independent trials are performed to solve the water distribution system problem. The first set of trials is conducted to identify the algorithmic parameters and the second set of trials is conducted to test the robustness of the algorithm. The results from various trials are discussed in detail in the following sections.

3.7.1. Algorithmic Parameters

A number of trials are performed to investigate the appropriate setting for the parameters μ and λ , and the number of generations is used as stopping criterion. During initial trial a 1/7 ratio of μ/λ was used as recommended in Eiben and Smith (2007). Different settings of μ and λ were also investigated with varying the μ/λ ratio such as 1, $\frac{1}{2}$, among others. For each parameter setting the hypervolume is calculated at every generation and the convergence of the algorithm is tested with respect to the hypervolume metric. Since the true Pareto front for the WDS problem is not known, the hypervolume metrics at convergence of the algorithm with different parameter values are compared. The parameter values those yield the maximum value of the hypervolume metric for the WDS problem are chosen as the best setting found so far. The best

parameter values identified during implementation of NSES-based search are: $\mu = 75$, $\lambda = 150$, and *stopping criterion* = 150 generations.

3.7.2. Algorithmic Convergence

After identifying the appropriate parameter values for the NSES algorithm applied to WDS multi-objective problem, 30 independent trials are conducted to test and evaluate the robust behavior of the proposed methodology. The convergence of the algorithm is measured in terms of hypervolume metric. The global worst point for this problem is identified as (1,1,1) in ‘fire flow-water quality-cost’ objective space.

From all 30 trials it is observed that the hypervolume increases with the progression of generation and reaches a plateau at 150 generation. The average hypervolume at convergence from 30 different trials are found to be 0.5324 with a standard deviation of 0.019. Such a small standard deviation value represents the robust behavior of the algorithm. The number of non-dominated solutions in the first front is also plotted with progression of generation. The convergence of NSES is shown in Fig. 3.9 and Fig. 3.10.

Although there are cases where the hypervolume fluctuates at the initial generations showing the loss of fitness quality (Fig. 3.9), however, this kind of response is due to the fact that the hypervolume is measured, not optimized in NSES methodology. Overall, the figures indicate that both hypervolume and number of non-dominated solutions appear to converge after 150 generation and further iterations of the algorithm would not likely to improve the results.

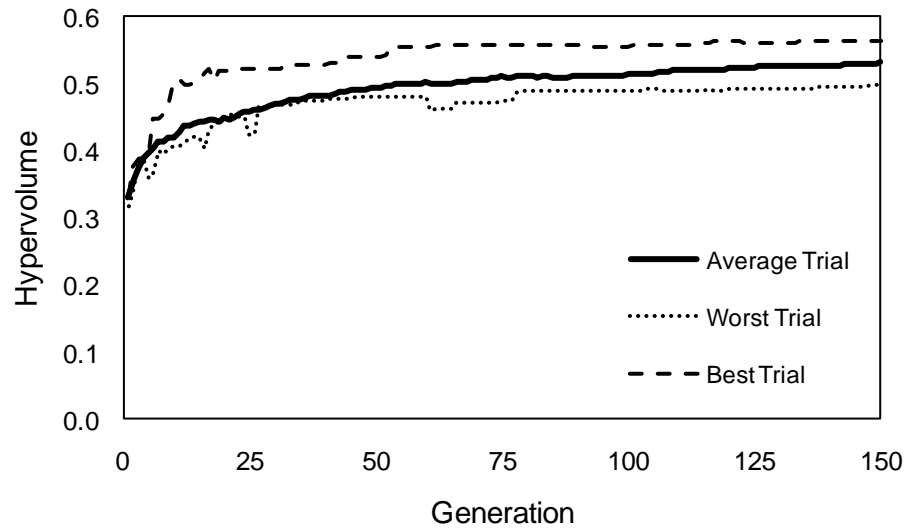


Fig. 3.9. Convergence of NSES for multi-objective water distribution system problem in terms of hypervolume metric

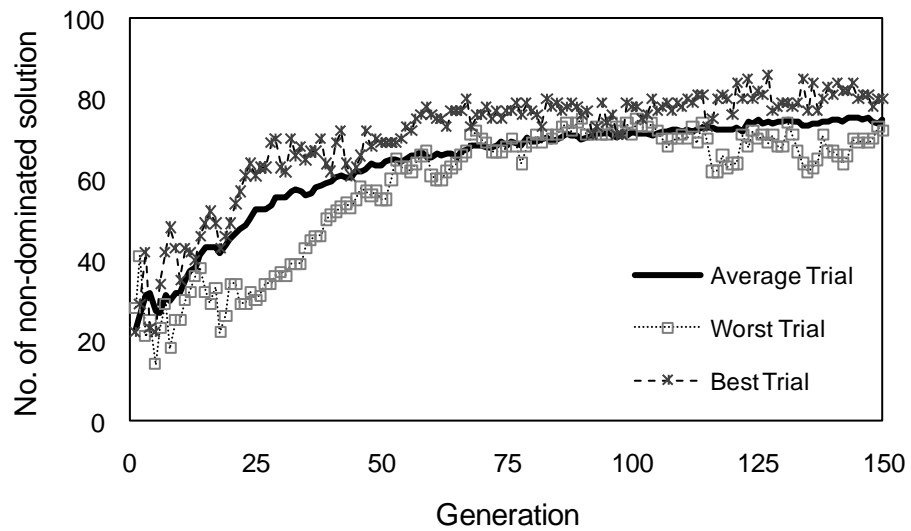


Fig. 3.10. Convergence of NSES for multi-objective water distribution system problem in terms of number of non-dominated solutions

3.7.3. Comparison of Non-dominated Solutions

The X-Y-Z scatter plots of the Pareto fronts from all of the 30 trials are compared in ‘fire flow-water quality-cost’ objective space where each point represents a solution indicating the aggregated fire flow, minimum residual chlorine, and the corresponding mitigation cost to implement that solution. Since the model minimizes the aggregated fire damage, the maximum chlorine deficiency, and the normalized cost of mitigation, consequently, the model returns maximized aggregated fire flow, maximized minimum residual chlorine, and minimum cost solutions. The scatter plots of the Pareto fronts from all 30 trials represent that the search is consistent. To get a better understanding of the Pareto front for the WDS problem, final solutions from the best trial are shown in a scatter plot in Fig. 3.11.

In existing condition, the available fire flows at hydrants HY29, HY53, and HY66 are 30 l/s (469 gpm), 55 l/s (873 gpm), and 55 l/s (869 gpm), respectively which generates an aggregated fire flow of 50 l/s (793 gpm). Although fire flow requirements vary regionally based on the development of the city and the population density, typically a fire flowrate of 63 l/s (1000 gpm) is required at fire hydrants serving single family residential buildings, and a flowrate of 158 l/s (2,500 gpm) is required at hydrants for multi-family residential/commercial/industrial buildings (BCS 2005). Thus in existing condition the Micropolis WDS fails to provide required fire fighting flows at all three hydrant locations. The minimum residual chlorine level in the existing condition is above the regulated minimum value of 0.2 mg/l.

Referring to Fig. 3.11 most of the Pareto-optimal solutions yield moderate to significant gain in both system wide fire flow and water quality with a few exceptions, however, each solution contributes to cost of mitigation with varying degrees. To understand the tradeoff relations between the conflicting objectives in detail, four non-dominated solutions, solution 1, solution 2, solution 3, and solution 4 are selected from the Pareto front, as shown in Fig. 3.11; the achieved objective values are listed in Table 3.2 and the decision variables (pipes) are shown in Fig. 3.12.

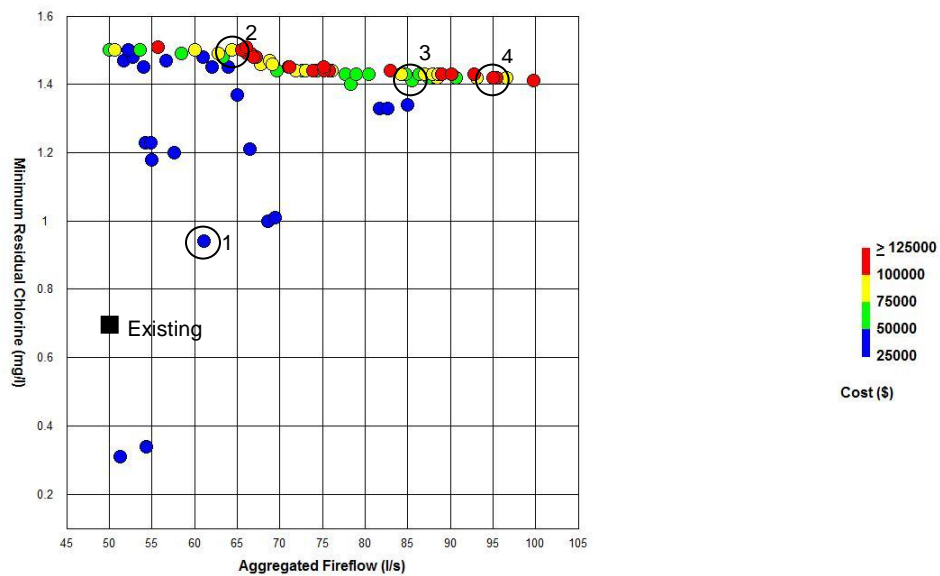


Fig. 3.11. X-Y-Z scatter plot of the Pareto-optimal solutions for the WDS after 150 generations, the WDS performance at existing condition is shown with a black square, solutions chosen for further discussion are enclosed in circles

Table 3.2. Comparison of Solutions in Fireflow Water Quality Cost Objective Space

Solution ID	Hydrant Fireflow			Aggregated Fireflow l/s	Minimum Residual Chlorine mg/l	Cost \$
	HY29 l/s	HY53 l/s	HY66 l/s			
Existing	30	55	55	50	0.71	0
1	77	58	55	61	0.94	33,364
2	74	64	56	64	1.50	82,132
3	131	79	64	85	1.41	57,187
4	160	85	67	95	1.42	107,290

Referring to Table 3.2, solution 1 provides sufficient fire flow at hydrant HY29 and less than required fire flows at both hydrants HY53 and HY66 resulting in an aggregated system wide flow of 61 l/s (967 gpm) which is a little less than the required one. The minimum residual chlorine level among ten water quality sensors for this solution is higher than the existing level. This solution involves 20 pipe enlargements with total length of 350 m (1,146 ft). Solution 2 involves 25 pipe enlargements (838 m [2748 ft]) and meets requirement of the system wide aggregated fire flow condition. This solution involves pipe enlargements near both the hydrants HY29 and HY53 thus provides improved fire flows at both the locations. Solutions 3 and 4 provide sufficient fire flows both at individual hydrant level and at aggregated level; solution 3 involves 23 pipe enlargements (630 m [2068 ft]) and solution 4 involves 28 pipe enlargements (949 m [3112 ft]). In the fire flow – water quality – cost objective space solution 1 is better than the other three in terms of the third objective: cost, but inferior to the others in terms of both aggregated fire flow and minimum residual chlorine; although the residual chlorine level is above the value required by government regulation. Solution 2 is better than solution 1 in terms of aggregated fire flow, however, is inferior to both solution 1

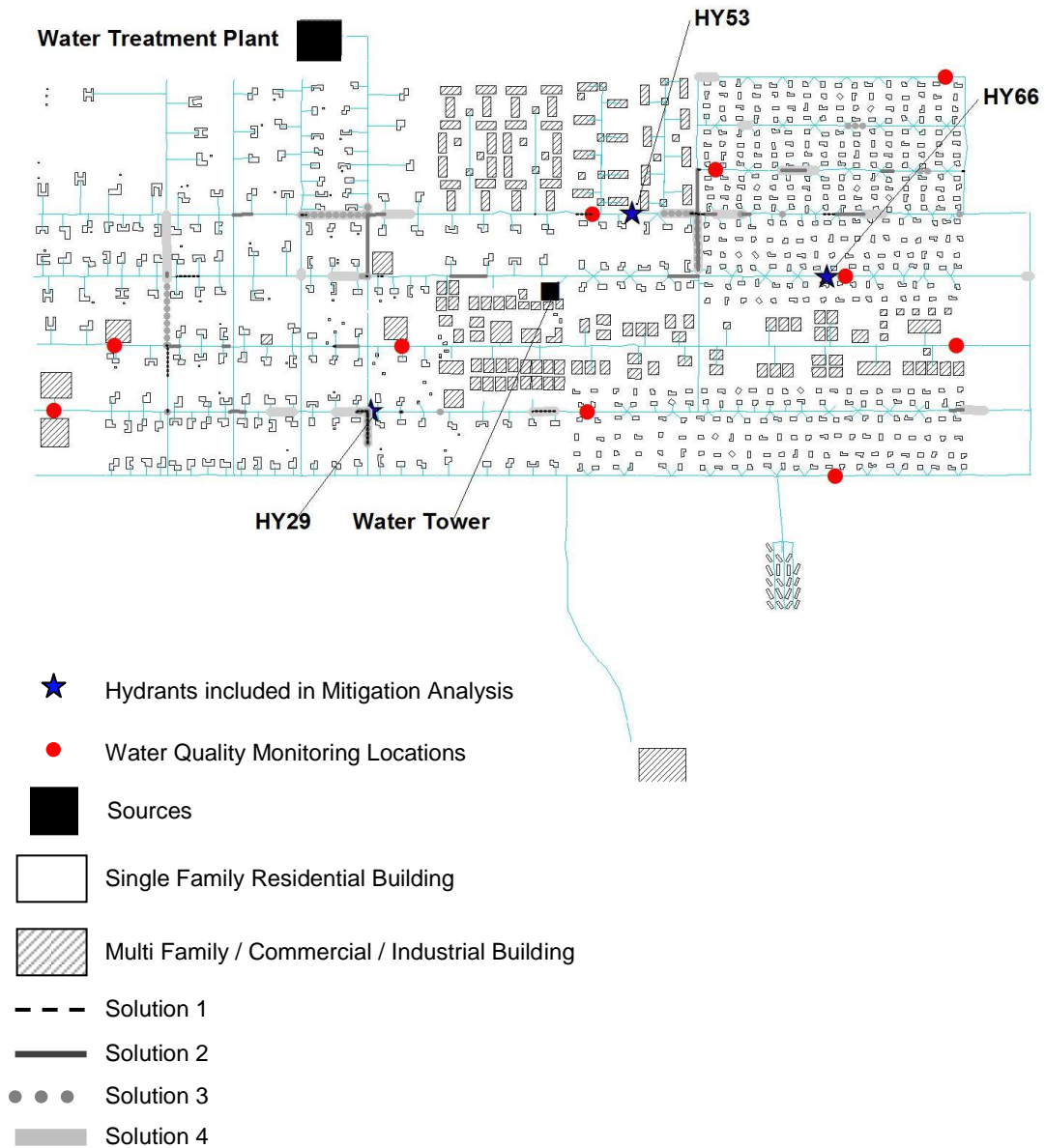


Fig. 3.12. Results (decision variables) of application of NSES to the multi-objective WDS problem

and solution 3 in terms of cost. Moreover, solution 2 produces the highest residual chlorine level among the four selected solutions. Similarly, solution 3 is better than both solution 1 and solution 2 in terms of the first objective, aggregated fire flow, and dominates solutions 2 and solution 4 in terms of cost and produces very different residual chlorine level than solution 1 and solution 2. Finally, solution 4 gives the most protection against fire event among the above mentioned solutions although it is inferior to solution 1, solution 2, and solution 3 in terms of cost.

From the above comparison it was observed that although the water quality fitness was mapped to satisfy the government regulation, however, there was not much of a variation in water quality between solution 3 and solution 4. This is due to the discontinuous set of decision variables which poses less effect on water age in this system. Overall, this comparison indicates that a tradeoff relationship does exist between the conflicting goals of WDS: fire flow, water quality, and cost.

3.8 Sensitivity to Variation in Water Distribution System's Fireflow Locations

To investigate the proposed methodology's applicability for different fire hydrant arrangements, NSES procedure is tested on Micropolis WDS with six fire hydrant locations. Among those six hydrants three are kept unchanged from previous investigation and three new fire hydrants are chosen from different parts of the city: one from the northwest region, one from the central business district, and one from the southeast region (Fig. 3.13). The weighting coefficients, α_i , to evaluate system wide aggregated fire flow are determined as described in section 3.6 and a required fire flow

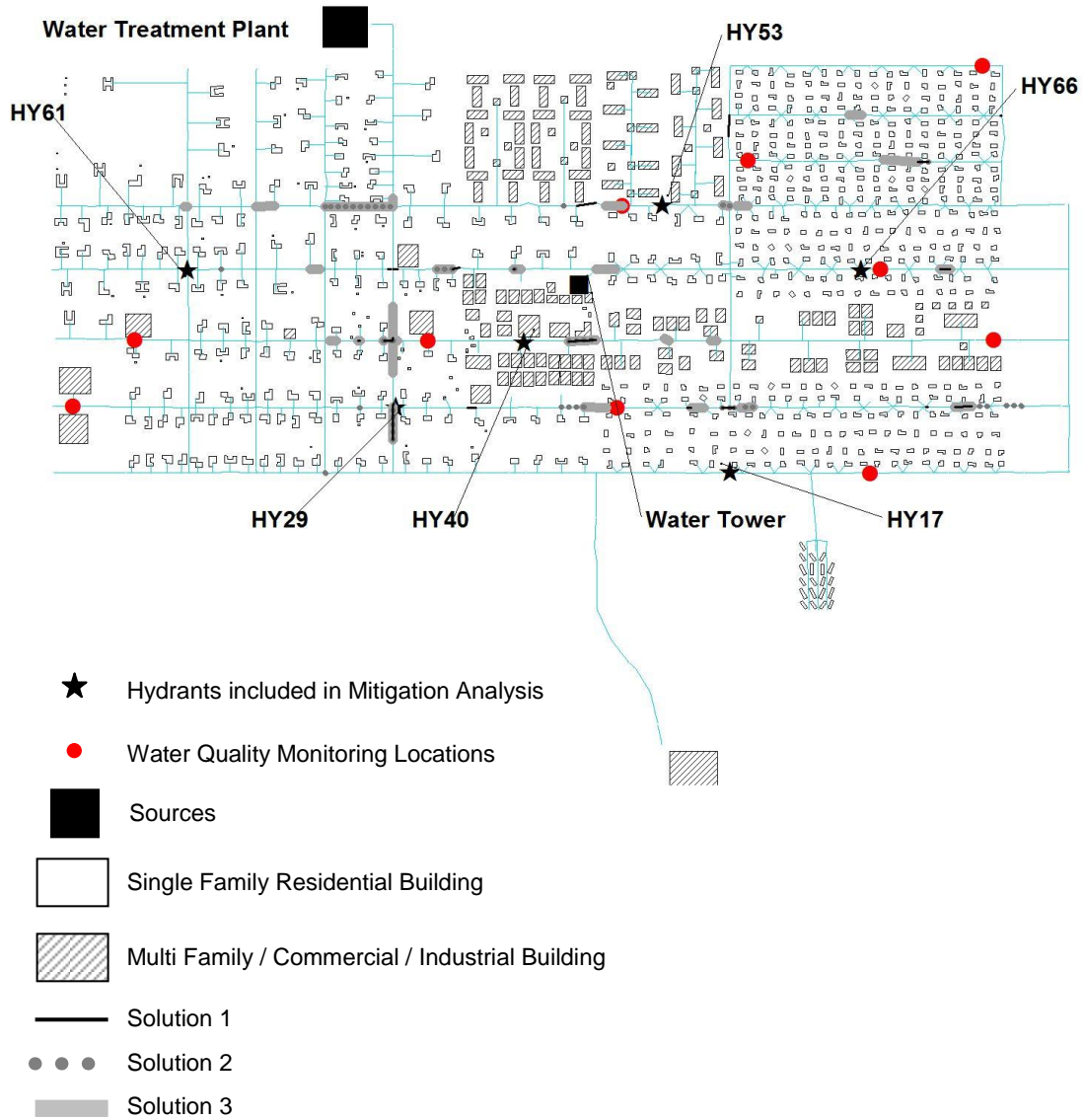


Fig. 3.13. Sensitivity analysis of application of NSES to the multi-objective WDS problem with six hydrant arrangements

of 63 l/s (1000 gpm) is considered at all six fire hydrants. The water quality sensors are kept unchanged. In this new problem the fire flow objective is optimized at more number of hydrant locations which makes the problem even harder. For this new arrangement, three different trials are conducted with the previously identified algorithmic parameters. The average hypervolume for this new arrangement is 0.4928 and the standard deviation of the hypervolume metrics is 0.005. Since the model optimizes fire flows at all six fire hydrants, the fitness values with respect to all three objectives changes and the Pareto fronts shifts from the previous analysis thus generates a slightly different hypervolume metric at convergence, which is as expected. The overall progression of both the hypervolume and the average number of non-dominated solutions with generation are consistent with that of previous analysis. Moreover, the Pareto fronts obtained with both previous and new analysis are similar in shape and in range. The X-Y-Z scatter plot of the Pareto optimal solutions from the best trial for this analysis is presented in Fig. 3.14. Three Pareto optimal solutions – solution 1, solution 2 and solution 3 - are chosen to further discuss the tradeoff relationship between the objectives.

As discussed in section 3.7.3 the system poses no fire protection at existing condition; the available fire flow at aggregated level as well as individual hydrant level is below the required fire flowrate of 63 l/s (1000 gpm) at all hydrant locations except at hydrant HY17. This condition obviously seeks for a new solution. Most of the solutions in the Pareto front yield moderate to significant gain of fire flow at all six fire hydrants. The minimum residual chlorine levels are also above the regulated value of 0.2 mg/l. Table 3.3 presents the objective values attained with solutions 1, 2, and 3. The locations

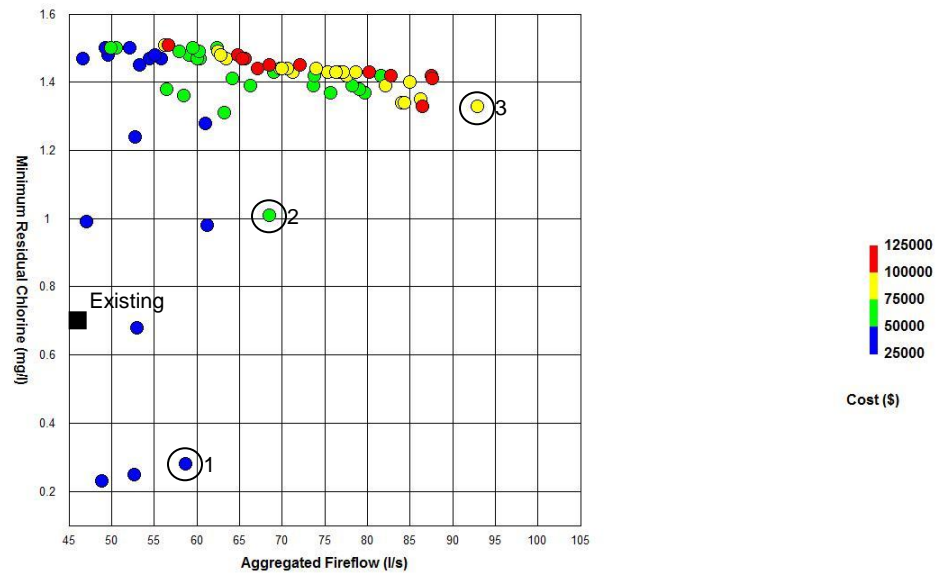


Fig. 3.14. X-Y-Z scatter plot of the Pareto-optimal solutions for the WDS with six hydrant arrangements after 150 generations, the WDS performance at existing condition is shown with a black square, solutions chosen for further discussion are enclosed in circles

Table 3.3. Comparison of Pareto-optimal Solutions from Sensitivity Analysis

Solution ID	Hydrant Fireflow						Aggregated Fireflow l/s	Minimum Residual Chlorine mg/l	Cost \$
	HY17 l/s	HY29 l/s	HY40 l/s	HY53 l/s	HY61 l/s	HY66 l/s			
Existing	71	30	19	55	59	55	46	0.71	0
1	72	72	48	56	59	56	59	0.28	34,728
2	100	96	52	62	73	60	68	1.01	52,148
3	160	171	59	74	98	71	93	1.33	99,071

of pipe enlargement (optimal decisions) for the three selected solutions are shown in Fig. 3.13. Referring to Table 3.3, solution 1 is better than the other two in terms of cost but

inferior to the others with respect to both fire flow and water quality objectives. Solution 2 is better than solution 1 in terms of both fire flow and water quality and better than solution 3 in terms of cost, however inferior to solution 3 with respect to fire flow. As a matter of fact, solution 3 produces the best fire flow for the new hydrant arrangements. The water quality attained with this solution is also very different than the other two; the cost is however the worst among the three solutions. It is worth to mention that hydrant HY40 is the most problematic in the system with a fire flow volume of 19 l/s (304 gpm) in existing condition. Fire flow volume at this location is significantly improved with all of the three solutions and also with all other solutions in the Pareto front; although solution 1 yields a little less than required fire flow. Finally it can be concluded from the analysis that the NSES procedure clearly demonstrates both persistency and robustness when applied to the Micropolis WDS with changed fire flow sensor arrangements.

3.9. Final Remarks

This paper illustrates a multi-objective optimization methodology for water distribution system which addresses the mitigation strategies during fire events. Although research on water systems' mitigation from natural and manmade hazard has been studied intensively in recent years; this paper introduces a new evolutionary computation-based multi-objective approach which effectively addresses the conflicting goals of the WDS: reliable delivery of water during normal as well as emergency conditions, meeting water quality standards, and finding cost-effective design and rehabilitation options.

An elitist non-dominated sorting genetic algorithm, NSGA-II (Deb et al. 2002), is modified by incorporating an ES-based search to develop the new approach, non-dominated sorted evolutionary strategy (NSES), to address difficulties for heuristic algorithms posed by WDS problems. The NSES algorithm has been applied to a number of test problems to measure the Pareto optimality. First, a deviation metric Δ , proposed by Deb et al. (2002), was evaluated for each of the test problems and the results were compared with NSGA-II. The test problem results indicate that the NSES algorithm is able to attain diversity among the solutions in the non-dominated objective space. Next, a scalar multi-objective metric, hypervolume (Fleischer 2003), was evaluated with the test problems. Hypervolume is a measure of both Pareto optimality and diversity. An efficient methodology for calculating hypervolume has been adopted from Fleischer (2003). NSES utilizes this metric explicitly at each generation and the results provide the evidence of both Pareto optimality and algorithmic convergence.

NSES methodology is then applied to a realistic problem in water distribution system's fire mitigation. Three objectives were considered during the analysis: (1) minimizing fire damages, (2) minimizing water quality deficiencies, and (3) minimizing the cost of mitigation. This methodology clearly generates Pareto-optimal solution surfaces that express the tradeoff relationship between fire damage, water quality, and least cost objectives; thus provides decision makers with the flexibility to choose a mitigation plan for urban fire events best suited for their circumstances. Each Pareto-optimal solution comprises a set of pipes to be enlarged to achieve increased fire flow and the corresponding diameters of these pipes. Although the model has the possibility

to add chlorine booster units as another set of decision variable, during the application of the model to the hypothetical case study, Micropolis, it was assumed that additional chlorine boosters will not be added. This is due to the fact that at existing condition the Micropolis WDS poses no system wide water quality deficiency. The Pareto optimal solutions also indicate that although there were variations among the solutions in terms of all three objectives, however, there were limited or no solutions in ‘high fire flow-low water quality-high cost’ region. Thus for this specific system it is difficult to conclude that a significant tradeoff relation exists between the emergency demand during an urban fire event and the water quality during normal demand condition. However, simulation of urban fire, if coupled with the water system, might show the actual fire consequences, mitigation strategies effectiveness, and the tradeoff relationship between fire damage, water quality, and least cost objectives.

Previous study of vulnerability and risk analysis (Section 2) introduced a new risk-based DP optimization approach which enables the water utilities to analyze the vulnerability and risk of the system during fire events. The probabilities of fire hazards, however, were not incorporated to perform a fire risk assessment for a coupled system of both water and fire response infrastructure. Previous studies also showed that the existing fire hazard and fire risk assessment methodologies neither consider probability of fire occurrences nor incorporate the actual WDS’s conditions, resulting in a defect in fire hazard assessment. Therefore, a novel methodology is needed to: (1) simulate the realistic fire consequences in a coupled system of water and fire model, (2) evaluate the real risks involved with it, and (3) the effectiveness of the Pareto-optimal mitigation

designs for the coupled system. The new investigation in fire hazard risk and mitigation assessment and its findings is discussed in detail as a separate article in Section 4.

4. A STOCHASTIC MODELING APPROACH FOR URBAN FIRE RISK ANALYSIS INCLUDING PERFORMANCE OF WATER AND FIRE RESPONSE INFRASTRUCTURES

4.1. Introduction

Urban fires can cause substantial damage to life and property, and fire safety is a major concern for infrastructure and emergency response planners, managers, and regulators. Fire hazard risk assessment has been practiced in regulatory systems for decades. However, avoidance and response to fire hazards is accomplished through a complex combination of systems (buildings, emergency responders, water distribution, being primary), and these systems are typically not assessed in a holistic manner with full understanding of dynamics and probabilities. Hence, a novel fire risk assessment approach is useful to estimate the probability of occurrence of fire variables and system performance metrics as well as to evaluate urban fire consequences.

A fire hazard is a condition or physical situation with a potential for undesirable consequences which results from a specific fire scenario in a specific environment. A fire scenario can be defined as a specific fire including its developmental variables, i.e., origin of fire, time of the day, wind speed and direction, temperature curve, etc. (Brannigan and Kilpatrick 1997). Water supply plays a vital role during fire. Studies of historical urban fires (Scawthorn et al. 2005) show that consequences from both earthquake fires (1906 San Francisco, California earthquake and fire, 1989 Loma Prieta, California earthquake and fire, 1994 Northridge, California earthquake and fire, among

others) and non-earthquake fires (1923 East Bay Hills, Berkeley, California fire, and 1991 East Bay Hills, San Francisco, California fire, among others) greatly depend upon water distribution system (WDS) performance during the events. Thus WDS failure can be considered as another variable to a fire scenario.

Scawthorn et al. (2005) view the occurrence of fire as a process which involves ignition, discovery, report, response, fire growth and spread, and suppression. Other key factors associated with a fire event are period of delay; which may occur during a report and/or during response, and liaison between the water and fire departments. Delays are particularly common following an earthquake and may promote fire growth and spread. Frank Blackburn, a former Fire Chief of San Francisco Fire Department has written:

Consistently providing adequate water supply for fire protection requires close liaison and cooperation between the fire and water departments. Unfortunately, these agencies are in most cases not part of the same governmental jurisdiction. As a result, understanding and awareness between the organizations can be lacking ... Coordination between the organizations can be complex and difficult to achieve... (Ballantyne et al. 1997)

Various combinations of the above mentioned fire variables along with the numerous factors of the fire process will result in varying degrees of consequences, both in terms of life and property. Bristow (2006) has developed a model of the interdependent water distribution and fire response infrastructures, to simulate various multi-mode attack and failure (MMAF) events and has outlined the process of effective mitigation design to reduce consequences of these MMAF scenarios. The method is however, iterative and does not provide any measure of urban fire risk. A need exists for an approach to effectively address the key aspects of urban fire risk including both the probabilities of occurrence and the consequences of fire scenarios.

In this study a novel urban fire risk assessment methodology was developed that includes simulation of urban fire dynamics, water distribution system performance, fire response, and the following risk factors: building ignition, WDS failure, and wind direction. The total annual probability of a given fire scenario was estimated as a joint probability of building ignition, wind direction, and WDS failure. A coupled model of water and fire response infrastructure (Bristow 2006) was utilized to evaluate fire consequences in terms of number of displaced people and cost of property damage. Urban fire risk (number of displaced people/year) for a particular scenario was then estimated as a product of total probability (per year) of a fire scenario and the fire consequences (number of displaced people). A Monte Carlo (MC) simulation (Hasofer et al. 2007) was utilized to generate numbers of possible fire scenarios sufficient to estimate the distribution of consequences with high confidence. Finally, a multi-objective approach, Non-dominated Sorting Evolution Strategy (NSES) was utilized to design effective mitigation strategies to manage the urban fire risk. The objectives considered in mitigation design were: (1) minimizing fire damages, (2) minimizing mitigation cost, and (3) minimizing water quality deficiencies. A virtual city was then used to demonstrate the application of the proposed methodology to an integrated water and fire response system. The specific goals of this research are to:

- Develop a methodology to assess urban fire risk including key aspects of and potential failure of water and fire response infrastructures;
- Identify critical scenarios based on the probabilities as well as consequences; and

- Design effective fire mitigation strategies in a multi-objective framework based on scenario-based results to manage the system wide urban fire risk.

The methodological steps involved in urban fire risk analysis with coupled water distribution and fire response services are presented in Fig. 4.1. The next section provides a brief introduction to existing fire models for consequence evaluation and the following sections describe the development of the methodology, implementation, and results in detail.

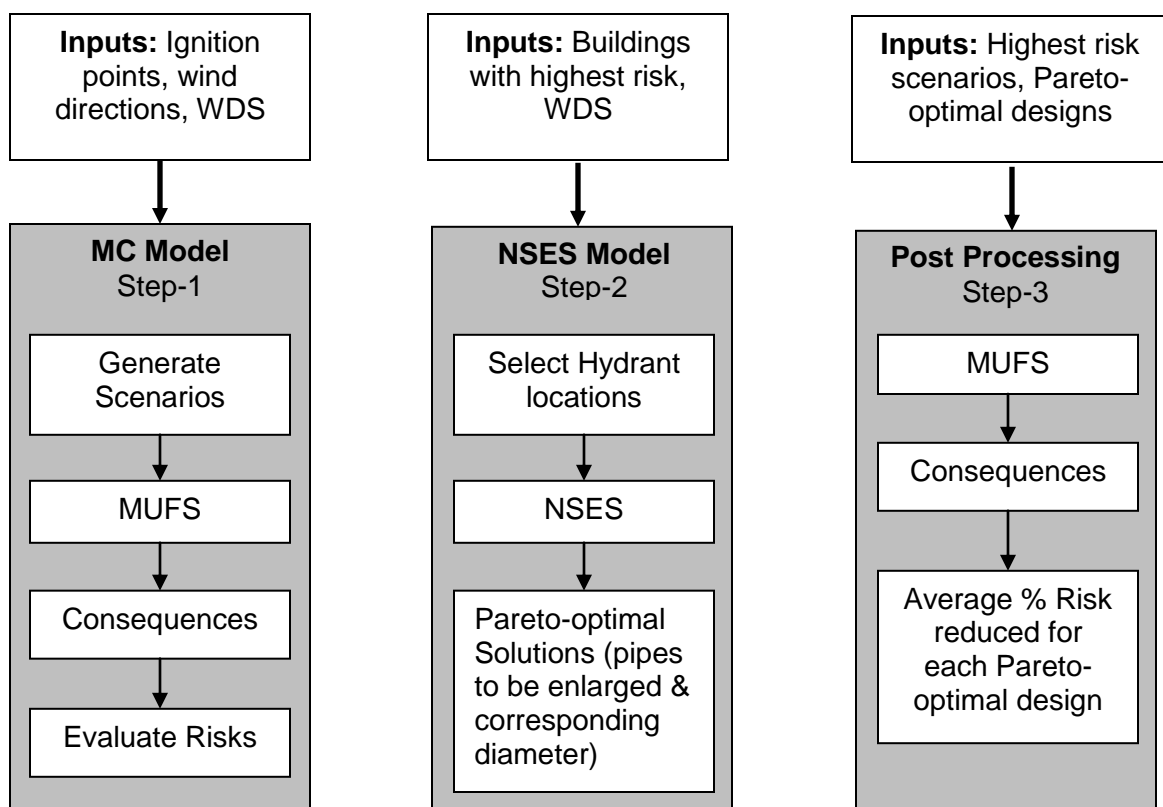


Fig. 4.1. Methodological steps in urban fire risk analysis

4.2. Computerized Fire Models

Many mathematical models of fire and smoke have developed throughout different countries in the world to study various aspects of fire risk and fire protection. These models include compartment fire models, fire-sprinkler interaction models, fire endurance models, fire spread models, fire suppression models, and smoke movement models (Friedman 1992). Scawthorn et al. (2005) discuss different fire growth and spread models developed during the last few decades. Some of those are discussed in detail below from Scawthorn et al. (2005).

- *The Hamada Model.* The most widely used urban fire spread equations are Hamada equations (Hamada 1951, 1975) which are derived empirically based on historical data from 1923 Kanto earthquake in Tokyo, Japan. Hamada equations are based on the assumption that the urban areas are series of equal blocks of buildings, and the buildings are equally spaced. The Hamada model estimates fire spread within one city block or a built-up district but does not account for fire spread across streets. Many subsequent fire spread models used the Hamada model as a foundation.
- *HAZUS.* HAZUS is a simulation modeling and planning tool which is used to produce loss estimates for earthquake risk mitigation (HAZUS 1999). The fire following earthquake module of HAZUS uses a fire ignition model, the Hamada fire spread model, and a fire suppression model that varies with availability of water during fire events. This tool is currently used by the Federal Emergency Management Agency (FEMA) as well as by federal, regional, and local

governments in planning for earthquake risk mitigation, emergency preparedness, response, and recovery. The ignition model under HAZUS operation predicts the urban fire's ignition points based on a design earthquake event; the model does not permit the user to specify ignition points. HAZUS utilizes the original Hamada fire spread model as described earlier. Finally, the model generates the urban fire's consequences in terms of potential dollar loss caused by fires. One of the major limitations of HAZUS is that the model assumes the water system inventory based on population density, not the actual characteristics of a water system.

- *MUFS*. One of the most recent developments in urban fire spread model is the MUFS (Model of Urban Fire Spread) (Bristow 2006). MUFS is a numerical model of fire ignition, fire spread, and fire suppression which can measure the span of burnt area resulting from a single or multi-ignition fire when the water system is partially or severely damaged. Unlike the Hamada model, MUFS can implement topology related building parameters for each individual building to determine the fire spread. Some of the topology related parameters include coordinates of vertices of each building, floor area and height, number of occupants, and building's fire proof construction. A building's fire proof construction parameters are: (i) Occupancy Hazard Classification (OHC) – an integer measure of fire danger posed by the building's contents, (ii) Exposure Factor (EF) – adjacency to other buildings, and (iii) Construction Classification Number (CCN) – level of fire proof construction techniques employed in

constructing the building. MUFS requires detailed information about the layout and connectivity of the community's water distribution system. MUFS utilizes building specific parameters, for instance: building size, construction materials, fireproofing techniques, to calculate the amount of water needed for fire suppression. MUFS also allows the user to specify the fire ignition points. Thus the inputs to MUFS are fire ignition points, building map and building properties, water distribution system information, fire truck availability schedule, wind speed, and wind direction. MUFS generates the fire spread vectors in terms of burn front coordinates, and estimates the fire consequences in terms of a list of burned buildings and the number of dislocated people from each burned building.

4.3 Components of Urban Fire Risk Assessment

Risk is the combination of the probability of an event and its consequences (ISO 2001). Traditionally, risk assessment addresses four basic questions: (1) What can go wrong? (2) How likely is it? (3) What are the consequences if it does go wrong? and (4) How certain is this knowledge? (Stern and Fineberg 2003). To answer these questions, the first step would be hazard identification; the second step would be estimation of probabilities for identified hazard scenarios; the third step would involve estimation of potential losses; and the last step would be analysis of uncertainty. Thus fire risk assessment would incorporate identification of fire scenarios; prediction of the probability distribution of fire hazards; evaluation of consequences resulting from fire growth and spread; and incorporation of uncertainty during both quantitative analysis

and risk characterization. The following sections describe the steps adopted in urban fire risk assessment.

4.3.1. Building Ignition Frequency

For quantitative assessment of urban fire risks, ignition frequency derived from regional fire statistics is the first step in fire risk assessment. From previous studies it has been found that ignition frequency depends upon both on floor area of buildings and building category (Tillander and Keski-Rahkonen 2002, Rahikainen and Keski-Rahkonen 2004, Lin 2005). Barrois, a French statistician, has proposed a generalized model where the ignition frequency is presented in the following form (Hasofer et al. 2007):

$$f(A) = c_1 A^r + c_2 A^s \quad (4.1)$$

where, $f(A)$ = average annual probability of a fire starting in a building in the category under study with area A (1/m²-anum); A = floor area of the building (m²); c_1, c_2, r, s = coefficients to be determined experimentally from observations for different building categories.

Tillander and Keski-Rahkonen (2002) study structural fires in Finland for the period 1996-1999 and fit the generalized Barrios model to observations on three different categories of buildings: (1) residential buildings, (2) industrial buildings and warehouses, and (3) all other buildings. It has found from the study that the generalized Barrois model is useful in determining the ignition frequency of buildings with a floor

area between 100 and 20,000 m^2 (square meters) (Tillander and Keski-Rahkonen 2002).

During the present study, the generalized Barrois model (Eq. 4.1) was used to estimate the probability of building fires in three categories of buildings: (1) residential buildings, (2) industrial buildings and warehouses, and (3) all other buildings. The model parameters used in the Finland study were applied accordingly and are presented in Table 4.1.

Table 4.1. Parameters of the Generalized Barrois Model Fitted to Observations in Finland (Tillander and Keski-Rahkonen 2002)

Building category	c_1	$c_2 \times 10^{-6}$	r	s
Residential buildings	0.01	5	-1.83	-0.05
Industrial buildings and warehouses	0.07	6	-1.48	-0.05
All buildings except residential and industrial buildings and warehouses	0.01	3	-1.25	-0.05

4.3.2. Wind Properties

Wind, particularly the wind direction, plays a vital role in determining the extent of fire spread in an urban area. Generally, fire does not spread only in the dominant wind direction or downwind direction - the direction wind is blowing to. Based on the dominant wind direction and speed, fire propagates in three other directions: upwind direction, the direction of the wind's origin; sidewind-left, the direction which is 90 degrees counter-clockwise from downwind direction; and sidewind-right, which is 90 degrees clockwise from downwind direction (Bristow 2006). The dominant wind

direction of a region varies geographically. The distribution of dominant wind direction for any region therefore, can be estimated from historical observations of meteorological data.

4.3.3. Water System Failure Probabilities

Water systems are vulnerable to various physical, chemical/biological, and cyber threats (Haines et al. 1998) which could cause potential damages to the systems. During this analysis, two failure scenarios of a water distribution system were considered during a fire event: (1) accidental failure due to soil-pipe interaction, and (2) accidental failure due to a seismic event.

Deterioration of pipes due to aging often cause pipe breaks and leaks and has been a major concern of water utility industries. Yamijala et al. (2009) have proposed a logistic generalized linear model (logistic GLM) for estimating the probability of pipe breakage due to soil-pipe interaction. Using historical (2000-2005) pipe break data from a major U.S. city, they have developed a statistical model to estimate the probability of pipe failure for a water distribution system. The results from their analysis showed that the variables that are statistically significant at a level of 5% for the studied system were: (1) pipe diameter, (2) pipe material, (3) pipe length, (4) land use type, and (5) soil type. For any given water system with known soil profile and zoning data, the likelihood of pipe failure at least once in a five year period caused by soil-pipe interaction for each individual pipe in the system can be estimated using the logistic GLM (Yamijala et al.

2009). Hence, in this article the logistic GLM (Yamijala et al. 2009) was used to estimate pipe failure probabilities due to pipe aging.

Seismic wave propagation often causes transient soil deformation and can produce well-dispersed damage to buried pipelines (Eidinger 2005). Studies showed that pipes that are made of cast iron or asbestos cement perform poorly during seismic events; ductile iron pipes, being more durable than cast iron, generally perform better than the other two. The level of ground shaking at any pipeline location is generally measured in terms of peak horizontal ground velocity (PGV). When the soil mass experiences long duration strong ground shaking, then landslides or liquefaction occurs and causes severe damage to the pipes. The amount of landslide or liquefaction movement is generally measured in terms of permanent ground displacement (PGD). Eidinger (2005) has developed a set of fragility curves using available pipe damage data from historical earthquakes. These curves are expressed as repair rates per unit length of pipe, and as a function of peak ground velocity (PGV) or permanent ground deformation (PGD). The pipe damage algorithm or fragility curves are expressed as follows (Eidinger 2005):

$$RR = K_1*(0.00187)*PGV \text{ (for wave propagation)} \quad (4.2)$$

$$RR = K_2*(1.06)*PGD^{0.319} \text{ (for permanent ground deformation)} \quad (4.3)$$

where, RR = repairs per 305 m (1000 ft) of main pipe; PGV = peak ground velocity in 0.0254 m/second (inch/second); PGD = permanent ground deformation in 0.0254 m

(inch); K_1 = ground shaking constants for fragility curve; and K_2 = permanent ground deformations constants for fragility curve. The constants K_1 and K_2 vary with different pipe material, joint type, soil, and pipe diameter. Detailed list of values for K_1 and K_2 can be found in Eidinger (2005). In this article only ground shaking hazard was considered, hence, equation (4.2) was applied.

4.3.4. Determination of Fire Consequences

Urban fires may result in several outcomes, such as property losses, dislocation of occupants, injuries, and human fatalities, among others. According to Stern and Fineberg (2003) ‘risk’ is a complex phenomenon and it has multiple dimensions. Thus urban fire risk also poses multi-dimensional risks such as social risk, economic risk, and risk to the ecosystem. All of the computerized fire models discussed in section 3 can generate consequences in terms of dollar losses or human fatalities. However, none of the fire models can handle the multi-dimensional nature of urban fire risk. Reviews of the literature show that there are arguments about converting human fatalities and injuries into monetary units (Stern and Fineberg 2003). MUFS can determine which buildings are burned at the end of the fire simulation period and can report the total number of dislocated people from those burned buildings as the urban fire’s final consequences. MUFS thus simplifies the dimensionality of urban fire risk without aggregating different dimensions into a single overall measure.

MUFS also has several advantages over other fire models, for example, it allows user defined inputs of the fire ignition point (or points), delay in report and response to

urban fire, building topology and spacing, and water supply system topology. Therefore, MUFS was used for consequence evaluation during urban fire.

4.3.5. Estimation of Urban Fire Risk

Risk estimation involves identification and probabilistic evaluation of failure scenarios (Hasofer et al. 2007); quantitatively:

$$\text{Risk} = (\text{Probability of an event}) * (\text{Consequence of an event}) \quad (4.4)$$

In this dissertation two expressions of risk will be defined and evaluated following from Eq. (4.4). First, “scenario risk” is determined for a specific convergence of probabilistic events; here, a fire scenario is considered as a “triplet” consisting of (i) ignition, (ii) wind direction, and (iii) WDS condition. Each element of this triplet itself is a random event and a combination of these events would result in another random event – consequences. The previous sections described the methods of estimating probabilities for different fire variables and evaluation of consequences. The probability of a specific scenario is the joint probability of the three events in the triplet. A common way to model different failure events during a fire hazard would be event tree and fault tree analysis (Pate-Cornell 1984); this could be extremely complex and would require great expense of time. On the other hand, a Monte Carlo method can generate a sample of fire consequences based on the probability distribution of the underlying random events - ignition, wind direction, and WDS failure. Therefore, a Monte Carlo simulation

approach was used to generate a large number of fire scenarios and thereby to estimate scenario risks. Fig. 4.2 shows the steps involved in Monte Carlo procedure to evaluate scenario risk.

A second expression of risk is “global risk,” defined as the aggregation of risk for a region (e.g., a city) across the universe of scenarios. Two different methods to estimate global risk are used herein. First, global risk can be estimated as:

$$E(\text{GlobalRisk}) = E(\text{Conseqs.}|\text{FireEvent}) * E(\text{FireEvent}) \quad (4.5)$$

where, $E(\text{GlobalRisk})$ = expectation of global risk expressed in consequences per year; $E(\text{Conseqs.}|\text{FireEvent})$ = expectation of consequences per fire event assuming that a fire event occurs; and $E(\text{FireEvent})$ = expectation of the number of fire events per year. Eq. (4.5) is based on the assumption that the random variables *Conseqs.* and *FireEvent* are independent; i.e., the consequences of any particular fire event are independent of the number of fire events that occurs in a given year. To estimate the global risk for an urban area using this method, both distribution of consequences per fire event and distribution of fire events for any given year are required.

A second means of estimating global risk is:

$$E(\text{GlobalRisk}) = E(\text{Conseqs.}\{\text{NoCond}\}) \quad (4.6)$$

where, $E(\text{Conseqs.}\{NoCond\})$ = expectation of consequences per year with no conditioning on occurrence of fire events (i.e., probability of non-ignition is included in

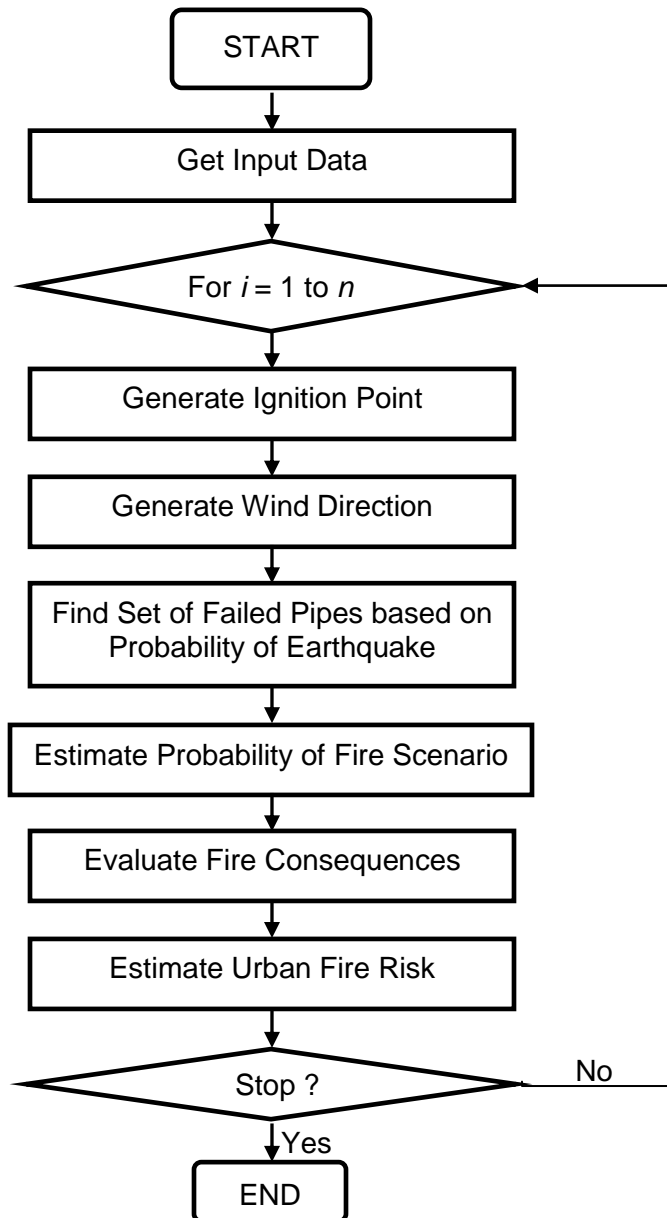


Fig. 4.2. Flowchart for Monte Carlo procedure to evaluate scenario risk

the expectation operator). To estimate the global risk using this method, the distribution of consequences per year (including non-ignition probability) is required. A Monte Carlo simulation can be utilized to estimate the annual distribution of consequences per year. A major difference between scenario risk and global risk is that scenario risk can be regarded as a “building-specific” risk; thus, individual building owners might be interested in scenario risks; global risk on the other hand provides risk for a particular region as it combines all possible scenario risks; thus, a city council might be interested in it. Generally, the global risk values are much higher than the scenario risk values.

4.4. Application of Urban Fire Risk Assessment Methodology to a Coupled Water and Fire Model

To demonstrate the risk assessment methodology for urban fire events, a hypothetical case study was performed for the virtual small town “Micropolis” (Brumbelow et al. 2005, 2007). Detailed description of available data and implementation of the methodology are presented in the following sections.

4.4.1. Description of Data and Estimation of Probabilities

“Micropolis” has an approximate area of 5.2 km^2 (2 mi^2) and a population of 5,000. It has a detailed water system model, a detailed building map, a soil map, and a geographic information system (GIS) database which are used throughout the analysis. The city has 868 buildings which include single-family, multi-family, commercial, and industrial buildings and warehouses. The WDS of the city has two major sources of

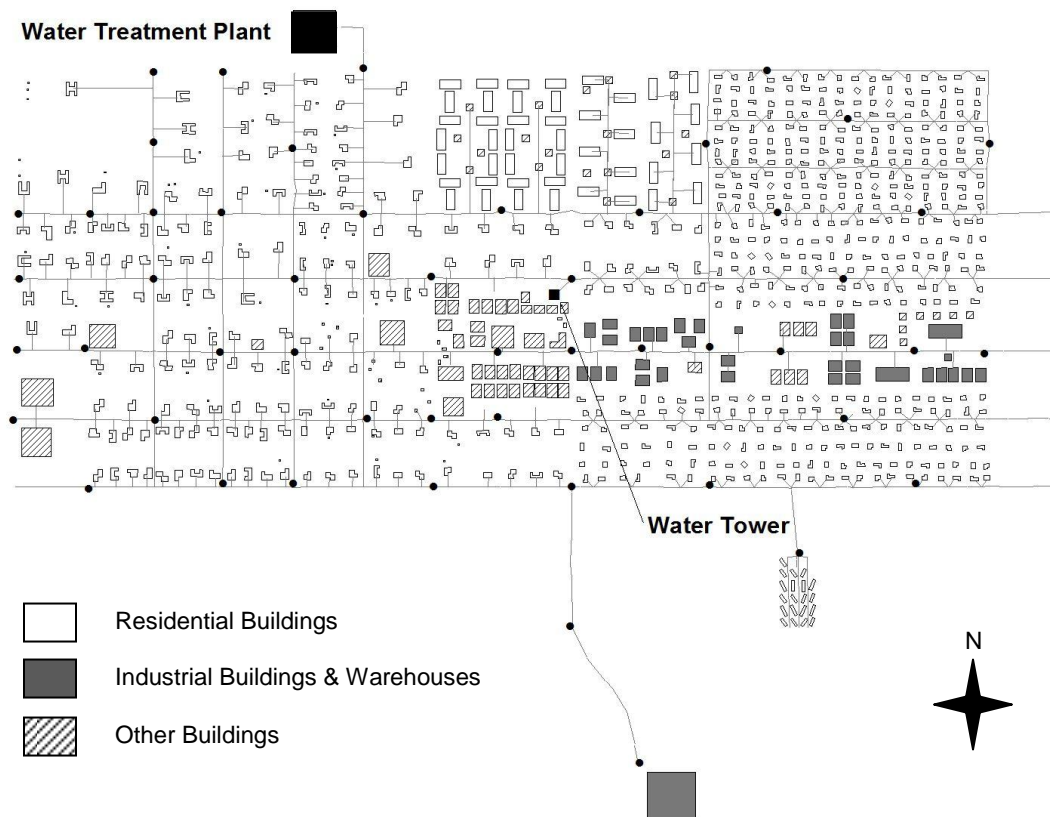


Fig.4.3. Building map of Micropolis with WDS shown in thin lines, water sources are shown in black squares, and fire hydrants are shown in black dots

water, a surface-water reservoir and a well field. Water from these sources is treated in a treatment plant. The current version of its water system model consists of a pumping station consisting of three pumps, one elevated storage tank, 1088 pipes, 1210 non-hydrant nodes, 52 fire hydrants, and 196 valves. Among the 1088 pipes there are 577

water mains and the remaining pipes are service and hydrant connections. Fig. 4.3 shows the building map of Micropolis with the water distribution system in thin lines.

The generalized Barrois model (Hasofer et al. 2007) was utilized to evaluate the ignition frequency of the buildings in Micropolis. First, all buildings were grouped into three categories: (1) residential buildings, (2) industrial buildings and warehouses, and (3) all other buildings. Using Barrois model for different building categories (Eq. 4.1), fifteen thousand Monte Carlo simulations were performed to estimate the annual probability of single fire in each building. Since the city's fire response unit solely depends upon the city's WDS capacity for firefighting flows and the daily demand of the WDS changes during the 24-hour period of a day, it is also important to estimate the probability of multiple ignitions during any day of the year for the city. The estimated annual probabilities of single ignition for buildings were converted to a daily probability of fire by a simple division by 365 days/year. Then fifteen thousand Monte Carlo simulations were performed to generate a distribution for number of building ignitions per day for the city. From this distribution it was found that the city has negligible threat of multiple ignitions in any day during a year (the probabilities of having 0, 1, and more than 1 ignition on a given day were 0.997, 0.003, and 0.000, respectively). Therefore, only single building ignition events were considered for further analysis.

The historical wind data (1984 – 2008) from Amarillo, Texas, was analyzed to determine a realistic frequency distribution of wind direction that could be used for Micropolis. The estimated annual wind frequencies in all eight directions are listed in

Table 4.2. A wind speed of 4.47 m/s (10 mph) was considered throughout this analysis following the findings of Bristow (2006).

Table 4.2. Annual Frequency Distribution of Wind Direction

Wind Direction	Probability
North (N)	0.127
Northeast (NE)	0.084
East (E)	0.050
Southeast (SE)	0.086
South (S)	0.303
Southwest (SW)	0.211
West (W)	0.087
Northwest (NW)	0.053

From the GIS database of Micropolis and the soil map of the area, the detailed information about pipe diameter, length, pipe material, pipe corrosivity to soil, soil type, and overlying land use data were extracted for each of the 577 water mains. Then using the logistic generalized linear model of Yamijala et al. (2009) the annual probability of failure of each of those 577 pipes was estimated.

To estimate pipe damage due to seismic risks the PGV-dependent model of Eidinger (2005) – Eq. (4.2) – was used. Data from the 1994 Northridge, California, earthquake on PGV values were used to estimate an exponential distribution for PGV.

Repair rates for cast iron (CI), asbestos cement (AC), and ductile iron (DI) pipes were estimated using Eidingger's fragility curves. Ten thousand Monte Carlo simulations of PGV magnitude were carried on with repair locations randomly assigned to pipes within each material class. The results of the Monte Carlo simulations were then aggregated to produce an annual seismic failure probability for each individual pipe.

4.4.2. Evaluation of Fire Consequences

The scenario risk approach described in section 4.3.5 was implemented in a computer code in Visual Basic 6.0 which utilizes iterative Monte Carlo solutions of MUFS evaluated under each scenario based on the distribution of the fire triplets – ignition, wind direction, and WDS failure. The specific outputs from MUFS under each scenario are: (1) a fire spread profile, (2) list of burned buildings, and (3) number of displaced people. Sample size (number of possible scenarios) of the Monte Carlo simulation was determined based on sample size convergence for stochastic analysis provided by Montgomery and Runger (1999) as follows:

$$n = \left(\frac{z_{\alpha/2} \sigma}{E} \right)^2 \quad (4.7)$$

where, n = sample size; $z_{\alpha/2}$ = upper $100\alpha/2$ percentage point of the standard normal distribution; σ = sample standard deviation; and E = specified error (absolute difference between the true mean and the sample mean).

Morgan and Henrion (1990) recommended that a small Monte Carlo run of ten simulations be used to get an initial estimate of sample standard deviation. Therefore, to determine the sample size using Eq. (4.7), ten Monte Carlo simulations were performed to get an initial estimate of the standard deviation of the consequences in terms of number of displaced people. It was found that $\sigma = 553$ displaced people. Then assuming the error $E \leq 15$ displaced people and desiring a 95% confidence interval ($z_{\alpha/2} = z_{0.05/2} = z_{0.025} = 1.96$), the necessary sample size was determined to be 5,221. Therefore, it was decided that 5,250 Monte Carlo simulations would be performed.

For each Monte Carlo run, the total probability of a scenario was estimated as a joint probability of ignition, wind direction, and WDS failure. Assuming independence of the three factors, the total probability of a fire scenario was estimated as:

$$\text{Probability of Fire Scenario} = P(I) * P(W) * P(F) \quad (4.8)$$

where, $P(I)$ = annual probability of building ignition; $P(W)$ = annual probability of wind direction; and $P(F)$ = annual probability of pipe failure. Finally, the risk from each scenario was estimated using Eq. (4.4).

4.5. Analyzing and Characterizing the Results

The methodology presented above generated 5,250 urban fire scenarios for the city Micropolis, each of which includes an ignition point, wind direction, and WDS condition. The model also generated the output for each scenario in terms of number of

displaced people as well as urban fire risks associated with those scenarios. Property losses were also estimated based on the replacement construction cost of burned buildings. Fig. 4.4 shows the histogram of fire consequences (number of displaced people) per scenario where each scenario is conditioned to a fire event.

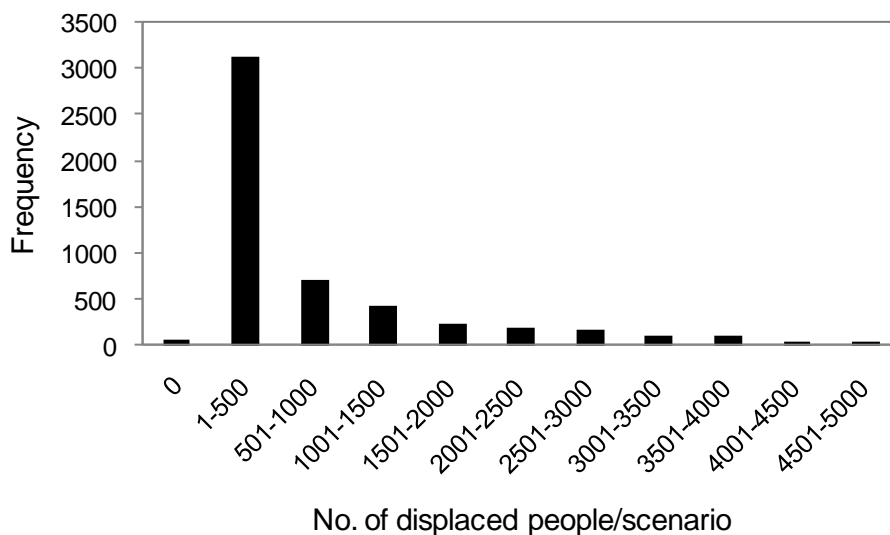


Fig.4.4. Histogram of fire consequences conditioned on ignition for Micropolis

To estimate the global urban fire risk for the city using Eq. (4.5), first the consequences from 5,250 scenarios were fitted to a gamma distribution (Haan 2002). The expectation of consequences per fire event conditioned on fire $[E(Conseqs.|FireEvent)]$ was estimated to be 739 displaced people/fire event. Then a binomial distribution (Haan 2002) was used to estimate the expectation of number of fire events in Micropolis for any given year $[E(FireEvent)]$ based on the estimated

probability of a single fire in any given day described in section 4.4.1. It was found that the expectation of fire [$E(\text{FireEvent})$] for the case study was 1.216 fires/year. Therefore, using Eq. (4.5) the expectation of risk or the global urban fire risk for the city was estimated to be 899 displaced people/year. To verify this global risk value, the second method [Eq. (4.6)] was used by implementing another Monte Carlo run not conditioned on ignition and the distribution of consequences per year was fitted to a gamma distribution (Fig. 4.5). The global risk using this method was estimated to be 825 displaced people/year. Implementation of both the methods of estimating global risk clearly verifies that the global urban fire risk for the city is pretty high.

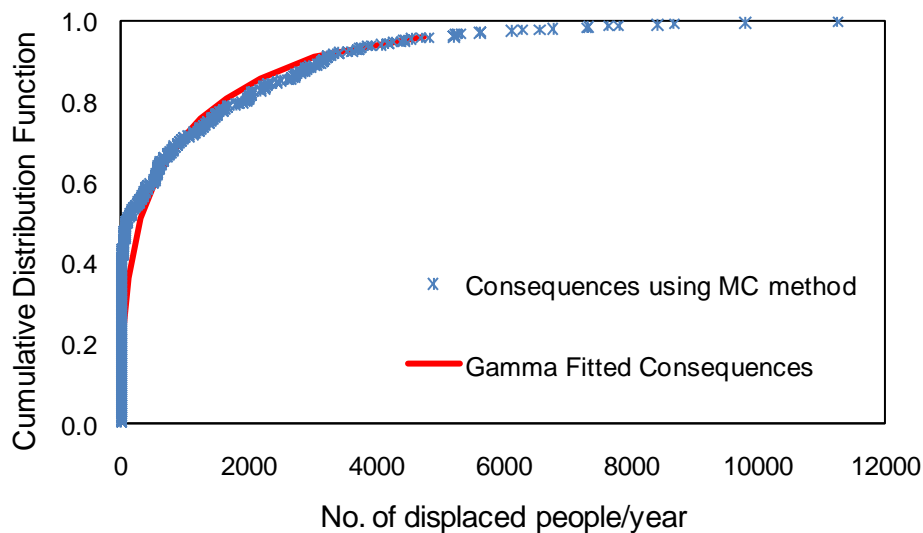


Fig.4.5. Gamma fitted distribution of consequences not conditioned on ignition for Micropolis

There are several reasons for evaluation of such a high global risk value for the city. First, MUFS output is highly dependent on the topology of an urban area. Currently in Micropolis database, several high occupancy buildings such as schools, churches, and industrial buildings, are located in the center of the city. Frequent occurrences of such high occupancy buildings constitute to larger consequences. Second, during consequence evaluation any building within the burn polygon is considered as fully burned; MUFS does not differentiate between partially burned and fully burned conditions resulting an overestimation of consequences in terms of displaced people. Third, determination of the extent of burned area is based on the interpolation of front points at each time step. This approach results in an exponential growth of burn polygon at each time step. Finally, as has been seen in previous sections the Micropolis WDS is in many locations insufficient to provide standard fire fighting flows even for single hydrants. Ignition of a fire near one of these poor performing sections of the WDS could allow the fire to grow unchecked to a large conflagration.

To analyze the scenario-based urban fire risk, the 5,250 scenarios were sorted in non-decreasing order of the risk value in terms of number of displaced people per year per scenario and 30 highest risk scenarios were chosen. Table 4.3 shows 30 highest risk scenarios for Micropolis. Based on the probabilities of fire triplets, the scenario-based urban fire risk was estimated in terms of both number of displaced people per year and property losses per year. Referring to Table 4.3, three important observations were made. First, none of the 30 highest risk scenarios involved any number of pipe failures; this indicates that the WDS was functioning with its usual capacity. Second, the

Table 4.3. Highest Risk Scenarios for Micropolis Generated from Monte Carlo Analysis

Scenario No.	Ignition Point	Facility Type	Wind Direction	No. of Failed Pipes	Joint Probability	Consequences		Risk	
						No. of Displaced People	Property Losses (\$)	No. of Displaced People/yr	Property Losses (\$/yr)
1	764	Warehouse	SW	0	0.0011	4,246	79,172,478	4.5	84,645
2	770	Industry	S	0	0.0020	2,155	40,542,987	4.4	81,888
3	833	Commercial	S	0	0.0010	3,590	69,079,623	3.7	71,122
4	822	Commercial	S	0	0.0010	3,689	67,856,386	3.6	65,753
5	762	Industry	SW	0	0.0012	2,958	62,004,610	3.4	71,521
6	787	Warehouse	S	0	0.0020	1,626	29,711,287	3.2	58,211
7	785	Warehouse	SW	0	0.0012	2,657	45,967,445	3.1	54,282
8	783	Warehouse	SW	0	0.0011	2,810	49,754,349	3.1	54,558
9	823	Commercial	SW	0	0.0007	4,265	81,533,444	3.1	58,457
10	771	Industry	S	0	0.0017	1,739	33,959,412	3.0	58,924
11	852	Commercial	S	0	0.0011	2,737	44,049,187	2.9	47,086
12	768	Warehouse	S	0	0.0020	1,442	28,585,973	2.9	57,131
13	784	Warehouse	SW	0	0.0013	2,242	38,364,959	2.9	49,107
14	769	Warehouse	N	0	0.0007	3,853	77,765,825	2.9	57,886
15	759	Industry	S	0	0.0019	1,488	29,681,094	2.8	56,354
16	785	Warehouse	S	0	0.0017	1,652	26,693,292	2.8	45,266
17	838	Apartment	S	0	0.0007	3,741	63,741,216	2.8	47,675
18	771	Industry	SW	0	0.0012	2,247	47,623,599	2.7	57,544
19	758	Industry	S	0	0.0015	1,661	33,401,738	2.6	51,281
20	863	Apartment	S	0	0.0007	3,818	67,026,592	2.5	44,653
21	757	Commercial	S	0	0.0009	2,922	55,371,339	2.5	48,122
22	791	Industry	SW	0	0.0019	1,313	20,369,698	2.5	38,959
23	741	Commercial	S	0	0.0012	2,014	33,262,806	2.5	40,995
24	825	Commercial	SW	0	0.0005	4,607	70,311,619	2.5	37,512
25	840	Apartment	S	0	0.0007	3,457	59,031,939	2.4	41,651
26	767	Warehouse	S	0	0.0019	1,246	26,249,229	2.4	49,838
27	782	Warehouse	S	0	0.0016	1,474	22,981,563	2.3	36,188
28	769	Warehouse	W	0	0.0005	4,458	92,923,729	2.3	47,334
29	823	Commercial	S	0	0.0010	2,189	43,036,428	2.3	44,309
30	821	Commercial	SW	0	0.0008	2,841	58,778,276	2.2	46,232

dominant wind direction or downwind direction was predominantly to south and to southwest. This accords with the wind frequency analysis in section 4.4.1 where the

probability of wind blowing to south and to southwest were the highest (0.303) and the second highest (0.211) respectively. Finally, the buildings with ignitions were mostly the industrial, warehouse, and commercial buildings which generally have larger floor areas. This reflects Tillander and Keski-Rahkonen's (2002) idea of ignition frequency's dependency on floor area.

It was initially surprising to observe that none of the highest risk scenarios included pipe failures, and further analysis appeared warranted. Of the 5,250 scenarios generated, 88 included at least one pipe failure. These 88 scenarios were sorted by order of consequences and the top twenty highest consequence scenarios with pipe failures are tabulated in Table 4.4. While these scenarios have very high levels of consequences, it can be seen for each scenario in Table 4.4 that the joint probability of simultaneous pipe failure and building ignition is so low that the risk values are far less than those presented in Table 4.3. This result is a classic example of the value of risk assessment versus consequences simulation alone.

To analyze the scenario-based urban fire risk further, the highest risk scenario (scenario-1 in Table 4.3) is selected and the progress of urban fire over time is mapped in Fig. 4.6. This scenario would cause 322 burned buildings with a property value of \$79.2 million and would cause 4246 displaced people if there were a 100% probability of ignition at the warehouse (Building # 764) and if the wind blew to southwest. The estimated risk was 4.5 displaced people per year or \$ 0.08 million of property losses per year. This scenario clearly burns the central business district and part of the multi-family residential area, destroying 50% of the city. To investigate further the reason for such a

Table 4.4. Scenarios Involved Pipe Failures for Micropolis Generated from Monte Carlo Analysis

Scenario No.	Ignition Point	Wind Direction	No. of Failed Pipes	Joint Probability	Consequences		Risk	
					No. of Displaced People	Property Losses (\$)	No. of Displaced People/yr	Property Losses (\$/yr)
P-1	677	E	1	0	4,763	78,632,931	0.0E+00	0.0E+00
P-2	5	E	495	1.3E-30	4,731	90,880,705	6.2E-27	1.2E-22
P-3	724	SE	503	2.9E-30	4,087	75,834,257	1.2E-26	2.2E-22
P-4	808	W	498	7.9E-31	4,074	66,089,777	3.2E-27	5.2E-23
P-5	90	SW	494	1.1E-27	3,982	71,787,568	4.2E-24	7.6E-20
P-6	856	S	496	2.8E-27	3,892	65,591,907	1.1E-23	1.9E-19
P-7	769	N	486	3.5E-27	3,885	78,650,758	1.4E-23	2.8E-19
P-8	134	SW	492	5.7E-27	3,884	71,046,948	2.2E-23	4.1E-19
P-9	638	E	494	4.5E-29	3,756	62,676,975	1.7E-25	2.8E-21
P-10	55	NE	497	4.2E-31	3,374	68,612,800	1.4E-27	2.9E-23
P-11	778	S	489	9.1E-29	3,326	64,263,850	3.0E-25	5.9E-21
P-12	393	W	495	1.4E-28	3,290	63,525,417	4.7E-25	9.1E-21
P-13	265	W	489	2.2E-29	3,282	62,891,271	7.2E-26	1.4E-21
P-14	714	E	487	1.9E-28	3,209	56,724,840	6.1E-25	1.1E-20
P-15	169	S	496	3.8E-29	3,143	60,254,854	1.2E-25	2.3E-21
P-16	264	N	492	1.9E-29	2,973	52,970,650	5.8E-26	1.0E-21
P-17	145	SE	504	1.0E-31	2,938	49,425,043	3.0E-28	5.1E-24
P-18	281	W	481	4.4E-27	2,921	53,625,965	1.3E-23	2.4E-19
P-19	649	E	497	0	2,776	55,242,194	0.0E+00	0.0E+00
P-20	310	N	480	4.4E-26	2,482	45,780,763	1.1E-22	2.0E-18

wide spread fire in a small town like Micropolis, three building characteristics were examined carefully; these are occupancy hazard classification (OHC), exposure factor(EF), and construction classification number (CCN). A building's OHC value indicates whether a building contains hazardous materials or not. Generally, OHC values are assigned as 3, 4, 5, 6, and 7 to indicate respectively severe hazard, high hazard, moderate hazard, low hazard, and light hazard occupancies (Eckman 1994). MUFS utilizes these values to prioritize the fire truck assignments. It was observed that

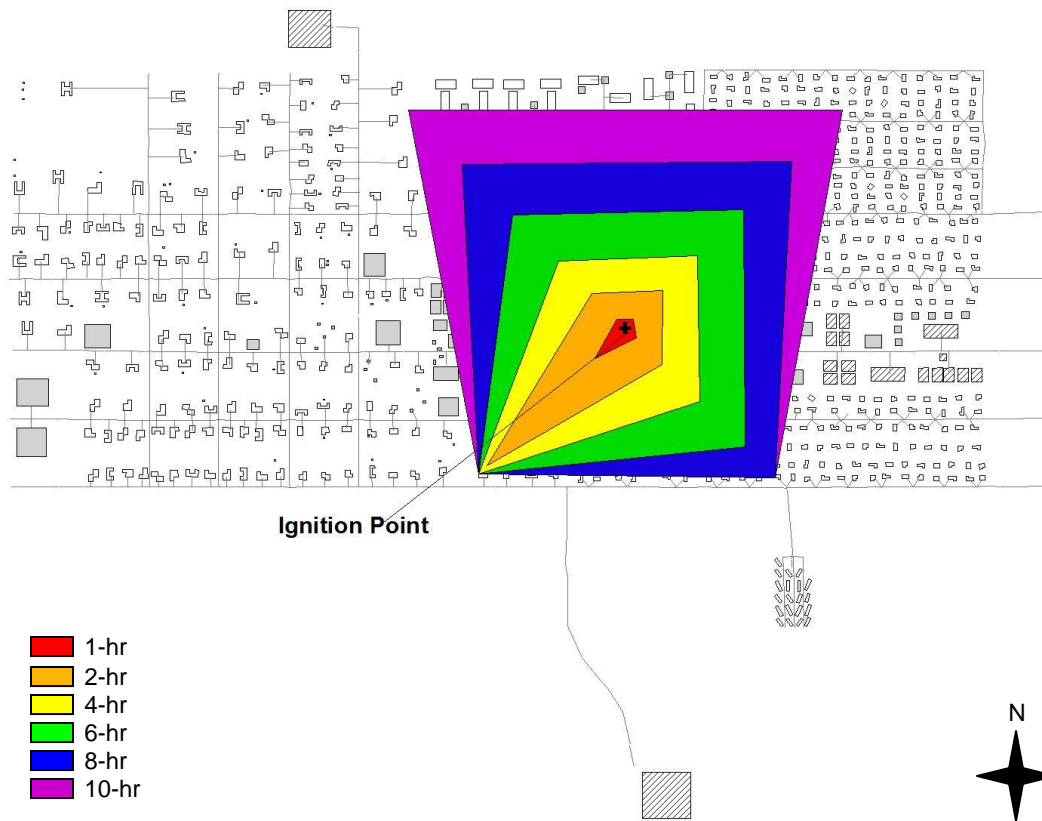


Fig. 4.6. Building map of Micropolis with fire spread profile for highest risk scenario (scenario-1)

8% of the total burned buildings under this scenario had high hazard occupancies such as building material storage, departmental stores, warehouses, etc.; 7% had moderate hazard occupancies for instance restaurants, libraries, etc; and the rest were low and light hazard occupancies such as churches, schools, residential dwellings, etc. This indicates that approximately 15% of the burned buildings were high to moderate hazard occupancies. A building's exposure factor (EF) indicates how close the building is from

its neighboring structures. Generally, the EF value of 1.0 indicates either the building has an area smaller than 9.3 m^2 (100 ft^2) or the building is more than 15.24 m (50 ft) away from the nearest structure; the EF value of 1.5 indicates that the building is close enough to the nearest neighbor to pose an exposure risk in case the surrounding structures catch a fire (Eckman 1994). While examining the EF values of the burned buildings, it was found that about 97% of the burned buildings had EF value of 1.5; which indicates the buildings were pretty close to each other. Finally, the burned buildings' CCN values were examined. A building's CCN value represents the type of fireproof construction techniques employed. A CCN value of 1.0 indicates a level of general fireproof construction, and lower CCN values indicate level of fire-resistant construction. From the Micropolis database it was found that all the burned buildings have CCN values of 1; indicating no fire-resistant construction techniques was employed in this region.

Following the above analysis, it can be concluded that there are several factors that caused the fire incident described by scenario-1 to spread rapidly. The two most important factors are the wind direction and WDS performance during fire event. Although the WDS was functioning normally during this fire scenario however, the system was unable to provide sufficient firefighting flows; this indicates that the highest risk factor is dominated by the poor design of WDS for this case study. Other major factors are the buildings nearness to each other and level of fireproof construction techniques. A combination of all these factors contributed to a higher urban fire risk for this community. Similar results were found for other high risk scenarios.

4.6. Managing Urban Fire Risk for the Case Study

Findings from the above analysis indicate that among the variables of fire hazard, both wind direction and WDS condition plays a vital role in fire propagation. Wind direction, however, depends upon a region's geographical location and atmospheric conditions; therefore, cannot be controlled. WDS performance, on the other hand, can be improved by pipe enlargement, among other measures. Previous studies have examined WDS vulnerability and risk during urban fire events and investigated rehabilitation for mitigation of potential fire events with a major focus on attaining adequate fire flows by pipe hardening and pipe enlargement. Pipe enlargement, however, can cause water quality problems and place public health at risk during normal operational periods. Thus a multi-objective approach is required to effectively address the conflicting goals of the WDS: reliable delivery of water during normal as well as emergency conditions such as fire, meeting water quality standards, and finding cost-effective design and rehabilitation options.

These goals can be achieved by identifying pipes for enlargement and their corresponding diameters, and the location of additional chlorine booster units. When more than one objective is considered in an optimization problem, no single solution may produce the best result with respect to all objectives. In such a case a set of solutions known as the Pareto optimal solutions or non-dominated solutions exist (Hans 1988), none of which is worse than any other with respect to all objectives. The Pareto optimal solutions provide the decision makers more information and flexibility in selection of a solution.

To mitigate the urban fire risk for this case study, a multi-objective evolutionary algorithm, Non-Dominated Sorting Evolution Strategy (NSES) (Kanta et al. 2009), was applied. NSES is a population based multi-objective evolutionary algorithm which produces Pareto-optimal solutions in an objective space. Implementing an evolution strategy (ES) (Rechenberg 1965) based search technique NSES utilizes a non-dominated sorting approach adopted from NSGS-II (Deb et al. 2002). Detailed discussion of NSES algorithm and its algorithmic performance in finding Pareto optimal solutions can be found in Kanta et al. (2009). The following sections describe the implementation of NSES approach to Micropolis WDS to mitigate potential urban fire events.

4.6.1. Model Formulation

The proposed model has three objectives: (1) minimizing the aggregated fire damage (f_1), (2) minimizing the maximum water quality deficiency (f_2), and (3) minimizing normalized mitigation cost (f_3). The multi-objective optimization problem, therefore, can be mathematically formulated as follows:

$$\text{Minimize } f_1 = \sum_{i=1}^n \alpha_i \frac{Q_{i_{req}} - Q_{i_{available}}}{Q_{i_{req}}} \quad (4.9)$$

$$\text{Minimize } f_2 = \max_j D_{C_j}; \quad j=1, 2, \dots, m \quad (4.10)$$

$$D_{C_j} = \begin{cases} 1; & C_{j_{available}} < 0.2, C_{j_{available}} \geq 4.0 \\ 1 - \frac{C_{j_{available}}}{3.8}; & 0.2 \leq C_{j_{available}} < 4.0 \end{cases} \quad (4.11)$$

$$\text{Minimize } f_3 = \frac{\sum_{k=1}^{np} C_k^P + \sum_{l=1}^{nb} C_l^B}{C_{worst}} \quad (4.12)$$

subject to:

$$D_k \in \{d\}; k = 1, 2, \dots, np \quad (4.13)$$

$$np \leq \phi \quad (4.14)$$

$$nb \leq \theta \quad (4.15)$$

where, $Q_{i_{req}}$ = required fire flow (l/s [gpm]) for hydrant i ; $Q_{i_{Available}}$ = available flow (l/s [gpm]) at minimum allowable residual pressure at hydrant i (typically set at 137.9 kN/m² [20 psi] by local code); α_i = weighting coefficient for hydrant i ; n = total number of fire hydrants considered for fire flow evaluation; D_{C_j} = chlorine deficiency (unitless) at monitoring node j ; $C_{j_{Available}}$ = available residual chlorine concentration (mg/l) at monitoring node j ; m = total number of monitoring nodes; C_k^P = cost of pipe k (\$); C_l^B = installation cost of booster station l (\$); C_{worst} = worst cost (\$); D_k = diameter (m [inch]) of pipe k ; d = commercially available discrete pipe sizes (m [inch]); N = total number of pipes in the network; np = number of pipe decision variables; ϕ = user defined maximum number of pipes to be replaced; nb = number of booster station decision variables; and θ = user defined maximum number of boosters to be installed.

4.6.2. Implementation of NSES to Mitigate WDS Fire Damages

The model decision variables are the pipes to be enlarged and the corresponding diameters; it is assumed that additional chlorine boosters will not be added, but the general problem formulated above includes this possibility. Micropolis WDS has 577 water mains among 1088 pipes each of which was considered as a potential pipe rehabilitation location. The diameter of rehabilitated pipes could be selected from the set of {0.15, 0.20, 0.25, 0.30, 0.36, 0.41, 0.46, 0.51, 0.61} m [{6, 8, 10, 12, 14, 16, 18, 20, 24} inch] diameter commercially available class 50 ductile iron pipes.

To manage the urban fire risk for Micropolis, all of the 30 highest risk scenarios were considered. Based on the location of the ignited buildings and the propagation of fire for each of the 30 scenarios, two unique sets of fire hydrants, each consisting of three hydrants, were chosen to improve the fire flow in high risk region. The first set consists of hydrants HY40, HY53, and HY66; the second set consists of hydrants HY1, HY42, and HY45 (Fig. 4.7). The aggregated fire damage (Eq. 4.9) was evaluated based on individual fire flow at each hydrants under study and the weighting coefficients, α_i , were selected to represent an average fire flow rate for the system. For this case a weight value of 0.333 was used for all hydrants, however, different α_i values can be assigned to prioritize the specific hydrant flows under study. A required fire flow of 63 l/s (1000 gpm) was considered at all fire hydrants.

Micropolis WDS has 751 valve nodes and junctions among 1210 non-hydrant nodes. To evaluate the system-wide residual chlorine levels, ten out of 751 nodes were selected as representative water quality monitoring nodes. The Surface Water Treatment

Rule (SWTR) requires the water distribution systems to maintain a “detectable” disinfectant residual level of 0.2 mg/l (for chlorine) throughout the system. Moreover, under the Stage 1 Disinfectant/Disinfection By-Products Rule, the residual should not exceed 4.0 mg/l for chlorine in any reach of the system (USEPA 2004). This is due to

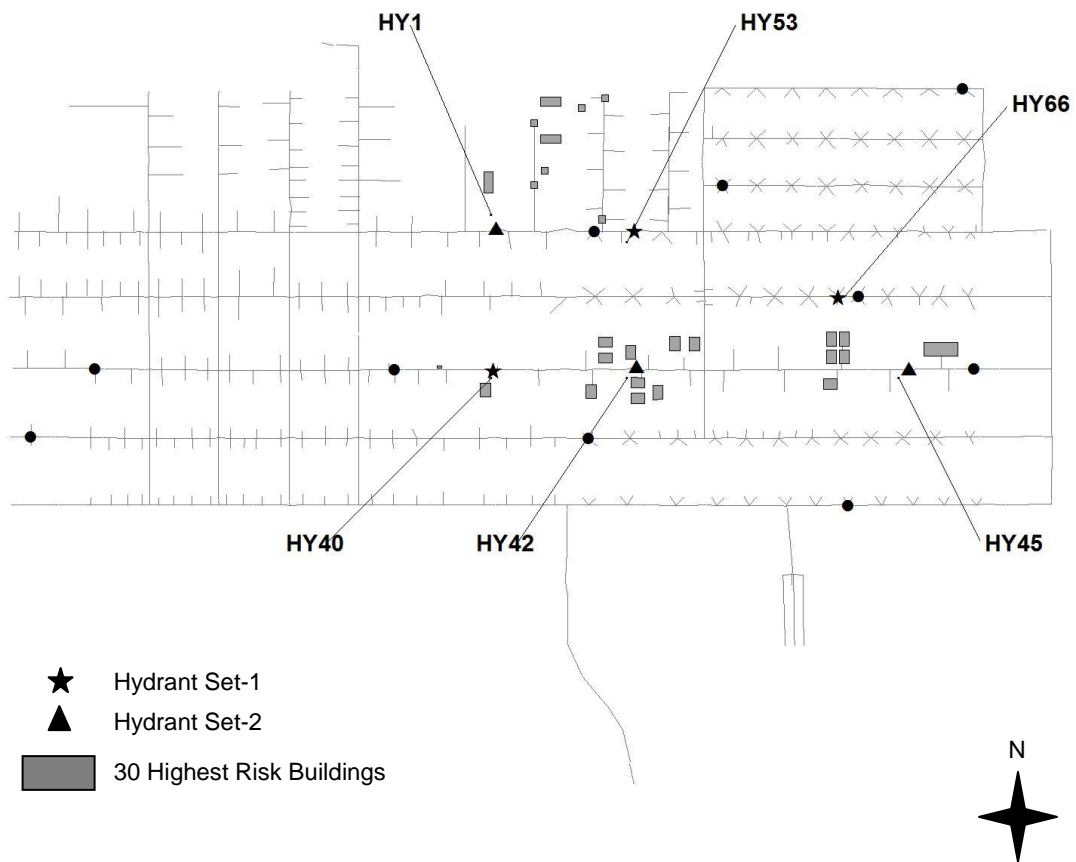


Fig.4.7. Building map of Micropolis with WDS shown in thin lines and water quality monitoring locations are shown in black dots

the fact that excessive levels of chlorine produces taste and odor problems, forms disinfectant by-products, and might accelerate pipe corrosion. Thus the water quality deficiency, expressed in Eq. (4.10), is defined to map the government regulation for drinking water quality and is evaluated at all ten monitoring nodes. Currently, a disinfectant dose of 4 mg/l is added at the treatment plant and there is no additional chlorine booster station in the system.

Finally, a normalized cost was evaluated as cost of pipe replacement for a current solution over the worst possible cost of rehabilitation (Eq. 4.12). The worst possible cost was evaluated by setting up a set of scenarios which maximizes the fire flow without cost or water quality constraints. The network is shown in Fig. 4.7.

The solution approach defined in this section was implemented in a computer code in Visual Basic 6.0 that utilizes iterative solution of the water distribution system's hydraulics and water quality under the objectives and constraints defined by Eq. (4.9) through Eq. (4.15). The NSES model is coupled with EPANet Programmer's Toolkit (Rossman 1999) to simulate the hydraulics and water quality in the network. To evaluate the aggregated fire damage, the required pressure head (14 m [46 ft]) was added simultaneously to all three hydrants' respective elevations and the emitter coefficient (Rossman 2000) at the corresponding hydrants was set to $44.5 \text{ l/s}/(\text{kN}/\text{m}^2)^{0.5}$ (1850 $\text{gpm}/\text{psi}^{0.5}$); then a single period simulation was performed. After running the hydraulic model, the available fire flow at each of the three hydrants was noted and the aggregated fire damage was calculated. To evaluate the water quality deficiency the hydraulics and water quality in the network were simulated separately without a fire flow demand over

a 168-hour time period to allow the system to reach a dynamic equilibrium condition with respect to disinfectant concentrations. It was assumed that a maximum number of 50 pipes or less needed to be replaced to increase the system-wide firefighting capability.

4.6.3. Mitigation Results

The multi-objective analysis was performed twice, one for each hydrant set, to check the robustness of the NSES algorithm. The algorithmic parameters used during implementation of NSES-based search were: $\mu = 150$, $\lambda = 300$, and *stopping criterion* = 350 generations.

The X-Y-Z scatter plots of the Pareto front for hydrant set-1 is shown in Fig. 4.8 where each point represents a solution indicating the aggregated fire flow, minimum residual chlorine, and the corresponding mitigation cost to implement that solution. In the following figure, the horizontal axis presents a maximization objective, and the vertical axis presents a minimization objective; thus, Pareto-front will be oriented from upper-right to lower-left with sub-optimal regions above and left of the front. Since the model simultaneously minimizes the aggregated fire damage, the maximum chlorine deficiency, and the normalized cost of mitigation, consequently, the model returns maximized aggregated fire flow, maximized minimum residual chlorine, and minimum cost solutions. In existing condition the system provides an aggregated fire flow of 23 l/s for hydrant set-1 and the minimum residual chlorine level was 0.71 mg/l which is above the regulated minimum value of 0.2 mg/l. Referring to Fig. 4.8 most of the Pareto-

optimal solutions yield moderate to significant gain in both system wide fire flow and water quality with a few exceptions, however, each solution contributes to cost of mitigation with varying degrees.

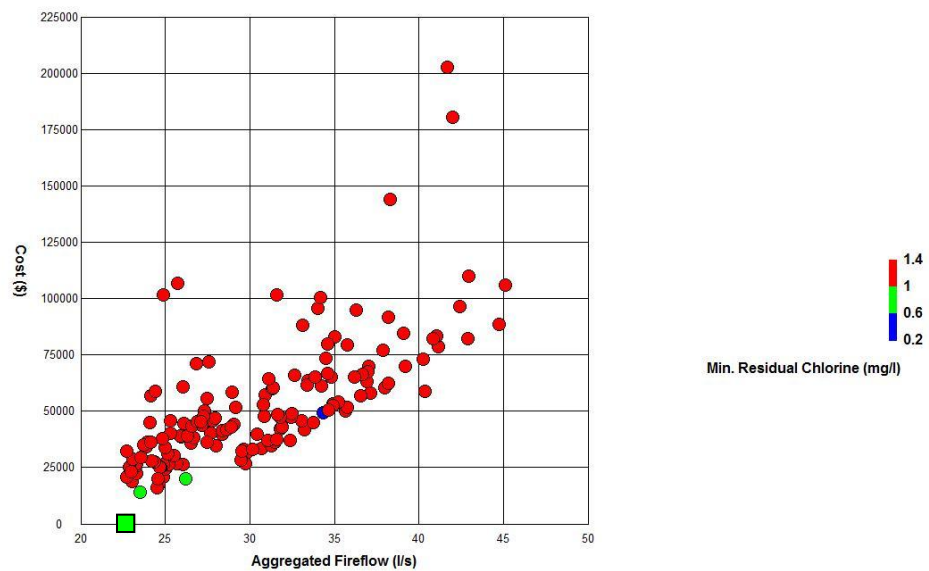


Fig. 4.8. X-Y-Z scatter plot of the Pareto-optimal solutions for the hydrant set-1 after 350 generations, the WDS performance at existing condition is shown with a square

The results from the risk assessment in section 4.5 showed that each highest risk scenario was unique, thus one Pareto-optimal solution which seemed very effective in reducing the risk for a particular scenario might not be as effective as for another scenario and vice versa. Therefore, the Pareto-optimal mitigation designs were evaluated for a number of scenarios. Finally, the average % of risk reduced for those scenarios by

each of the mitigation design was used as a measure of mitigation effectiveness for that particular design.

During the mitigation effectiveness analysis, first, 15 Pareto-optimal solutions were chosen from the Pareto front. Then, for each of the 15 solutions, the urban fire consequences were evaluated for each of the 30 highest risk scenarios. Finally, the average percent of risk reduced by implementing each of the 15 designs were evaluated. The achieved objective values are listed in Table 4.5. The 15 Pareto-optimal designs in fire flow-cost-water quality objective space for hydrant set-1 are shown in Fig. 4.9 and the Pareto front in scenario risk-cost-water quality objective space for hydrant set-1 is shown in Fig. 4.10.

Table 4.5. Comparison of Pareto-optimal Solutions in the Objective Space for Hydrant Set-1

Solution	Hydrant Flow			Aggregated Fireflow	Average % Risk Reduced <i>% displaced people per yr</i>	Cost \$	Minimum Residual Chlorine mg/l
	HY40 <i>l/s</i>	HY53 <i>l/s</i>	HY66 <i>l/s</i>				
Existing	10	25	33	23	0	0	0.71
1	10	31	34	25	14	26,469	1.27
2	11	34	36	27	12	38,238	1.46
3	11	32	41	28	12	45,833	1.47
4	12	35	41	29	14	44,205	1.47
5	13	39	40	31	16	47,799	1.43
6	13	41	43	32	14	47,174	1.40
7	13	43	47	34	21	49,193	0.26
8	14	44	48	35	18	54,202	1.27
9	32	38	41	37	24	57,896	1.07
10	12	56	45	38	22	60,464	1.39
11	15	50	56	40	29	58,989	1.34
12	38	40	45	41	32	78,708	1.40
13	13	55	60	43	31	82,258	1.43
14	16	58	60	45	32	88,525	1.46
15	16	55	64	45	28	106,014	1.07

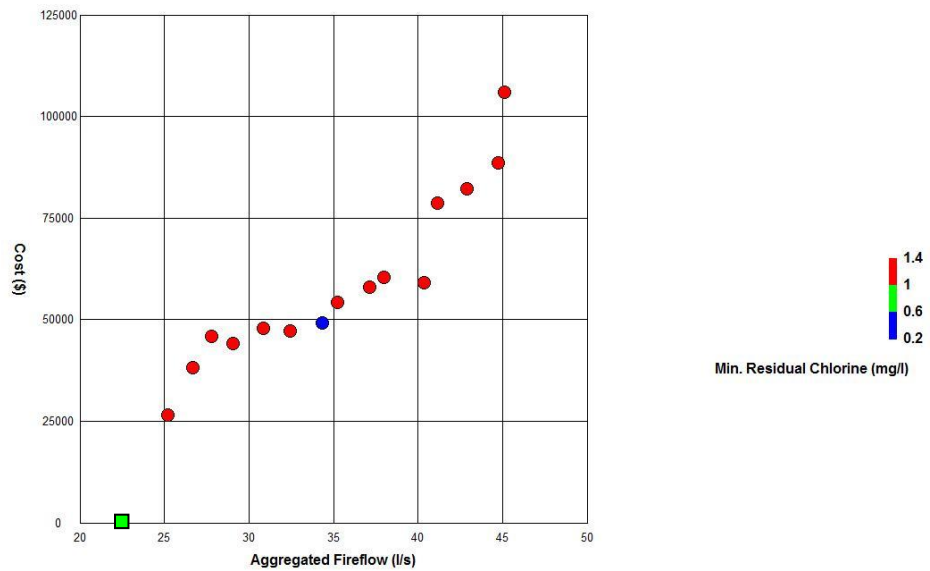


Fig. 4.9. X-Y-Z scatter plot of 15 Pareto-optimal solutions in fireflow-cost-water quality space (hydrant set-1), the WDS performance at existing condition is shown with a square

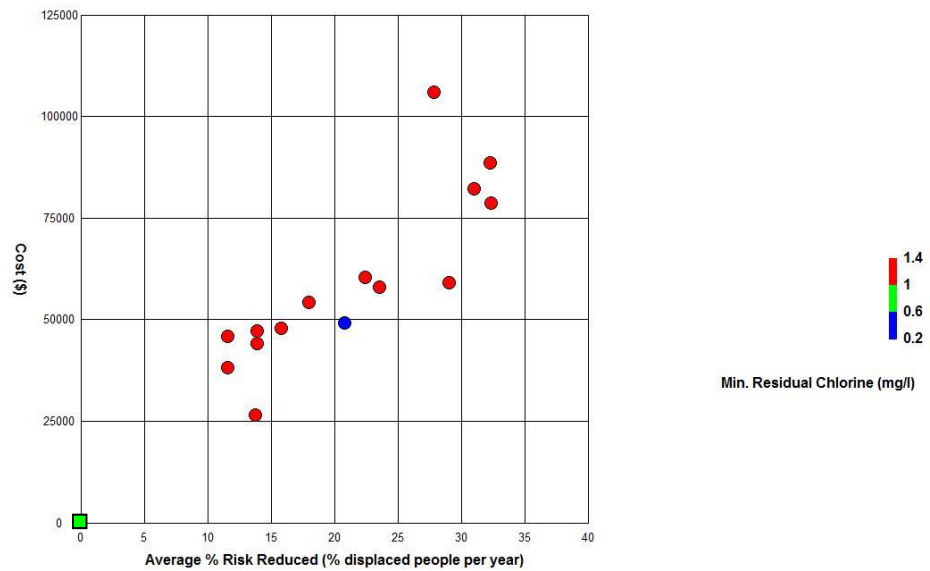


Fig. 4.10. X-Y-Z scatter plot of the Pareto front in scenario risk-cost-water quality space (hydrant set-1), the WDS performance at existing condition is shown with a square

Referring to Table 4.5, in fire flow-cost-water quality objective space, solution 1 is better than solution 2 in terms of cost, but inferior to solution 2 in terms of both aggregated fire flow and Water quality. This tradeoff relation between solutions 1 and 2 while translated in risk-cost-water quality objective space showed that solution 1 is better than solution 2 in terms of both average % of scenario risk reduced and cost but inferior to solution 2 in terms of water quality. Similar comparisons could be made for all other Pareto-optimal solutions. Referring to Fig. 4.9, Fig. 4.10 and Table 4.5, there clearly a tradeoff relationship exists between fire flow and mitigation cost or average % of scenario risk reduced and mitigation cost. Although each of the Pareto-optimal solutions produced vary different water quality, it is difficult to conclude that a significant tradeoff relation exists between fire flow and water quality during normal demand condition for this case study.

To test the robustness of the mitigation approach, both the multi-objective analysis and mitigation effectiveness analysis were performed using hydrant set-2. The achieved objective values are listed in Table 4.6. The Pareto-optimal designs in fire flow-cost-water quality objective space using hydrant set-2 are shown in Fig. 4.11 and the Pareto front in scenario risk-cost-water quality objective space for hydrant set-2 is shown in Fig. 4.12. Referring to Fig. 4.11, Fig. 4.12, and Table 4.6, a tradeoff relationship was found between fire flow and mitigation cost or average % of scenario risk reduced and mitigation cost; however, as in the case with hydrant set-1, there is not much of a tradeoff between fire flow demand and water quality under normal demand condition for this city. Results for both the hydrant sets were consistent in terms of

average % of scenario risk reduction and cost of mitigation; hence provides justification of robustness of the proposed methodology.

Table 4.6. Comparison of Pareto-optimal Solutions in the Objective Space for Hydrant Set-2

Solution	Hydrant Flow			Aggregated Fireflow <i>l/s</i>	Average % Risk Reduced <i>% displaced people per yr</i>	Cost \$	Minimum Residual Chlorine <i>mg/l</i>
	HY1 <i>l/s</i>	HY42 <i>l/s</i>	HY45 <i>l/s</i>				
Existing	18	0	62	27	0	0	0.71
1	28	0	104	44	19	47,608	1.37
2	34	3	109	49	19	49,081	1.33
3	35	5	109	49	21	50,647	1.05
4	36	8	111	52	28	53,255	1.41
5	36	12	111	53	29	55,394	1.03
6	41	7	114	54	28	60,861	1.47
7	32	17	117	55	24	66,299	1.14
8	40	19	116	58	27	85,689	1.43
9	40	23	116	60	28	96,810	1.46
10	37	24	123	61	27	75,024	1.42

4.7. Final Remarks

This paper illustrates a new approach for urban fire risk assessment for a coupled water and fire response system utilizing a stochastic model. Although various fire hazard and fire risk assessment methodologies have been developed and studied for decades, this paper introduces a stochastic approach: (1) by incorporating three important fire variables: ignition, wind direction, and water distribution system's failure, and (2) by

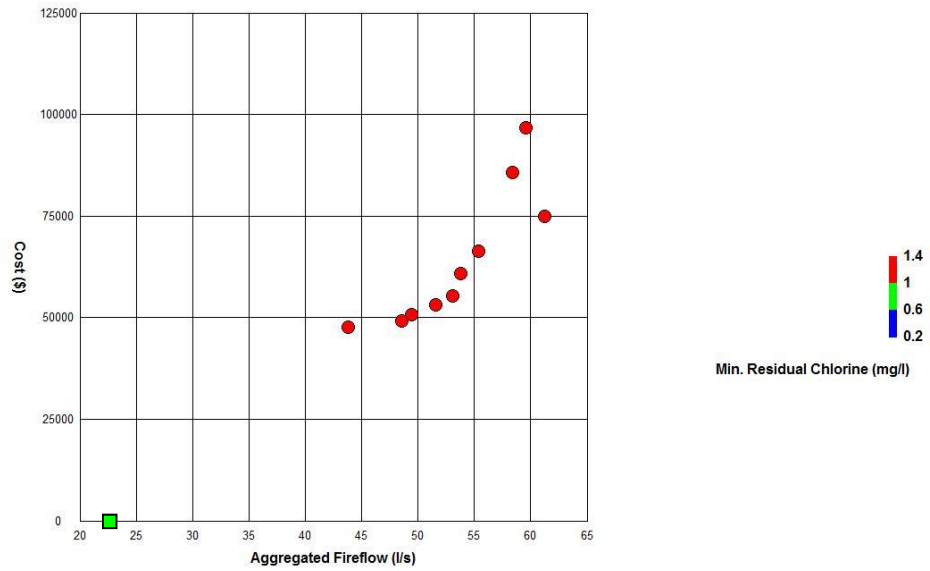


Fig. 4.11. X-Y-Z scatter plot of 10 Pareto-optimal solutions in fireflow-cost-water quality space (hydrant set-2), the WDS performance at existing condition is shown with a square

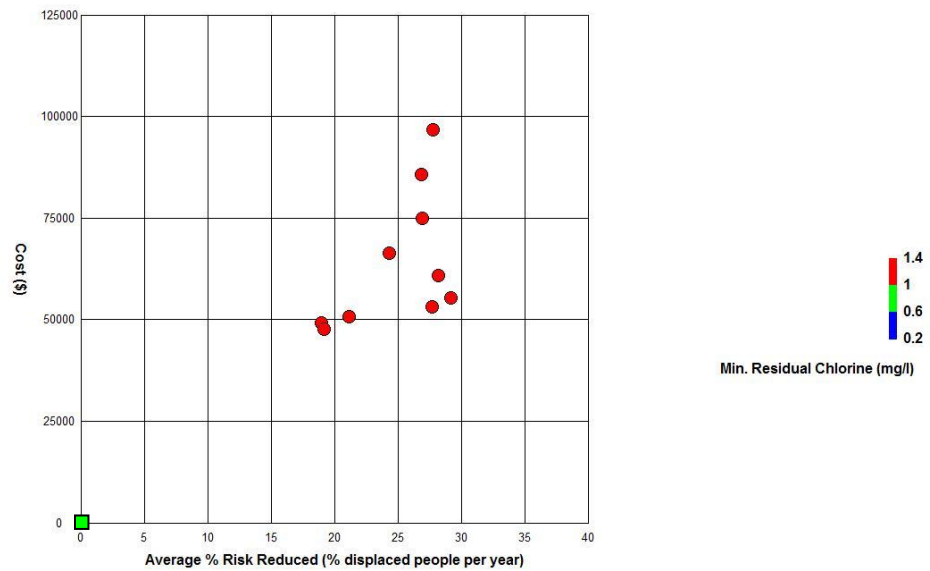


Fig. 4.12. X-Y-Z scatter plot of the Pareto front in scenario risk-cost-water quality space (hydrant set-2), the WDS performance at existing condition is shown with a square

introducing both building fire and wind direction probabilities as well as an actual WDS failure probabilities.

The Barrois model (Hasofer et al. 2007) was used to estimate building ignition frequencies. Wind frequencies were estimated from historical wind data. Pipe failure probabilities due to soil-pipe interaction were estimated using Yamijala et al. (2009) model and pipe failure probabilities due to seismic event were estimated using Eidingger (2005) model. A computerized fire spread model, MUFS (Bristow 2006), was used to evaluate the fire consequences. Risk was quantified in two different levels: scenario risk and global risk. Scenario risk was evaluated in terms of number of displaced people/year per scenario. Each scenario for a fire event was defined as a triplet consisting of ignition, wind property, and WDS condition; and the probability of occurrence of a particular scenario was estimated as a joint probability of those fire variables. Scenario-based urban fire risk for a particular scenario was then estimated as a product of total probability of a fire scenario and the fire consequences. A Monte Carlo simulation was utilized to generate all possible fire scenarios as well as the distribution of consequences. Global risk on the other hand was evaluated in two different methods: with and without conditioning on fire events and expressed as number of displaced people/year. Global risk is an aggregation of all possible scenario risk and thus estimated much higher than individual scenario risk.

The proposed methodology was implemented for a realistic case study, Micropolis. The results of Monte Carlo simulation showed that both global and scenario-based urban fire risk for the case study was quite high and varied with different

scenarios. The two most important factors found to be critical during urban fire events were: the wind direction and WDS performance. Although the WDS was functioning normally (no failure) during most of the high risk fire scenarios under study, the system was unable to provide sufficient firefighting flows. This result indicates that the highest risk factor was dominated by the poor design of WDS for this case study.

To mitigate the urban fire risk for this case study, a multi-objective evolutionary algorithm, Non-Dominated Sorting Evolution Strategy (NSES), was applied to effectively address the conflicting goals of the WDS: reliable delivery of water during normal as well as emergency conditions such as fire, meeting water quality standards, and finding cost-effective design and rehabilitation options. This methodology clearly generates Pareto-optimal solution surfaces that express the tradeoff relationship between fire damage, water quality, and least cost objectives; this provides decision makers with the flexibility to choose a mitigation plan for urban fire events best suited for their circumstances. Each Pareto-optimal solution comprises a set of pipes to be enlarged to achieve increased fire flow and the corresponding diameters of these pipes. To examine the effectiveness of the solutions in reducing urban fire risk, the Pareto-optimal mitigation designs were then evaluated for 30 highest risk scenarios. Finally, the average % of risk reduced for those scenarios by each of the mitigation design was used as a measure of mitigation effectiveness for that particular design.

Analysis of the results showed that most of the Pareto-optimal solutions reduced the average risk for 30 scenarios with varying degrees. The results also showed that a tradeoff relationship exists between fire flow and mitigation cost or average % of risk

reduced and mitigation cost. Although each of the Pareto-optimal solutions produced vary different water quality, it was difficult to conclude that a significant tradeoff relation exists between fire flow during emergency condition and water quality during normal demand condition for this case study. The analysis was performed with two different sets of hydrant arrangements to examine the robustness of the mitigation methodology. Results for both the hydrant sets were consistent in terms of average % of risk reduction and cost of mitigation; hence provides justification of robustness of the proposed methodology.

5. SUMMARY AND CONCLUSIONS

This dissertation has focused on developing new methodologies to address risk and consequences of and effective mitigation strategies for urban fire events focusing on two critical infrastructures – water systems and emergency services. While risk assessment is the preferred approach to address and assess fire hazards, estimation of probabilities of various fire variables as well as interdependency between water and fire services are often ignored. New risk-based techniques were developed to address these issues and were implemented to an illustrative case study to generate a risk-based WDS vulnerability assessment tool, a set of Pareto-optimal WDS fire mitigation designs, and a set of Pareto-optimal risk management plans for urban fire events.

To extend the basic knowledge of vulnerabilities in the water systems during occurrence of fire and to incorporate the risk associated with the water system failure for fire events in decision making processes, a risk-based dynamic programming modeling approach was developed to identify the critical components of a WDS during fire events under three failure scenarios: (1) accidental failure due to soil-pipe interaction, (2) accidental failure due to a seismic activity, and (3) intentional failure or malevolent attack. Fire damage consequences for the water system were evaluated as the normalized differences in hydrant flows based on regional fire flow requirements. The risk-based DP methodology was then applied to a realistic case study, Micropolis WDS, to assess vulnerability and risk to the water system posed by fire hazard. Several mitigation designs were proposed based on the concept of hardening specific sets of water mains

(those appeared as the most vulnerable components for fire at all locations under consideration). Simulations of the mitigation strategies showed that the system risk could be reduced significantly by adapting some of the mitigation measures and the system's resiliency could be improved as well. However, some of the proposed mitigation plans were not adequate when the number of pipe failure due to malevolent actions was small. This observation called for an investigation on the mitigation measures in a more systematic way.

For systematic generation of fire mitigation strategies for WDS, a new EA-based decision making tool Non-dominated Sorting Evolution Strategy (NSES), was developed and then applied to Micropolis WDS to yield Pareto-optimal mitigation designs for WDS fire events based on three primary objectives: (1) minimizing fire damage, (2) minimizing water quality problem, and (3) minimizing mitigation cost. Each Pareto-optimal solution comprised a set of pipes to be enlarged to achieve increased fire flow and the corresponding diameters of those pipes. The objective of developing this tool was to identify a set of Pareto-optimal solutions in the 'fire damage - water quality – cost objective space that could help utility managers understand the trade-offs between those objectives. The Pareto optimal solutions for the case study indicated that although there were variations among the solutions in terms of all three objectives, however, for this specific system it was difficult to conclude that a significant tradeoff relation exists between the emergency demand during an urban fire event and the water quality during normal demand condition.

To assess urban fire risk in a complex combination of systems, such as buildings, emergency responders, water distribution, being primary, a risk-based stochastic modeling approach was developed by introducing both fire hazard and wind direction probabilities and by incorporating actual WDS failure probabilities. A computerized fire spread model, MUFS (Bristow 2006), was used to evaluate the fire consequences in terms of number of displaced people. The methodology was applied to the Micropolis case study, and urban fire risk was estimated at two different levels: (1) scenario risk for a large number of possible fire scenarios, and (2) global risk aggregated across scenarios by utilizing separate Monte Carlo simulations. Results showed that both global and scenario-based urban fire risk for the case study were quite high and varied with different scenarios. The two most important factors found to be critical during urban fire events were: the wind direction and WDS performance. Although the WDS was functioning normally (no pipe failure) during most of the high risk fire scenarios under study, the system was unable to provide sufficient firefighting flows. This result indicates that the highest risk factor was the poor design of WDS for this case study. To mitigate the urban fire risk for this case study, NSES was applied with three objectives: (1) minimizing fire damage, (2) minimizing mitigation cost, and (3) minimizing water quality problem. The Pareto front in ‘fire flow – cost – water quality’ objective space was then translated into ‘average percent of scenario risk reduction – cost – water quality’ objectives to validate the effectiveness of the mitigation plans. Analysis of the results showed that most of the Pareto-optimal solutions reduced the average risk for the scenarios under study with varying degrees. The results also showed that a tradeoff

relationship exists between fire flow and mitigation cost or average % of risk reduction and mitigation cost. Although each of the Pareto-optimal solutions produced vary different water quality, it was difficult to conclude that a significant tradeoff relation existed between fire flow during emergency condition and water quality during normal demand condition for this case study.

Although the vulnerability analysis for water systems has been a topic of intense study in recent years, it is a difficult decision how best to respond to the possibility of high-consequence but relatively low probability events when resources are limited. Therefore, a risk analysis framework was used for the water systems to understand the changing nature of system vulnerability versus failure probabilities. The risk-based vulnerability assessment tool can help utility managers understand the value of risk mitigation. The multi-objective approach (NSES) for WDS fire mitigation was developed to effectively address the conflicting goals of the water systems: reliable delivery of water during normal as well as emergency conditions, meeting water quality standards, and finding cost-effective design and rehabilitation options. The multi-objective optimization tool generates Pareto optimal solutions in ‘fire flow-water quality-cost’ objective space and thus can provide the decision makers more information and flexibility in selection of a particular mitigation design best suited for their situation. Finally, the urban fire risk analysis tool for the coupled water distribution and fire response model was developed to provide Pareto-optimal risk management plans for urban fire events. The tools were successfully implemented to the case study, thus provides enough justification of the applicability to any real world problem. Although the

outcome of the implementation of the proposed methodology showed that a significant tradeoff relation did not exist between fire flow during emergency condition and water quality during normal demand condition for this case study, it is expected that a real world application of this methodology would find a tradeoff relation between those conflicting goals beyond the illustrative case study. Finally, the application of the methodologies presented in this dissertation would guide the water utility managers, emergency response personnel, and affiliated decision makers to address and assess urban fire risk and appropriate risk management strategies and thereby would enhance decision making process in both water systems planning and management and emergency services throughout the country.

Future research based on this dissertation is appropriate to address several remaining issues. First, the mitigation design for urban fire events using the NSES approach was based on discontinuous/discrete decisions on small sections of water main. In real systems, however, pipe replacement typically involves much longer sections of water main. Revisions to the methodology would be appropriate and could be done by skeletonizing the distribution network between major highway intersections and important hydrant locations. Second, a sensitivity analysis of NSES with respect to the number of hydrants under consideration in reducing urban fire risk should be investigated. Third, MUFS output is highly dependent on both the topology of an urban area and approximation of interpolation of burn polygon(s) at each time step. Moreover, MUFS does not account for estimation of number of displaced people based on percentage of building burned; thus any building within the burn polygon is considered

as fully burned during consequence evaluation. This approach results in an overestimation of consequences resulting in a higher risk values. This issues with MUFS need to be improved in future. At a larger scale of research, future efforts will address interdependence of critical infrastructures such as water supply, transportation, power, and emergency services. The risk and reliability of complex systems caused by cascading failures within critical infrastructures and development of mitigation measures through analysis and validation of modeling and optimization tools will also be investigated.

REFERENCES

- Al-Zahrani, M. A., and Moied, K. (2001). "Locating optimum water quality monitoring stations in water distribution system." *Proc., World Water and Environmental Resources Congress*, ASCE, Reston, VA.
- American Water Works Association(AWWA). (1998). *AWWA Manual M31 – Distribution System Requirements for Fire Protection*, AWWA, Denver, CO.
- American Water Works Association Research Foundation (AWWARF) and Sandia National Laboratories. (2002). *Risk Assessment Methodology for Water Utilities (RAM-WTM)*, AWWARF, Denver, CO.
- Arulraj, G. and Rao, H. (1995). "Concept of significant index for maintenance and design of pipe networks." *Journal of Hydraulic Engineering*, ASCE, 121(11), 833-837.
- Atiquzzaman, M., Liong, S., and Yu, X. (2006). "Alternative decision making in water distribution network with NSGA-II." *Journal of Water Resources Planning and Management*, ASCE, 132(2), 122-126.
- Ballantyne, Donald, B., and Crouse, C. B. (2997). *Reliability and Restoration of Water Supply Systems for Fire Suppression and Drinking Following Earthquakes*, National Institute and Standards and Technology, NIST GRC 97-730, Gaithersburg, MD.
- Brannigan, V. M. and Kilpatric, A. (1997). "Performance-based codes: reengineering the regulatory system." *Proc. 1996 International Conference on Performance Based Codes and Fire Safety Design Methods*, SFPE 1997, 139-149.
- Bristow, E. C. (2006). *Interdependent Infrastructures and Multi-mode Attacks and Failures: Improving the Security of Urban Water Systems and Fire Response*, Doctoral dissertation, Texas A&M University, Civil Engineering, College Station, TX.
- Bristow, E. C., Brumbelow, K., and Kanta, L. (2007). "Vulnerability assessment and mitigation methods for interdependent water distribution and urban fire response systems." *Proc. World Environmental and Water Resources Congress 2007*, ASCE, Tampa, FL.
- Brumbelow, K., Bristow, E. C., and Torres, J. (2005). "Micropolis: A virtual city for water distribution systems research applications." *Proc. AWRA 2006 Spring Specialty Conference: GIS and Water Resources IV*, American Water Resources Association, Denver, CO.

- Brumbelow, K., Torres, J., Guikema, S., Bristow, E. C., and Kanta, L. (2007). "Virtual cities for water distribution and infrastructure system research." *Proc. World Environmental and Water Resources Congress 2007*, ASCE, Reston, VA.
- Brumbelow, K. and Bristow, E. C. (2008). "Tradeoffs in water distribution system design for normal versus emergency flows: quantity, quality, and cost/benefits." *Proc. World Environmental and Water Resources Congress 2008*, ASCE, Honolulu, HI.
- Cities of Bryan and College Station (2005). *B/CS Unified Design Guideline Manual, Water, Sewer, and Streets*, Available: www.bcsunited.net/2005Files/DesignManual2005.pdf
- Clemen, R. T. and Reilly, T. (2001). *Making Hard Decisions*, Duxbury, Pacific Grove, CA.
- Deb, K., Agrawal, S., Pratap, A., and Meyarivan, T. (2002). "A fast elitist non-dominated sorting genetic algorithm for multi-objective optimization: NSGA-II." *IEEE Transactions on Evolutionary Computation*, 6(2), 182-197, Piscataway, NJ.
- Dorn, J. L. (2004). *Evolutionary Algorithms to Aid Watershed Management*, Doctoral dissertation, North Carolina State University, Civil Engineering, Raleigh, NC.
- Eckman, W. F. (1994). *The Fire Department Water Supply Handbook*, Fire Engineering Books & Videos, Saddle Brook, NJ.
- Eiben, A. E. and Smith, J. E. (2007). *Introduction to Evolutionary Computing*, Springer-Verlag, New York.
- Eidinger, J. (2005). *Seismic Guidelines for Water Pipelines*, G&E Report 80.01.01, Revision 0, American Lifelines Alliance, Oakland, CA.
- Ezell, B. C., Farr, J. V., and Wiese, I. (2000). "Infrastructure risk analysis model." *Journal of Infrastructure Systems*, ASCE, 6(3), 114-117.
- Farmani, R., Walters, G. A., and Savic, D., A. (2005). "Trade-off between total cost and reliability for Anytown water distribution network." *Journal of Water Resources Planning and Management*, ASCE, 131(3), 161-171.
- Fleischer, M. (2003). "The measure of Pareto optima – applications to multi-objective metaheuristics." *Evolutionary Multi-Criterion Optimization*, Springer-Verlag, Faro, Portugal.

- Friedman, R. (1992). "An international survey of computer models for fire and smoke." *Journal of Fire Protection Engineering*, 4(3), 81-92.
- Haan, C. T. (2002). *Statistical Methods in Hydrology*, Iowa State Press, Ames, IA.
- Haimes, Y. Y. (1981). "Hierarchical holographic modeling." *IEEE Trans. on Sys., Man, and Cybernetics*, SMC-11(9), 606-617.
- Haimes, Y. Y., Matalas, N. C., Lambert, J. H., Jackson, B. A., and James, F. R. (1998). "Reducing vulnerability of water supply systems to attack." *Journal of Infrastructure Systems*, ASCE, 4(4), 164-177.
- Haimes, Y. Y. (2002). "Strategic responses to risks of terrorism to water resources." *Journal of Water Resources Planning and Management*, ASCE, 128(6), 383-389.
- Hamada, M. (1951). *On Fire Spreading Velocity in Disasters*, Sagami Shobo, Tokyo, Japan (in Japanese).
- Hamada, M. (1975). *Architectural Fire Resistant Themes*, No. 21 in *Kenchiku-gaku Taikei*, Shokoku sha, Tokyo, Japan (in Japanese).
- Hans, A. E. (1988). "Multicriteria optimization for highly accurate systems: Multicriteria optimization in engineering and science." *Mathematical Concepts and Methods in Science and Engineering*, E. Stadler, ed., Plenum Press, New York, 19, 309-352.
- Hasofer, A. M., Beck, V. R., and Bennetts, I. D. (2007). *Risk Analysis in Building Fire Safety Engineering*, Butterworth-Heinemann, Oxford, UK.
- HAZUS. (1999). *Earthquake Loss Estimation Methodology, HAZUS^R 99*, Service Release 2 (SR2) Technical Manual, Developed by Federal Emergency Management Agency, Washington, DC through agreements with National Institute of Building Sciences, Washington, DC.
- Holland, J. H. (1975). *Adaptation in Natural and Artificial Systems*, The University of Michigan Press, Ann Arbor, MI.
- Horn, J., Nafpliotis, N., and Goldberg, D. E. (1994). "A niched Pareto genetic algorithm for multiobjective optimization." *IEEE Conference on Evolutionary Computation*, IEEE Service Center, Piscataway, NJ, 82-87.
- International Organization of Standards (ISO). (2001). *Draft ISO Guide 73*. Technical Management Board Working Group on Risk Management Terminology, Geneva.

- Jeong, H. S. and Abraham, D. M. (2006). "Operational response model for physically attacked water networks using NSGA-II." *Journal of Computing in Civil Engineering*, ASCE, 20(5), 328-338.
- Kanta, L. and Brumbelow, K. (2008). "Vulnerability, risk, and mitigation assessment of water supply systems for insufficient fire flows." *Proc. World Environmental and Water Resources Congress 2008*, ASCE, Honolulu, HI, 1-10.
- Kanta, L., Brumbelow, K., and Zechman, E. (2009). "A multi-objective evolutionary computation approach to hazards mitigation designs for water distribution systems." *Proc. World Environmental and Water Resources Congress 2009*, ASCE, Kansas City, MO.
- Kanta, L. R. (2006). *Vulnerability Assessment of Water Supply Systems for Insufficient Fire Flows*, M.S. Thesis, Texas A&M Engineering, Civil Engineering, College Station, TX.
- Knowles, J. and Corne, D. (1999). "The Pareto archived evolutionary strategy: a new baseline algorithm for multi-objective optimization." *Proc. 1999 Congress on Evolutionary Computation*, IEEE Service Center, Piscataway, NJ, 98-105.
- Lewis, T. G. (2006). *Critical Infrastructure Protection in Homeland Security: Defending a Networked Nation*, John Wiley & Sons, New York.
- Mays, L. W., ed. (1996). *Water Resources Handbook*, McGraw-Hill, New York.
- Mays, L. W., ed. (2000). *Water Distribution Systems Handbook*, McGraw-Hill, New York.
- Mays, L. W., ed. (2004). *Urban Water Supply Management Tools*, McGraw-Hill, New York.
- Modarres, M. (2006). *Risk Analysis in Engineering Techniques, Tools, and Skills*, Taylor & Francis, Boca Raton, FL.
- Montgomery, D. C. and Runger, G. (1999). *Applied Statistics and Probability for Engineers*, John Wiley & Sons Inc., New York.
- Morgan, M. G. and Henrion, M. (1990). *Uncertainty – A Guide to Dealing with Uncertainty in Quantitative Risk and Policy Analysis*, Cambridge University Press, New York.
- National Research Council. (1994). *Science and Judgment in Risk Assessment*, National Academy Press, Washington, DC.

- Ostfeld, A., and Salomons, E. (2004). "Optimal layout of early warning detection stations for water distribution systems security." *Journal of Water Resources Planning and Management*, ASCE, 130(5), 377-385.
- Pate-Cornell, M. (1984). "Fault trees vs. event trees in reliability analysis." *Society for Risk Analysis*, 4(3), 177-186.
- Prasad, T., Walters, G., and Savic, D. (2004). "Booster disinfection of water supply networks: multiobjective approach." *Journal of Water Resources Planning and Management*, ASCE, 130(5), 367-376.
- Prasad, T. D. and Park, N. (2004). "Multiobjective genetic algorithms for design of water distribution networks." *Journal of Water Resources Planning and Management*, ASCE, 130(1), 73-82.
- Rahikainen, J. and Keski-Rahkonen, O. (2004). "Statistical determination of ignition frequency of structural fires in different premises in Finland." *Fire Technology*, 40, 335-353.
- Ranjithan, S. R. (2005). "Role of evolutionary computation in environmental and water resources systems analysis." *Journal of Water Resources Planning and Management*, ASCE, 131(1), 1-2.
- Rechenberg, I. (1965). *Cybernetic Solution Path of an Experimental Problem* (Royal Aircraft Establishment Translation No. 1122, B. F. Toms, Trans.), Ministry of Aviation, Royal Aircraft Establishment, Farnborough Hants, UK.
- Rossman, L. A. (1999). "The EPANET programmer's toolkit for analysis of water distribution systems." *29th Annual Water Resources Planning and Management Conference*, Erin M. Wilson, ed., June, 1999, Tempe, AZ.
- Rossman, L. A. (2000). *EPANET 2 Users Manual*. EPA/600/R-00/057. National Risk Management Research Laboratory, U.S. Environmental Protection Agency, Cincinnati, OH.
- Saylor Publications, Inc. (2004). *Current Construction Costs, 41st Annual Edition*, Saylor Publications, Chatsworth, CA.
- Scawthorn, C., Eidinger, J. M., and Schiff, A. J., ed. (2005). *Fire Following Earthquake*, Technical Council on Lifeline Earthquake Engineering, Monograph No. 26, ASCE, Danvers, MA.

- Skolicki, Z., Wadda, M. M., Houck, M. H., and Arciszewski, T. (2006). "Reduction of physical threats to water distribution systems." *Journal of Water Resources Planning and Management*, ASCE, 132(4), 211-217.
- Srinivas, N. and Deb, K. (1995). "Multi-objective function optimization using non-dominated sorting genetic algorithms." *Evolutionary Computation*, 2(3), 221-248.
- Stern, P. C. and Fineberg, H. V., ed. (2003). *Understanding Risk: Informing Decisions in a Democratic Society*, National Academy Press, Washington, DC.
- Tidwell, V. C., Cooper, J. A., and Silva, C. J. (2005). "Threat assessment of water supply systems using markov latent effects modeling." *Journal of Water Resources Planning and Management*, ASCE, 131(3), 218-227.
- Tillander, K. and Keski-Rahkonen, O. (2002). "The ignition frequency of structural fires in Finland 1996-99". *Proc. 7th International Symposium on Fire Safety Science*, Worcester, MA, 1051-1062.
- USEPA (2002). *Effects of Water Age on Distribution System Water Quality*, A report prepared by AWWA with assistance from Economic and Engineering Services Inc., prepared for Office of Ground Water and Drinking Water Standards and Risk Management Division, Washington, DC.
- USEPA (2004). *The Effectiveness of Disinfectant Residuals in the Distribution System*, Office of Ground Water and Drinking Water Standards and Risk Management Division, Washington, DC.
- White House (2003). *National strategy for the physical protection of critical infrastructures and key assets*, A report prepared by the office of the President of the United States, Washington, DC. Available: www.whitehouse.gov/pcipb/physical.html
- Yamijala, S., Guikema, S., and Brumbelow, J. K. (2009). "Statistical estimation of water distribution system pipe reliability." *Reliability Engineering & System Safety*, ELSEVIER, 94, 282-293.
- Zechman, E. M. and Ranjithan, S. R. (2009). "Evolutionary computation-based methods for characterizing contaminant sources in a water distribution system." *Journal of Water Resources Planning and Management*, ASCE, 135(5), 334-343.
- Zitzler, E. and Thiele, L. (1998). "Multiobjective optimization using evolutionary algorithms - A comparative case study." *Proc. 5th International Conference on Parallel Problem Solving from Nature*, PPSNV, Berlin, Germany, 292-304.

Zitzler, E. and Thiele, L. (1999). "Multiobjective evolutionary algorithms: A comparative case study and the strength Pareto approach." *IEEE Transactions on Evolutionary Computation*, 3(4), 257-271.

VITA

Lufthansa Rahman Kanta was born in Dhaka, Bangladesh, the first of three children to Lutfor and Mahmuda Rahman. She earned a Bachelor of Science degree in civil engineering from Bangladesh University of Engineering and Technology, Dhaka, Bangladesh, in 1995. She worked as a Hydraulic Engineer at Surface Water Modeling Center, Dhaka, Bangladesh, for five years after completion of her undergraduate education. She enrolled as a graduate student in the Zachry Department of Civil Engineering at Texas A&M University, College Station, Texas, in 2003 and earned a Master of Science in civil engineering with a specialty in water resources engineering in December 2006 under the supervision of Dr. Kelly Brumbelow. She continued her studies at Texas A&M University and worked toward a Doctor of Philosophy degree, developing a methodology of assessing risk and consequences of and generating effective mitigation measures within two critical infrastructures – water system and fire response. She earned a Doctor of Philosophy in civil engineering with a specialty in water resources engineering in December 2009. She will begin work as a Post-doctoral Research Associate in the Zachry Department of Civil Engineering at Texas A&M University. Her intent is to continue as a post-doctoral researcher and teacher in the field of systems analysis in environmental and water resources planning and management.

She may be reached by e-mail at: lufthansa_kanta@neo.tamu.edu or by contacting Dr. Kelly Brumbelow at: Zachry Department of Civil Engineering, WERC Building, Room 205L, 3136 TAMU, College Station, TX 77843-3136.